UNIVERSITY OF CALIFORNIA
RIVERSIDE

Structural and Functional Characterization of the *Xylella fastidiosa* O Antigen: Contribution to Bacterial Virulence, Insect Transmission, and Modulation of Innate Immune Recognition in Grapevine

A Dissertation submitted in partial satisfaction
of the requirements for the degree of

Doctor of Philosophy

in

Plant Pathology

by

Jeannette Nicole Rapicavoli

August 2016

Dissertation Committee:
Dr. M. Caroline Roper, Chairperson
Dr. Hailing Jin
Dr. Patricia Manosalva

The Dissertation of Jeannette Nicole Rapicavoli is approved:

_____

_____

_____

Committee Chairperson

University of California, Riverside

ACKNOWLEDGMENTS

Chapter 1 in its entirety is reprinted with permission as appears in Rapicavoli, J. N., Kinsinger, N., Perring, T. M., Backus, E. A., Shugart, H. J., Walker, S., & Roper, M. C. 2015. Appl. Environ. Microbiol. *81*(23), 8145-8154. This work was supported by an award to M. Caroline Roper by the California Department of Food and Agriculture Pierce's Disease and Glassy-Winged Sharpshooter Board. Structural characterization in Chapter II was supported in part by the Chemical Sciences, Geosciences and Biosciences Division, Office of Basic Energy Sciences, U.S. Department of Energy grant (DE-FG02-93ER20097) to the Complex Carbohydrate Research Center at the University of Georgia in Athens. Brian Ingel also contributed to writing the general introduction.

First and foremost, I would like to express my deepest appreciation for my advisor, Dr. Caroline Roper. I feel truly blessed to have been accepted into your lab. Thank you for your dedication to my success. You have shaped me into the scientist that I am today. I would also like to thank the members of my dissertation committee, Dr. Hailing Jin and Dr. Patricia Manosalva for their guidance and support. I would like to acknowledge all members of the Roper lab, past and present, including Brian Ingel, Nichole Ginnan, Polrit Viravathana, and Claudia Castro, with special thanks to Dr. Lindsey Burbank for her scientific insight and helpful discussions. I would also like to acknowledge our undergraduate lab helper, Chi Lok Leung, for his diligence in the lab and for assisting me with my experiments. In addition, I would like to give special consideration to all of my collaborators and the members of their labs: Drs. Elaine A. Backus, Thomas M. Perring, Sharon Walker, and Dario Cantu. Thank you for your

valuable contributions to the work in this dissertation. I would also like to give special recognition to my undergraduate professors at Cal Poly in San Luis Obispo, Drs. Michael Yoshimura and David Headrick. Thank you for your dedication to my success, for your guidance and encouragement as I struggled to navigate life as a first-generation college student, and for your truly unwavering support. You have transformed the way that I look at science, and I hope to carry that with me as I embark on my professional career. You are a constant source of inspiration for me, and I can only hope that I will impact someone's life in a similar way. Last, but not least, I would like to thank all of my family and friends for their encouragement throughout my graduate studies, with special acknowledgment to my husband, Evan Rathje. Thank you for going on this academic journey with me.

DEDICATION

This dissertation is dedicated to Dr. Michael Yoshimura, whose passion for Plant Pathology deeply inspired me and forever changed my life.

ABSTRACT OF THE DISSERTATION

Structural and Functional Characterization of the *Xylella fastidiosa* O Antigen: Contribution to Bacterial Virulence, Insect Transmission, and Modulation of Innate Immune Recognition in Grapevine

by

Jeannette Nicole Rapicavoli

Doctor of Philosophy, Graduate Program in Plant Pathology
University of California, Riverside, August 2016
Dr. M. Caroline Roper, Chairperson

Xylella fastidiosa is a xylem-limited, insect transmitted bacterium that causes fatal diseases in economically important crops, most notably, Pierce's disease of grapevine. Due to its unique dual lifestyle, *X. fastidiosa* utilizes different mechanisms to facilitate colonization of its plant and insect hosts. While research has focused heavily on the role of surface-associated proteins, we establish the major cell surface carbohydrate, lipopolysaccharide (LPS), as an important bacterial virulence factor and modulator of innate immunity in grapevine.

We focused our attention on the terminal O antigen moiety of the LPS molecule, which serves as a key point of contact between potential hosts and the environment. Biochemical and structural analysis identified the major O antigen polysaccharide as a linear α1-2 linked rhamnan polymer. By targeting an O antigen polymerase (Wzy), we found that loss of the rhamnose-rich O antigen considerably altered bacterial adhesion dynamics in the blue-green sharpshooter vector. Scanning electron microscopy confirmed

that this defect in initial attachment compromised subsequent biofilm formation within vector foreguts, thus impairing pathogen acquisition. During the plant host-pathogen interaction, successful pathogens must overcome plant immune responses to establish and cause disease. Due to the fact that *X. fastidiosa* lacks the quintessential type III secretion system, and its arsenal of effectors, we sought to determine the contribution of O antigen to this complex biological process. Using RNAseq, we found that in intact cells, O antigen functions as a shield; this allows *X. fastidiosa* to delay early recognition by the grapevine immune system, thus promoting bacterial survival and the establishment of infection.

The results presented in this dissertation provide a comprehensive understanding of the composition and structure of this major cell surface polysaccharide and offer valuable insight into its diverse functions. Specifically, the studies detailing the implication of O antigen in the evasion of basal defense responses in grapevine present a novel and unprecedented mechanism employed by this unique xylem-dwelling bacterial pathogen.

TABLE OF CONENTS

LIST OF FIGURES

CHAPTER I

CHAPTER II

CHAPTER III

LIST OF TABLES

CHAPTER I

CHAPTER II

CHAPTER III

GENERAL INTRODUCTION

Xylella fastidiosa is a Gram-negative, xylem-limited bacterium belonging to the Xanthomonadaceae family (1). This destructive agricultural pathogen is obligately transmitted by sharpshooter insect vectors and causes diseases in several economically important crops, namely Pierce's disease (PD) of grapevine and Citrus Variegated Chlorosis (CVC). It has also recently been implicated in Olive quick decline syndrome in Italy (2, 3). Many studies exploring *X. fastidiosa* biology have utilized the *X. fastidiosa* subsp. *fastidiosa* strain, the grapevine host, and *Homalodisca vitripennis* (the Glassy-winged sharpshooter) and/or *Graphocephala atropunctata* (the Blue-green sharpshooter). Thus, most of what we know about the plant- and vector-microbe interactions are in the context of the PD pathosystem, so the majority of this introduction will focus on PD and its impact in California. It is likely that many of the findings in grape can be extrapolated to other plant systems; however, we must be mindful that there are likely important differences in *X. fastidiosa* interactions with different plant hosts and insect vectors.

Host Ranges and Strain Differences. *X. fastidiosa* has an incredibly broad host range, comprising 309 different plant species in 63 plant families (4), which includes economically important hosts such as coffee, citrus, and grapevine. *X. fastidiosa* also causes diseases in almond, peach, plum, and oleander and in ornamental trees such as elm, sycamore, and maple (5). While *X. fastidiosa* is often referred to as a generalist, due to the large numbers of plant species in which the bacterium resides, very few plants actually sustain long-term infections and become symptomatic (6). The bacterium can

reside in a wide range of plants as a harmless endophyte and has been detected in hundreds of asymptomatic plant species (3, 7, 8). Fortunately, most *X. fastidiosa* strains do not move systemically in symptomless hosts (9, 10), but these plants can still serve as sources of inoculum for vectors to acquire the bacterium (11).

There are distinct differences in the host ranges of the different strains of *X. fastidiosa*. Although all *X. fastidiosa* isolates were assigned to the same species, they have been further classified to the subspecies level, which correlates strongly with host specificity (12, 13). Three distinct clades of *X. fastidiosa* have been identified in North America, corresponding to the different subspecies: *X. fastidiosa* subsp. *fastidiosa,* which is found in grapevines, almond, and alfalfa; *X. fastidiosa* subsp. *multiplex*, which is found predominantly in trees (e.g. almond, peach, plum, and oak); *X. fastidiosa* subsp. *sandyi*, which thus far has only been found in oleander; and *X. fastidiosa* subsp. *pauca*, which is primarily found in citrus and coffee in South America (12), although a recent strain associated with olive quick decline syndrome in Italy was found to be genetically related (14). It is important to note that there is significant plant host-pathogen specificity among the subspecies, i.e. the oleander strain cannot infect grapevine and vice versa. However, the mechanisms dictating this specificity remain unknown.

Disease symptoms. Most *X. fastidiosa*-related diseases appear as leaf scorch symptoms concentrated around the leaf margin. In the context of PD, *X. fastidiosa* can also cause raisining of grape clusters, irregular periderm development (termed “green islands”), abnormal abscission of petioles (termed “matchstick petioles”), and general stunting of

vines. PD symptoms generally appear in late spring and begin with leaf-scorching. As the infection progresses, additional symptoms (e.g. green islands, matchstick petioles, and berry desiccation) increase into the late summer. Interestingly, in some host interactions, *X. fastidiosa* does not cause leaf scorch. For example, symptoms of citrus variegated chlorosis (CVC) include foliar wilt and interveinal chlorosis on the upper surfaces of leaves (similar to Zn deficiency), which correspond with necrotic, gum-like regions on the undersides of the leaves. Additional symptoms of CVC include defoliation, dieback, and hardening of fruits (15). Another example is phony peach disease, which exhibits flat, dark green leaves, earlier bloom, shortened internodes, delayed leaf senescence, and reduced fruit size. Some occlusions occur in the xylem vessels, but there is no foliar wilting, chlorosis, or necrosis symptoms (5).

Insect transmission. The *X. fastidiosa* life cycle is unique in that it involves both plant and insect hosts. *X. fastidiosa* is obligately transmitted by xylem sap-feeding insects belonging to the hemipteran family Cicadellidae, primarily sharpshooters; additional vectors, such as spittlebugs (Hemiptera, Cercopidae), have also been reported (7, 16). *X. fastidiosa* is the only known insect-transmitted plant pathogen that is persistent within the vector but non-circulative (17). It is semi-persistent in nymphs, i.e. the bacterium is lost after each vector molt, but persistent in adult vectors (which do not molt) (7, 17). *X. fastidiosa* is also propagative within vectors, allowing the insects to inoculate the pathogen for months after acquisition from an infected plant (7). There is no evidence of transstadial or transovarial transmission, meaning there is no pathogen transfer through

insect life stages or to offspring, respectively (16). Native vectors in California include the blue-green sharpshooter, *Graphocephala atropunctata* (Signoret); the green sharpshooter, *Draeculacephala minerva* (Ball); and the red-headed sharpshooter, *Xyphon fulgida* (Nottingham) (16, 18). Invasive vectors include the glassy-winged sharpshooter, *Homalodisca vitripennis* (Say) (19). Both the blue-green sharpshooter (BGSS) and the glassy-winged sharpshooter (GWSS) are important vectors of PD in California. CVC and additional *X. fastidiosa*-related diseases in other parts of the world have their own distinct vectors. In contrast with *X. fastidiosa* strain specificity in plant hosts, there is a lack of vector-*X. fastidiosa* strain specificity. For example, the glassy-winged sharpshooter is capable of transmitting a South American isolate of *X. fastidiosa*, albeit with variable efficiency (20).

Transmission of *X. fastidiosa* consists of three main steps: pathogen acquisition from an infected host plant, retention of the pathogen within the vector, and inoculation of the pathogen into a susceptible plant host (21). Vectors can acquire *X. fastidiosa* and immediately inoculate it into a new host, indicating there is no latent period required for transmission (22). Upon acquisition during the ingestion of xylem sap, *X. fasitidiosa* attaches to and forms biofilms within the functional foregut of the insect in a manner similar to its biofilm formation in plants (21, 23). Cells initially attach laterally, which increases cell surface area in contact with the insect cuticle. Interestingly, in the later stages of biofilm formation, the cells become polarly attached to the foregut cuticle, presumably to allow for maximal exposure to the nutrient dilute xylem sap (7, 23, 24). *X. fastidiosa* colonizes two major regions of the foregut: the precibarium and the cibarium.

Colonization of these regions were first shown microscopically (22, 25) and later correlated with inoculation of *X. fastidiosa* to plant hosts during feeding. While the cibarium has been suggested to act as a reservoir for bacterial inoculum within the foregut (17), colonization of the precibarium, specifically, has been associated with transmission of *X. fastidiosa* to plants (24).

The vector foregut is an extremely turbulent environment, as xylem sap flow rates have been estimated to reach nearly 8 cm/s (26). Therefore, attachment is not a trivial process, and it relies on numerous factors at the vector-pathogen interface. Several surface-associated bacterial components, such as type I pili, hemagglutinin adhesins, and fimbriae contribute to the adhesive properties of *X. fastidiosa* that are imperative for colonization in insect vectors (7, 23, 27-29). These traits are regulated by the *rpf* cell-cell signaling system (29-31). In addition, cell surface polysaccharides, namely lipopolysaccharide (LPS) and exopolysaccharide (EPS), also play a role in the transmission process. Rapicavoli et al. (2015) demonstrated that LPS contributes to the early stages of acquisition of *X. fastidiosa* by the BGSS (32). A mutant strain exhibiting LPS structural alteration was impaired in attachment to the insect foregut cuticle lining, and thus acquisition of the pathogen was disrupted. EPS has also been implicated in the transmission of *X. fastidiosa* by the BGSS, as mutants impaired in EPS production were not transmitted efficiently (33).

Disease cycle. *X. fastidiosa* is found exclusively in the xylem vessels of plant hosts and the mouthparts of its insect vectors. In both environments, it forms biofilms that are

important for plant infection and insect transmission processes. While disease cycles will vary slightly depending on the specific disease, the progression of disease follows the same trend. *X. fastidiosa* cells are delivered directly into xylem vessels through vector feeding, which differs from other bacterial plant pathogens (e.g. species and pathovars of *Xanthomonas*) that enter the host through natural openings or wounds (7, 34). In susceptible hosts, such as grapevine, *X. fastidiosa* multiplies and systemically colonizes the xylem tissue through active degradation of xylem pit membranes: a process that is facilitated by cell wall-degrading enzymes and Type IV pili-mediated motility (35, 36). In many hosts, the bacterium multiplies to high titers within the vessels, and bacterial populations are heterogeneously distributed throughout the plant. Insects can then acquire *X. fastidiosa* from plants harboring the bacterium and transmit them to a new plant. As previously mentioned, both symptomatic and asymptomatic hosts are important reservoirs of the bacteria. The development of disease relies on the ability of the pathogen to spread from the point of infection and establish itself systemically in the xylem tissue (7, 35, 37). For some perennial hosts (e.g. grapevine), in which bacterial concentrations are high in symptomatic leaf veins and petioles, populations typically decline in the fall as the plant enters dormancy and defoliates (38).

Geographic Distribution. Historically, *X. fastidiosa* has been limited to North America where the first epidemic of PD occurred in Los Angeles, California in the late 1880s (16). It has since spread throughout the United States but is most prominent in California and the southern United States. Diseases caused by *X. fastidiosa* are rare or absent in parts of

North America with cold winters, with an exception being the occurrence of leaf scorch on landscape trees in Canada (39, 40). There have been experimental observations that freezing can be therapeutic for PD (41, 42), which suggests that winter climates limit where PD can occur. *X. fastidiosa* also causes important disease of fruit trees, such as almond leaf scorch, which is prevalent in the San Joaquin Valley of California (43, 44).

In the coastal regions of California, PD persists mainly in "PD hot spots" along parts of the vineyard adjacent to riparian areas (e.g. streambeds). The dominant vector in this region is the native BGSS, which enters vineyards from these riparian areas in the spring and summer, following overwintering, to feed and reproduce. PD incidence is the highest in these hot spots, creating what is known as the PD "edge effect" (3), meaning that infection remains primarily along the edges of the vineyard. In addition, BGSS prefer to feed on succulent, new growth, so any *X. fastidiosa* cells that have not reached the vines' permanent arms or trunk will likely be pruned out when vines enter dormancy in the winter. Thus, PD does not typically persist from year to year in these areas (monocyclic disease). The introduction of the invasive GWSS into Southern California in the 1990s, however, drastically changed the epidemiology of PD in California to a polycyclic disease. Compared with California-native vectors, adult GWSS are polyphagous (feeding on over 100 species of plants), highly mobile, and they feed on a greater variety of plant parts (40, 45). GWSS have a strong tendency to feed at the bases of new shoots, even through the scaly bark of branches on grapevines, and they will also feed on dormant canes. This difference in feeding behavior can increase the

establishment of chronic infections, persisting from year to year, as these portions of the vine are permanent and not pruned annually (3).

In South America, CVC was first observed in Brazil in 1987 (26). Since its discovery, CVC has become widely distributed in the major citrus-growing regions of Brazil (46), where it also causes a leaf scorch disease on coffee (47). Following the resurgence of PD in California, in the 1990s, there has also been an emergence of new *X. fastidiosa*-related diseases in other parts of the world. For example, *X. fastidiosa* appeared in Taiwan in pear trees and grapevines (48, 49) and was more recently identified in olive trees in Italy that are affected with olive quick decline syndrome, representing the first confirmed detection of *X. fastidiosa* in the European Union (50). The introduction of *X. fastidiosa* into Italy is an important and significant change in the geographical distribution of this pathogen, where, to our knowledge, the plant communities have not been exposed.

Economic Impact. *X. fastidiosa* causes economic losses in many agriculturally important crops, but here we will focus primarily on PD and CVC, as the economic impacts of these diseases have been the most extensively studied. PD represents a significant threat to the California table, raisin, and winegrape industries, which were valued at over $5 billion in 2014 (51). Following the introduction of GWSS into Southern California, and subsequently, the Pierce's disease epidemic in Temecula in the late 1990s, production losses resulted in an estimated $37.9-million-dollar reduction in California state income (52). Despite the presence of the PD Control Program (PDCP), established by the

California Department of Food and Agriculture in 2001, PD still costs producers over $100 million dollars per year in crop loss and efforts to mitigate the disease. This amount excludes an additional $50 million per year spent on preventative measures, including vector control. (45). Alston *et al*. (2013) evaluated the costs and benefits of PD research in the winegrape industry, and they estimated that PD would cost an additional $189 million per year if the PDCP ended (53). Therefore, the benefits of PD research clearly outweigh the costs in terms of preventing another major outbreak.

The potential for GWSS to spread to other parts of California has caused great concern for growers as this could change the epidemiology of existing *X. fastidiosa*-related diseases or cause an emergence of new diseases. For example, the presence of GWSS in Southern California caused the appearance of a new, lethal leaf scorch disease of oleander (*Nerium oleander*). Due to its low maintenance and drought tolerant nature, oleander is an important shrub to California's landscape industry. In addition, the California Department of Transportation (Caltrans) maintains oleander in over 2,100 miles of freeway median (54). Damage to these freeway plantings, caused by OLS, has cost an estimated $52 million (55). In California, almond leaf scorch is a relatively minor problem in the San Joaquin Valley that could become a major problem if GWSS establishes itself, as this could lead to a rapid increase in disease severity and spread (54).

Citrus is another important host of *X. fastidiosa* in South America. CVC was first described in Brazil in 1987, and affects all major commercial sweet orange cultivars (56). It is considered one of the most important diseases affecting the Brazilian citrus industry, which accounts for 30% of sweet orange production and 85% of exports of frozen orange

juice concentrate worldwide (57, 58). Currently, 40% of citrus plants in Brazil are affected by CVC, and economic losses due to the disease can reach $120 million annually (56, 58).

Virulence Factors

Adhesins. Biofilm formation plays an essential role in the plant and insect lifestyles of *X. fastidiosa*, and relies on the ability of the bacteria to attach to host surfaces and to each other (31). These biofilm-related behaviors are facilitated by several bacterial cell surface proteins and structures, including fimbrial and afimbrial adhesins, type IV pili, outer membrane proteins, and exopolymers (59).

X. fastidiosa Type I fimbrial adhesins are pilliform structures encoded by the *fim* operon. Knockout mutations of *fimA*, which encodes the major subunit, and *fimF, which* encodes the anchor protein, affected fimbriae production and failed to induce biofilm formation at the air-liquid interface in liquid culture (27, 60). Furthermore, these mutants failed to attach to a glass surface and form aggregates. These mutations also affected *X. fastidiosa* virulence, as disease severity was significantly reduced in Cabernet Sauvignon grapevines (27). With respect to afimbrial adhesins, *X. fastidiosa* possesses hemagglutinin proteins, HxfA and HxfB (61). Knockout mutations in *hxfA* and *hxfB* resulted in hypervirulent phenotypes after inoculation into Chardonnay, Chenin Blanc, and Thompson Seedless grapevines. However, research done by Feil et al (2007) determined that Δ*hxfB* had reduced virulence when inoculated into Cabernet Sauvignon grapevines (27). This discrepancy could be caused by the physiological differences that exist between red and white grape varieties, which could affect how the pathogen

interacts with its host in the xylem (62). Both *hxfA* and *hxfB* mutants also displayed significantly decreased cell-cell aggregation but retained the ability to adhere to surfaces (61, 63). Interestingly, in addition to their location on the bacterial outer membrane, HxfA and HxfB are also found in outer membrane vesicles, which have been implicated in mediating biofilm formation and colonization (63, 64).

Additional surface proteins have been implicated in facilitating attachment of bacteria to host cells. A knockout mutation in the outer membrane protein XadA resulted in reduced adhesion to glass surfaces, but the mutation did not appear to affect cell-cell aggregation (27). The Δ*xadA* mutant strain also failed to produce biofilm, which is likely a consequence of defects in cell-cell aggregation: a key step in biofilm formation.

Motility. The process by which *X. fastidiosa* moves within plants differs substantially from closely related *Xanthomonas* pathovars and other prominent bacterial pathogens, which utilize flagellar-driven motility. Although *X. fastidiosa* is non-flagellate, it is able to migrate upstream through the use of Type IV-mediated twitching motility (65), which provides the means for long-range systemic movement *in planta*. Twitching motility occurs through the extension, attachment, and then retraction of Type IV pili, which are approximately 1-6 μm in length (66). This type of motility has also been observed in other xylem-dwelling bacterial plant pathogens, such as *Ralstonia solanacearum* (66). Knockout mutations in *pilB* and *pilQ* in *X. fastidiosa*, which are involved in the assembly of Type IV pili, increased the production of biofilm; however, basipetal movement *in planta* was significantly reduced (65).

In addition to motility, Type IV pili also contribute to autoaggregation in *X. fastidiosa*. Cell-cell aggregation is a critical step in microcolony formation and constructing a mature biofilm, and *X. fastidiosa* has a high propensity to aggregate in culture. Using a *pilB* mutant, De La Fuente et al. (2008) demonstrated that cells lacking type IV pili do not form spherical or compact aggregates. Instead, these cells were loosely attached to each other. Under flow conditions, these cells were eventually displaced downstream (67).

Cell surface polysaccharides. Like many other plant pathogenic bacteria, cell surface polysaccharides, namely lipopolysaccharide (LPS) and exopolysaccharide (EPS), play important roles in *X. fastidiosa* pathogenesis and virulence. LPS and EPS are among the predominant macromolecules found on the cell surface and thus contribute to the cell's interaction with the environment and potential hosts. In addition to facilitating adhesion, these polysaccharides perform a diverse array of functions for the cells (e.g. providing structural integrity and protection against host defense responses and toxic substances) (68-70), and thus greatly influence pathogen biology.

LPS occupies more than 75% of the bacterial cell surface and is comprised of a conserved lipid A-core oligosaccharide component and a variable O antigen (71). The O antigen of an *X. fastidiosa* subsp. *fastidiosa* (PD) isolate has been characterized as a high molecular weight heteropolymer consisting predominantly of α1-2 linked rhamnose subunits (Chapter II). Incorporation of rhamnose into the O antigen is mediated specifically by the Wzy polymerase, which catalyzes the polymerization of the individual

O-units that comprise the long chain (72). Targeted mutation of the *X. fastidiosa* Wzy polymerase resulted in a truncated O antigen that was primarily depleted of rhamnose. This structural alteration to the O antigen affected the net surface charge of the bacterial cell, disrupting surface attachment and cell-cell aggregation. The *wzy* mutant hyperattached to a glass surface but was deficient in cell-cell aggregation, consequently resulting in a thinner and rougher biofilm. Furthermore, the *wzy* mutant was severely impaired in virulence and colonization in grapevine, demonstrating that the O antigen is an important virulence factor in the development of PD in grapevine (73). More recently, Rapicavoli et al (2015) established a role for the O antigen in the early stages of acquisition of *X. fastidiosa* by the BGSS (32). Loss of the rhamnose-rich O antigen caused a consistent change in the net surface charge of the cell, which impaired cell attachment to vector foreguts. This severely compromised biofilm formation and thus impaired pathogen acquisition. In efforts to further determine its role in the host-pathogen interactions of the *X. fastidiosa* pathosystem, comprehensive investigations into the structural characterization of the O antigen are ongoing.

X. fastidiosa also produces a novel EPS, termed fastidian gum (74). *In silico* analysis revealed the presence of an operon closely related to the xanthan gum operon of *Xanthomonas campestris* pv *campestris*, minus three genes (*gumG*, *I*, and *L)*, which are all involved in the assembly and decoration of the terminal mannose residue of the repeating oligosaccharide subunit in the polymer (33, 74, 75). Thus, *X. fastidiosa* EPS is predicted to be similar to xanthan gum but is likely missing the terminal mannose residue

found on the repeating side chains. Secretion of both polymers is also predicted to be similar (33).

Antibodies raised against a modified xanthan gum polymer (structurally similar to *X. fastidiosa* EPS) revealed that *X. fastidiosa* produces relatively small amounts of EPS *in vitro* compared with *X. campestris* pv *campestris,* which produces an abundance of EPS in culture (75). Furthermore*,* this EPS was shown to be associated with the cells in a loose slime layer, with smaller amounts present as a tightly bound capsule. Spatiotemporal localization of EPS during the different stages of biofilm formation indicated that there is very little EPS associated with initial microcolony formation but can be seen intercalating the mature biofilm structure. Thus, EPS seems to contribute more to three-dimensional architecture and stability of the mature biofilm, as opposed to initial surface attachment of the cells (75). Findings by Souza et al (2006) corroborate this, as EPS mutants in the CVC strain of *X. fastidiosa* were not affected in surface attachment but showed a reduced capacity to form biofilms (76). Immunolocalization in PD-infected grapevines showed that an EPS matrix was associated with *X. fastidiosa* cell aggregates in the plant xylem vessels, where it also contributed to vessel occlusions (75).

The creation of mutants compromised in EPS production has confirmed the role of EPS in plant and insect colonization in *X. fastidiosa*. Mutations in *gumD* (putatively encoding a glycosyltransferase that initiates the synthesis of the tetrasaccharide) and *gum H* (putatively encoding a glycosyltransferase) significantly affected EPS production in *X. fastidiosa.* These mutants were also deficient in biofilm formation, sustained lower populations *in planta*, and were impaired in systemic colonization of grapevine.

Furthermore, both mutants were poorly transmitted by the blue-green sharpshooter, and results indicated that these cells are likely not retained within the vector over time (33). Indeed, Almeida and Purcell indicated the presence of cells embedded in an EPS matrix during the initial stages of colonization of the insect foregut, implicating EPS in the transmission process (24). Gene expression was also impacted in both mutants. Mutation of *gumD* and *H* resulted in an up-regulation of genes belonging to the *X. fastidiosa rpf* cell-cell signaling system (activated by a diffusible signaling factor, DSF), which regulates the expression of genes involved in motility and attachment. Killiny et al (2013) speculate that EPS may facilitate the accumulation of DSF near the cell surface or aid in signal binding to receptors (33).

Cell wall-degrading enzymes. *X. fastidiosa* maintains an array of cell wall-degrading enzymes (CWDE) in its genome that are critical for systemic colonization of plant hosts (e.g. polygalacturonase (PG), endoglucanases, xylanases) (31, 77). The xylem network is comprised of many interconnected vessels that are finite but variable in length (78, 79). Xylem vessels are connected to each other by bordered pits and separated by porous primary cell wall membranes; these are comprised of cellulose microfibrils embedded in a meshwork of hemicellulose and pectin (80, 81). Pit membranes allow for the exchange of water and small solutes between vessels and also serve as a barrier against air embolisms and pathogen movement (79, 82). *X. fastidiosa* is too large to passively move through the small pores of pit membranes (83). Therefore, it must enzymatically degrade the membrane (62, 84).

Endo-PGs facilitate the hydrolytic cleavage of polygalacturonic acid, which is a critical component of xylem pit membranes (80, 85). *X. fastidiosa* possesses only one endo-PG, encoded by the gene *pglA*, which is critical for pathogenicity in grapevine (86). A *pglA*- mutant failed to systemically colonize Chardonnay grapevines. Furthermore, the *pglA*- mutant did not induce Pierce's disease symptoms, indicating this enzyme is necessary for pathogenicity. However, *pglA* alone is not sufficient for pit membrane degradation, and requires the cooperation of endoglucanases (7).

In addition to the roles of these CWDE in plant hosts, there is also evidence that *X. fastidiosa* may secrete similar enzymes in the foreguts of its insect vectors. Killiny et. al. (2010) discovered a functional chitinase (ChiA) in the *X. fastidiosa* genome (87). Chitin is the primary polysaccharide constituent of the insect cuticle. The authors demonstrated that *X. fastidiosa* could utilize chitin as a carbon source, and bacterial populations increased in the presence of chitin. Furthermore, the presence of chitin in growth media induced phenotypic and transcriptional changes in *X. fastidiosa*, such as an increase in adhesiveness, that that would be conducive to life in the insect.

Secretion systems. In contrast with other prominent bacterial pathogens, *X. fastidiosa* does not possess a Type III secretion system or its arsenal of effectors to suppress plant innate immune responses (88). However, *X. fastidiosa* is able to produce components of the Type I, II, and V secretion systems (84, 89). The Type I secretion system is a general secretory pathway that has many functions, including multidrug resistance efflux and secretion of various proteases, hydrolases, and toxins (90). Often called the Type I

translocator, this sealed channel is ATP-dependent and is comprised of two inner membrane proteins that attach to TolC, a periplasm/outer membrane protein that is highly conserved among many phytopathogenic bacteria (91). *X. fastidiosa* maintains only a single copy of the *tolC* gene in its genome. An *X. fastidiosa tolC* mutant stain did not induce any PD symptoms (92). However, bacteria could not be isolated from these mutant-inoculated grapevines, suggesting that the mutation is lethal. The mutant strain also displayed a high level of sensitivity to several phytochemicals, detergents, and crude plant extracts, highlighting the importance of TolC-mediated multidrug efflux in the viability of *X. fastidiosa*.

The Type II secretion system (T2SS) is a general secretory pathway that is comprised of 12-15 different proteins, depending on the bacterial species (93). *X. fastidiosa* maintains a 12-protein T2SS that is closely related to those found in *Xanthamonas campestris* pv. *campestris* and *Xanthomonas oryzae* pv. *oryzae* (94). The T2SS is made up of three parts: (i) the outer membrane pore, (ii) the inner membrane complex, and (iii) the pseudopilin complex (95). XpsD forms the outer membrane pore, which is connected to the inner membrane complex (XpsF, L, M, E) by XpsN. The pseudopilin complex in comprised of XpsG, H, I, and K, which have their protein leader sequences removed by XpsO before pseudopilin assembly (96). *X. fastidiosa* proteins secreted through this pathway are transported into the periplasm via the Sec-dependent pathway and loaded into the T2SS. Pseudopilin formation is driven by XpsE: an ATPase that facilitates the stacking of additional pseudopilin subunits that push the loaded protein out into the extracellular environment (94). While the T2SS is defined as a general

secretory pathway, the proteins secreted by this system are often proteases and CWDE and typically have a variable sequence signal that directs their transport (95). It has been hypothesized that the T2SS facilitates the secretion of *X. fastidiosa* proteases and cell wall-degrading enzymes. However, a definitive connection has yet to be established.

The Type V secretion system is comprised of a family of autotransporter proteins (97). Autotransporter proteins typically contain three domains: (i) an N-terminal leader domain that initiates transport across the inner membrane via the Sec-dependent pathway, (ii) a variable passenger domain that acts as the virulence determinant, and (iii) a C-terminal helper domain that is required for transport across the outer membrane (98). *X. fastidiosa* maintains six genes predicted to encode members of the AT-1 autotransporter family, one of which is *xatA* (99). Its C-terminal helper domain interacts with the bacterial outer membrane, and also outer membrane vesicles, and its passenger domain is released into the extracellular environment. An *X. fastidiosa* mutant strain lacking a functional *xatA* gene formed smaller bacterial aggregates and subsequently, smaller biofilms compared to the wild type Temecula1 strain. When inoculated into grapevines, the *xatA* mutant strain did not induce Pierce's disease symptoms and was significantly impaired in host colonization.

Regulation of virulence factors. *X. fastidiosa* is able to coordinate gene expression in a cell density-dependent fashion, primarily through the production of a fatty acid diffusible signaling factor (DSF), which is synthesized by the *rpf* gene cluster. The synthesis of DSF modulates the production of virulence mechanisms in both the plant and insect

environments (29). The *rpfF* gene, which functions as a DSF synthase, is required for DSF production in *X. fastidiosa* and in species of its close relative *Xanthomonas* (31). In addition to signal production, signal reception is also critical for the coordination of virulence factors. The *rpfC* gene serves as a DSF receptor and is involved in the autoregulation of DSF production.

X. fastidiosa rpfF mutants were impaired in colonization of an insect vector, which resulted in significantly reduced transmission rates. Interestingly, this same mutant exhibited hypervirulence in grapevines, maintaining higher populations *in planta* and producing more intense PD symptoms (29). *X. fastidiosa rpfC* mutants exhibited a phenotype opposite to that of DSF-deficient *rpfF* mutants (29, 31). The *rpfC* mutants of *X. fastidiosa* were deficient in systemic colonization and virulence and maintained lower populations *in planta* than the wild-type strain. Furthermore, the *rpfC* mutants were acquired by insects feeding on infected plants but were somewhat deficient in transmission (31). The current model for DSF-mediated gene regulation indicates that DSF promotes the expression of genes in a manner opposite that of other prominent bacterial pathogens. That is, at high cell densities, accumulation of DSF induces the expression of adhesins and gum production, which contribute to the insect acquisition phase. Conversely, at lower cell densities, reduction in DSF abundance increases the expression of Type IV pili and extracellular enzymes, which contribute to motility and systemic colonization of the plant host. Because traits optimal for each environment are in conflict with each other, it has been proposed that *X. fastidiosa* maintains a mixed

population of cells in the plant (that are likely spatially and temporally separated), and DSF serves as the switch to coordinate each lifestyle (7).

In addition to the well-characterized *rpf* regulon, additional two-component regulatory systems have been implicated in the regulation of quorum sensing processes contributing to *X. fastidiosa* pathogenicity. For example, Pierce and Kirkpatrick (2015) investigated the role of the PhoP/PhoQ system, which consists of a response regulator and sensor kinase, respectively. Single knockout mutations of either *phoP* or *phoQ* caused a significant reduction in biofilm formation and cell-cell aggregation compared with wild type. Furthermore, these mutants were avirulent in grapevines, showing no PD symptoms (100). Additionally, mutation of a response regulator, XhpT, caused a significant reduction in surface attachment, an increase in exopolysaccharide production, and a reduction in virulence in a susceptible grapevine host (101).

LITERATURE CITED

1. **Wells JM, Raju BC, Hung H-Y, Weisburg WG, Mandelco-Paul L, Brenner DJ.** 1987. *Xylella fastidiosa* gen. nov., sp. nov: gram-negative, xylem-limited, fastidious plant bacteria related to *Xanthomonas spp*. International Journal of Systematic Bacteriology **37:**136-143.

2. **Saponari M, Boscia D, Nigro F, Martelli G.** 2013. Identification of DNA sequences related to *Xylella fastidiosa* in oleander, almond and olive trees exhibiting leaf scorch symptoms in Apulia (Southern Italy). Journal of Plant Pathology **95**.

3. **Hopkins D, Purcell A.** 2002. *Xylella fastidiosa*: cause of Pierce's disease of grapevine and other emergent diseases. Plant Disease **86:**1056-1066.

4. **Baker R, Bragard C, Caffier D, Candresse T, Gilioli G, Grégoire J-C, Holb I, Jeger MJ, Karadjova OE, Magnusson C.** 2015. Scientific Opinion on the risks to plant health posed by *Xylella fastidiosa* in the EU territory, with the identification and evaluation of risk reduction options. EFSA Journal **13:**3989.

5. **Hopkins D.** 1989. *Xylella fastidiosa*: xylem-limited bacterial pathogen of plants. Annual Review of Phytopathology **27:**271-290.

6. **Almeida RP, Nunney L.** 2015. How do plant diseases caused by *Xylella fastidiosa* emerge? Plant Disease.

7. **Chatterjee S, Almeida RPP, Lindow S.** 2008. Living in two Worlds: The Plant and Insect Lifestyles of *Xylella fastidiosa*. Annual Review of Phytopathology **46:**243-271.

8. **Raju B, Nome S, Docampo D, Goheen A, Nyland G.** 1980. Alternative hosts of Pierce's disease of grapevines that occur adjacent to grape growing areas in California. American Journal of Enology and Viticulture **31:**144-148.

9. **Hill B, Purcell A.** 1995. Multiplication and movement of *Xylella fastidiosa* within grapevine and four other plants. Phytopathology **85:**1368-1372.

10. **Purcell A, Saunders S.** 1999. Fate of Pierce's disease strains of *Xylella fastidiosa* in common riparian plants in California. Plant Disease **83:**825-830.

11. **Hill B, Purcell A.** 1997. Populations of *Xylella fastidiosa* in plants required for transmission by an efficient vector. Phytopathology **87:**1197-1201.

12. **Scally M, Schuenzel EL, Stouthamer R, Nunney L.** 2005. Multilocus sequence type system for the plant pathogen *Xylella fastidiosa* and relative contributions of

recombination and point mutation to clonal diversity. Applied and Environmental Microbiology **71:**8491-8499.

13. **Schuenzel EL, Scally M, Stouthamer R, Nunney L.** 2005. A multigene phylogenetic study of clonal diversity and divergence in North American strains of the plant pathogen *Xylella fastidiosa*. Applied and Environmental Microbiology **71:**3832-3839.

14. **Giampetruzzi A, Chiumenti M, Saponari M, Donvito G, Italiano A, Loconsole G, Boscia D, Cariddi C, Martelli GP, Saldarelli P.** 2015. Draft genome sequence of the *Xylella fastidiosa* CoDiRO strain. Genome Announcements **3:**e01538-01514.

15. **Bove JM, Ayres AJ.** 2007. Etiology of three recent diseases of citrus in Sao Paulo State: Sudden death, variegated chlorosis and huanglongbing. Iubmb Life **59:**346-354.

16. **Janse JD, Obradovic A.** 2010. *Xylella fastidiosa*: its biology, diagnosis, control and risks. Journal of Plant Pathology **92:**S1. 35-S31. 48.

17. **Alhaddad H, Coudron TA, Backus EA, Schreiber F.** 2011. Comparative behavioral and protein study of salivary secretions in *Homalodisca spp.* sharpshooters (Hemiptera: Cicadellidae: Cicadellinae). Annals of the Entomological Society of America **104:**543-552.

18. **Redak RA, Purcell AH, Lopes JRS, Blua MJ, Mizell Iii RF, Andersen PC.** 2004. The biology of xylem fluid-feeding insect vectors of *Xylella fastidiosa* and their relation to disease epidemiology. Annual Reviews in Entomology **49:**243-270.

19. **Sorensen J, Gill R.** 1996. A range extension of *Homalodisca coagulata* (Say)(Hemiptera: Clypeorrhyncha: Cicadellidae) to southern California. Pan-Pacific Entomologist **72:**160-161.

20. **Damsteegt VD, Brlansky RH, Phillips PA, Roy A.** 2006. Transmission of *Xylella fastidiosa*, causal agent of citrus variegated chlorosis, by the glassy-winged sharpshooter, *Homalodisca coagulata*. Plant Disease **90:**567-570.

21. **Killiny N, Almeida RPP.** 2014. Factors affecting the initial adhesion and retention of the plant pathogen *Xylella fastidiosa* in the foregut of an insect vector. Applied and Environmental Microbiology **80:**420-426.

22. **Purcell AH, Finlay AH.** 1979. Evidence for noncirculative transmission of Pierce's disease bacterium by sharpshooter leafhoppers. Phytopathology **69:**393-395.

23. **Killiny N, Almeida RPP.** 2009. *Xylella fastidiosa* Afimbrial Adhesins Mediate Cell Transmission to Plants by Leafhopper Vectors. Applied and Environmental Microbiology **75:**521-528.

24. **Almeida RPP, Purcell AH.** 2006. Patterns of *Xylella fastidiosa* colonization on the precibarium of sharpshooter vectors relative to transmission to plants. Annals of the Entomological Society of America **99:**884-890.

25. **Brlansky RH, Timmer LW, French WJ, McCoy RE.** 1983. Colonization of the sharpshooter vector, *Oncometopia nigricans* and *Homalodisca coagulata* by xylem-limited bacteria. Phytopathology **73:**530-535.

26. **Retchless AC, Labroussaa F, Shapiro L, Stenger DC, Lindow SE, Almeida RPP.** 2014. Genomic insights into *Xylella fastidiosa* interactions with plant and insect hosts, p 177-202, Genomics of Plant-Associated Bacteria. Springer.

27. **Feil H, Feil WS, Lindow SE.** 2007. Contribution of fimbrial and afimbrial adhesins of *Xylella fastidiosa* to attachment to surfaces and virulence to grape. Phytopathology **97:**318-324.

28. **Guilhabert MR, Kirkpatrick BC.** 2005. Identification of *Xylella fastidiosa* antivirulence genes: hemagglutinin adhesins contribute to *X. fastidiosa* biofilm maturation and colonization and attenuate virulence. Molecular Plant-Microbe Interactions **18:**856-868.

29. **Newman KL, Almeida RPP, Purcell AH, Lindow SE.** 2004. Cell-cell signaling controls *Xylella fastidiosa* interactions with both insects and plants. Proceedings of the National Academy of Sciences of the United States of America **101:**1737-1742.

30. **Almeida RPP, Killiny N, Newman KL, Chatterjee S, Ionescu M, Lindow SE.** 2012. Contribution of rpfB to cell-to-cell signal synthesis, virulence, and vector transmission of *Xylella fastidiosa*. Molecular Plant-Microbe Interactions **25:**453-462.

31. **Chatterjee S, Wistrom C, Lindow SE.** 2008. A cell–cell signaling sensor is required for virulence and insect transmission of *Xylella fastidiosa*. Proceedings of the National Academy of Sciences **105:**2670-2675.

32. **Rapicavoli JN, Kinsinger N, Perring TM, Backus EA, Shugart HJ, Walker S, Roper MC.** 2015. O Antigen Modulates Insect Vector Acquisition of the Bacterial Plant Pathogen *Xylella fastidiosa*. Applied and Environmental Microbiology **81:**8145-8154.

33. **Killiny N, Martinez RH, Dumenyo CK, Cooksey DA, Almeida RPP.** 2013. The Exopolysaccharide of *Xylella fastidiosa* Is Essential for Biofilm Formation, Plant Virulence, and Vector Transmission. Molecular Plant-Microbe Interactions **26:**1044-1053.

34. **Yadeta KA, Thomma BPHJ.** 2013. The xylem as battleground for plant hosts and vascular wilt pathogens. Frontiers in Plant Science **4**.

35. **Roper MC, Greve LC, Warren JG, Labavitch JM, Kirkpatrick BC.** 2007. *Xylella fastidiosa* requires polygalacturonase for colonization and pathogenicity in Vitis vinifera grapevines. Molecular Plant-Microbe Interactions **20:**411-419.

36. **Meng YZ, Li YX, Galvani CD, Hao GX, Turner JN, Burr TJ, Hoch HC.** 2005. Upstream migration of *Xylella fastidiosa* via pilus-driven twitching motility. Journal of Bacteriology **187:**5560-5567.

37. **Perez-Donoso AG, Sun Q, Roper MC, Greve LC, Kirkpatrick B, Labavitch JM.** 2010. Cell Wall-Degrading Enzymes Enlarge the Pore Size of Intervessel Pit Membranes in Healthy and *Xylella fastidiosa*-Infected Grapevines. Plant Physiology **152:**1748-1759.

38. **Hopkins DL.** 1981. Seasonal concentration of the Pierce's disease bacterium in grapevine stems, petioles, and leaf veins. Phytopathology **71:**415-418.

39. **Goodwin P, Zhang S.** 1997. Distribution of *Xylella fastidiosa* in southern Ontario as determined by the polymerase chain reaction. Canadian Journal of Plant Pathology **19:**13-18.

40. **Hoddle MS.** 2004. The potential adventive geographic range of glassy-winged sharpshooter, Homalodisca coagulata and the grape pathogen *Xylella fastidiosa*: implications for California and other grape growing regions of the world. Crop Protection **23:**691-699.

41. **Purcell A.** 1980. Environmental therapy for Pierce's disease of grapevines. Plant Disease **64:**388-390.

42. **Lieth J, Meyer M, Yeo K-H, Kirkpatrick B.** 2011. Modeling Cold Curing of Pierce's Disease in *Vitis vinifera* 'Pinot Noir' and 'Cabernet Sauvignon' Grapevines in California. Phytopathology **101:**1492-1500.

43. **Groves R, Chen J, Civerolo E, Freeman M, Viveros M.** 2005. Spatial analysis of almond leaf scorch disease in the San Joaquin Valley of California: factors affecting pathogen distribution and spread. Plant disease **89:**581-589.

44. **Turner WF, Pollard HN.** 1959. Insect transmission of phony peach disease, vol 1193. US Dept. of Agriculture.

45. **Alston JM, Fuller KB, Kaplan JD, Tumber KP.** 2015. Assessing the returns to R&D on perennial crops: the costs and benefits of Pierce's disease research in the California winegrape industry. Australian Journal of Agricultural and Resource Economics **59:**95-115.

46. **Beretta M, Barthe G, Ceccardi T, Lee R, Derrick K.** 1997. A survey for strains of *Xylella fastidiosa* in citrus affected by citrus variegated chlorosis and citrus blight in Brazil. Plant Disease **81:**1196-1198.

47. **De Lima J, Miranda V, Hartung J, Brlansky R, Coutinho A, Roberto S, Carlos E.** 1998. Coffee leaf scorch bacterium: axenic culture, pathogenicity, and comparison with *Xylella fastidiosa* of citrus. Plant Disease **82:**94-97.

48. **Su C-C, Chang C-M, Chang C-J, Su W-Y, Deng W-L, Shih H-T.** 2013. The occurrence of Pierce's disease of grapevines and its control strategies in Taiwan, p 145-162. *In* (ed)

49. **Su C, Deng W, Jan F, Chang C, Huang H, Chen J.** 2014. Characterization of *Xylella fastidiosa* pear leaf scorch strain in Taiwan through whole genome sequence analyses. In *American Phytopathological Society Abstracts* (Vol. 104, No. S3, p. 115).

50. **Loconsole G, Potere O, Boscia D, Altamura G, Djelouah K, Elbeaino T, Frasheri D, Lorusso D, Palmisano F, Pollastro P.** 2014. Detection of *Xylella fastidiosa* in olive trees by molecular and serological methods. Journal of Plant Pathology **96:**1-8.

51. **CDFA.** 2014. California agricultural production statistics https://www.cdfa.ca.gov/statistics/.

52. **Siebert J.** 2001. Economic impact of Pierce's disease on the California grape industry. In *California Department of Food and Agriculture Pierce's Disease Research Symposium* (p. 111-116).

53. **Alston J, Fuller K, Kaplan J, Tumber K.** 2013. The Costs and Benefits of Pierce's Disease Research in the California Winegrape Industry, p. *In* (ed), Agricultural and Applied Economics Association.

54. **Blua M, Phillips P, Redak R.** 1999. A new sharpshooter threatens both crops and ornamentals. California Agriculture **53:**22-25.

55. **Lytle J, Bernal J, Morse J.** 2012. Biology of *Pseudoligosita plebeia* (Hymenoptera: Trichogrammatidae), an egg parasitoid of *Homalodisca spp.* (Hemiptera: Cicadellidae) collected from northwestern Mexico as a potential biocontrol agent of *H. vitripennis* in California. Journal of Economic Entomology **105:**1532-1539.

56. **Gonçalves F, Stuchi E, Lourenço S, Hau B, Amorim L.** 2012. Relationship between sweet orange yield and intensity of Citrus Variegated Chlorosis. Plant Pathology **61:**641-647.

57. **Rodrigues CM, de Souza AA, Takita MA, Kishi LT, Machado MA.** 2013. RNA-Seq analysis of Citrus reticulata in the early stages of *Xylella fastidiosa* infection reveals auxin-related genes as a defense response. BMC genomics **14:**676.

58. **Gonçalves FP, Stuchi ES, Lourenço SA, Kriss AB, Gottwald TR, Amorim L.** 2014. The effect of irrigation on development of citrus variegated chlorosis symptoms. Crop Protection **57:**8-14.

59. **Gerlach RG, Hensel M.** 2007. Protein secretion systems and adhesins: The molecular armory of Gram-negative pathogens. International Journal of Medical Microbiology **297:**401-415.

60. **Feil H, Feil WS, Detter JC, Purcell AH, Lindow SE.** 2003. Site-directed disruption of the fimA and fimF fimbrial genes of *Xylella fastidiosa*. Phytopathology **93:**675-682.

61. **Guilhabert MR, Kirkpatrick BC.** 2005. Identification of *Xylella fastidiosa* antivirulence genes: Hemagglutinin adhesins contribute to *X. fastidiosa* biofilm maturation and colonization and attenuate virulence. Molecular Plant-Microbe Interactions **18:**856-868.

62. **Sun QA, Greve LC, Labavitch JM.** 2011. Polysaccharide Compositions of Intervessel Pit Membranes Contribute to Pierce's Disease Resistance of Grapevines. Plant Physiology **155:**1976-1987.

63. **Voegel TM, Warren JG, Matsumoto A, Igo MM, Kirkpatrick BC.** 2010. Localization and characterization of *Xylella fastidiosa* haemagglutinin adhesins. Microbiology-Sgm **156:**2172-2179.

64. **Grenier D, Mayrand D.** 1987. Functional-Characterization of Extracellular Vesicles Produced by Bacteroides-Gingivalis. Infection and Immunity **55:**111-117.

65. **Meng Y, Li Y, Galvani CD, Hao G, Turner JN, Burr TJ, Hoch H.** 2005. Upstream migration of *Xylella fastidiosa* via pilus-driven twitching motility. Journal of Bacteriology **187:**5560-5567.

66. **Li Y, Hao G, Galvani CD, Meng Y, Fuente LDL, Hoch HC, Burr TJ.** 2007. Type I and type IV pili of *Xylella fastidiosa* affect twitching motility, biofilm formation and cell–cell aggregation. Microbiology **153:**719-726.

67. **De La Fuente L, Burr TJ, Hoch HC.** 2008. Autoaggregation of *Xylella fastidiosa* cells is influenced by type I and type IV pili. Applied and Environmental Microbiology **74:**5579-5582.

68. **Pel MJC, Pieterse CMJ.** 2013. Microbial recognition and evasion of host immunity. Journal of Experimental Botany **64:**1237-1248.

69. **D'Haeze W, Holsters M.** 2004. Surface polysaccharides enable bacteria to evade plant immunity. Trends in Microbiology **12:**555-561.

70. **Rodrigues C, Takita M, Coletta-Filho H, Olivato J, Caserta R, Machado M, de Souza A.** 2008. Copper resistance of biofilm cells of the plant pathogen *Xylella fastidiosa*. Applied Microbiology and Biotechnology **77:**1145-1157.

71. **Lerouge I, Vanderleyden J.** 2002. O-antigen structural variation: mechanisms and possible roles in animal/plant–microbe interactions. FEMS Microbiology Reviews **26:**17-47.

72. **Raetz CRH, Whitfield C.** 2002. Lipopolysaccharide endotoxins. Annual Review of Biochemistry **71:**635.

73. **Clifford JC, Rapicavoli JN, Roper MC.** 2013. A Rhamnose-Rich O-Antigen Mediates Adhesion, Virulence, and Host Colonization for the Xylem-Limited Phytopathogen *Xylella fastidiosa*. Molecular Plant-Microbe Interactions **26:**676-685.

74. **da Silva FR, Vettore AL, Kemper EL, Leite A, Arruda P.** 2001. Fastidian gum: the *Xylella fastidiosa* exopolysaccharide possibly involved in bacterial pathogenicity. FEMS Microbiology Letters **203:**165-171.

75. **Roper MC, Greve LC, Labavitch JM, Kirkpatrick BC.** 2007. Detection and Visualization of an Exopolysaccharide Produced by *Xylella fastidiosa* In Vitro and In Planta. Applied and Environmental Microbiology **73:**7252-7258.

76. **Souza LC, Wulff NA, Gaurivaud P, Mariano AG, Virgílio AC, Azevedo JL, Monteiro PB.** 2006. Disruption of *Xylella fastidiosa* CVC gumB and gumF genes

affects biofilm formation without a detectable influence on exopolysaccharide production. FEMS Microbiology Letters **257:**236-242.

77. **Hill BL, Purcell AH.** 1997. Populations of *Xylella fastidiosa* in plants required for transmission by an efficient vector. Phytopathology **87:**1197-1201.

78. **Thorne ET, Young BM, Young GM, Stevenson JF, Labavitch JM, Matthews MA, Rost TL.** 2006. The structure of xylem vessels in grapevine (vitaceae) and a possible passive mechanism for the systemic spread of bacterial disease. American Journal of Botany **93:**497-504.

79. **Tyree MT, Zimmermann MH, Zimmermann MH.** 2002. Xylem structure and the ascent of sap, 2nd ed. Springer, Berlin ; New York.

80. **Buchanan BB, Gruissem W, Jones RL.** 2000. Biochemistry & molecular biology of plants. American Society of Plant Physiologists, Rockville, Md.

81. **Choat B, Jansen S, Zwieniecki MA, Smets E, Holbrook NM.** 2004. Changes in pit membrane porosity due to deflection and stretching: the role of vestured pits. Journal of Experimental Botany **55:**1569-1575.

82. **Stevenson JF, Matthews MA, Greve LC, Labavitch JM, Rost TL.** 2004. Grapevine susceptibility to Pierce's disease II: Progression of anatomical symptoms. American Journal of Enology and Viticulture **55:**238-245.

83. **Mollenhauer HH, Hopkins DL.** 1974. Ultrastructural Study of Pierces Disease Bacterium in Grape Xylem Tissue. Journal of Bacteriology **119:**612-618.

84. **Simpson AJG, Reinach FC, Arruda P, Abreu FA, Acencio M, Alvarenga R, Alves LMC, Araya JE, Baia GS, Baptista CS, Barros MH, Bonaccorsi ED, Bordin S, Bove JM, Briones MRS, Bueno MRP, Camargo AA, Camargo LEA, Carraro DM, Carrer H, Colauto NB, Colombo C, Costa FF, Costa MCR, Costa-Neto CM, Coutinho LL, Cristofani M, Dias-Neto E, Docena C, El-Dorry H, Facincani AP, Ferreira AJS, Ferreira VCA, Ferro JA, Fraga JS, Franca SC, Franco MC, Frohme M, Furlan LR, Garnier M, Goldman GH, Goldman MHS, Gomes SL, Gruber A, Ho PL, Hoheisel JD, Junqueira ML, Kemper EL, Kitajima JP, Krieger JE, et al.** 2000. The genome sequence of the plant pathogen *Xylella fastidiosa*. Nature **406:**151-157.

85. **Jayani RS, Saxena S, Gupta R.** 2005. Microbial pectinolytic enzymes: A review. Process Biochemistry **40:**2931-2944.

86. **Roper MC, Greve LC, Warren JG, Labavitch JM, Kirkpatrick BC.** 2007. *Xylella fastidiosa* requires polygalacturonase for colonization and pathogenicity in *Vitis vinifera* grapevines. Molecular Plant-Microbe Interactions **20:**411-419.

87. **Killiny N, Prado SS, Almeida RPP.** 2010. Chitin utilization by the insect-transmitted bacterium *Xylella fastidiosa*. Applied and Environmental Microbiology **76:**6134-6140.

88. **Dow JM, Daniels MJ.** 2000. *Xylella* genomics and bacterial pathogenicity to plants. Yeast **17:**263-271.

89. **Van Sluys MA, de Oliveira MC, Monteiro-Vitorello CB, Miyaki CY, Furlan LR, Camargo LEA, da Silva ACR, Moon DH, Takita MA, Lemos EGM, Machado MA, Ferro MIT, da Silva FR, Goldman MHS, Goldman GH, Lemos MVF, El-Dorry H, Tsai SM, Carrer H, Carraro DM, de Oliveira RC, Nunes LR, Siqueira WJ, Coutinho LL, Kimura ET, Ferro ES, Harakava R, Kuramae EE, Marino CL, Giglioti E, Abreu IL, Alves LMC, do Amaral AM, Baia GS, Blanco SR, Brito MS, Cannavan FS, Celestino AV, da Cunha AF, Fenille RC, Ferro JA, Formighieri EF, Kishi LT, Leoni SG, Oliveira AR, Rosa VE, Sassaki FT, Sena JAD, de Souza AA, Truffi D, et al.** 2003. Comparative analyses of the complete genome sequences of Pierce's disease and citrus variegated chlorosis strains of *Xylella fastidiosa*. Journal of Bacteriology **185:**1018-1026.

90. **Delepelaire P.** 2004. Type I secretion in gram-negative bacteria. Biochimica Et Biophysica Acta-Molecular Cell Research **1694:**149-161.

91. **Holland IB, Schmitt L, Young J.** 2005. Type 1 protein secretion in bacteria, the ABC-transporter dependent pathway (Review). Molecular Membrane Biology **22:**29-39.

92. **Reddy JD, Reddy SL, Hopkins DL, Gabriel DW.** 2007. ToIC is required for pathogenicity of *Xylella fastidiosa* in *Vitis vinifera* grapevines. Molecular Plant-Microbe Interactions **20:**403-410.

93. **Korotkov KV, Sandkvist M, Hol WGJ.** 2012. The type II secretion system: biogenesis, molecular architecture and mechanism. Nature Reviews Microbiology **10:**336-351.

94. **Jha G, Rajeshwari R, Sonti RV.** 2005. Bacterial type two secretion system secreted proteins: Double-edged swords for plant pathogens. Molecular Plant-Microbe Interactions **18:**891-898.

95. **Sandkvist M.** 2001. Biology of type II secretion. Molecular Microbiology **40:**271-283.

96. **Cianciotto NP.** 2005. Type II secretion: a protein secretion system for all seasons. Trends in Microbiology **13:**581-588.

97. **van Ulsen P, Rahman SU, Jong WSP, Daleke-Schermerhom MH, Luirink J.** 2014. Type V secretion: From biogenesis to biotechnology. Biochimica Et Biophysica Acta-Molecular Cell Research **1843:**1592-1611.

98. **Henderson IR, Navarro-Garcia F, Desvaux M, Fernandez RC, Ala'Aldeen D.** 2004. Type V protein secretion pathway: the autotransporter story. Microbiology and Molecular Biology Reviews **68:**692-+.

99. **Matsumoto A, Huston SL, Killiny N, Igo MM.** 2012. XatA, an AT-1 autotransporter important for the virulence of *Xylella fastidiosa* Temecula1. Microbiologyopen **1:**33-45.

100. **Pierce BK, Kirkpatrick BC.** 2015. The PhoP/Q two-component regulatory system is essential for *Xylella fastidiosa* survival in *Vitis vinifera* grapevines. Physiological and Molecular Plant Pathology **89:**55-61.

101. **Voegel TM, Doddapaneni H, Cheng DW, Lin H, Stenger DC, Kirkpatrick BC, Roper MC.** 2013. Identification of a response regulator involved in surface attachment, cell–cell aggregation, exopolysaccharide production and virulence in the plant pathogen *Xylella fastidiosa*. Molecular Plant Pathology **14:**256-264.

CHAPTER I. O antigen modulates insect vector acquisition of the bacterial plant pathogen *Xylella fastidiosa*

Reprinted with permission from:
Rapicavoli, J. N., Kinsinger, N., Perring, T. M., Backus, E. A., Shugart, H. J., Walker, S., & Roper, M. C. (2015). *Applied and Environmental Microbiology*, *81*(23), 8145-8154.

ABSTRACT

Hemipteran insect vectors transmit the majority of plant pathogens. Acquisition of pathogenic bacteria by these piercing/sucking insects requires intimate associations between the bacterial cells and insect surfaces. Lipopolysaccharide (LPS) is the predominant macromolecule displayed on the cell surface of Gram-negative bacteria and thus mediates bacterial interactions with the environment and potential hosts. We hypothesized that bacterial cell surface properties mediated by LPS would be important in modulating vector-pathogen interactions required for acquisition of the bacterial plant pathogen *Xylella fastidiosa,* the causative agent of Pierce's disease of grapevine. Utilizing a mutant that produces truncated O antigen (the terminal portion of the LPS molecule), we present results that link this LPS structural alteration to a significant decrease in the attachment of *X. fastidiosa* to blue-green sharpshooter foreguts. Scanning electron microscopy confirmed that this defect in initial attachment compromised subsequent biofilm formation within vector foreguts, thus impairing pathogen acquisition. We also establish a relationship between O antigen truncation and significant changes in the physiochemical properties of the cell, which in turn affect the dynamics of *X. fastidiosa* adhesion to the vector foregut. Lastly, we couple measurements of the physiochemical properties of the cell with hydrodynamic fluid shear rates to produce a

Comsol model that predicts primary areas of bacterial colonization within blue-green sharpshooter foreguts, and we present experimental data that support the model. These results demonstrate that, in addition to reported protein adhesin-ligand interactions, O antigen is crucial for vector-pathogen interactions, specifically in the acquisition of this destructive agricultural pathogen.

INTRODUCTION

Insect vectors transmit numerous pathogens to a wide range of animal and plant hosts. Hemipteran vectors, such as aphids, leafhoppers, and whiteflies, are an economically important group of insects because they are the dominant vectors of plant pathogens (1). The molecular determinants of transmission have been explored for only a few phytopathosystems (compared to mammalian systems), with virus-vector interactions being the most extensively studied. Surface entities, such as virion capsid components, have been shown to be important for the retention and transmission of plant viruses (2), indicating the importance of pathogen surface properties in mediating these interactions. However, we have much less information regarding the molecular mechanisms of insect transmission of bacterial pathogens, specifically those infecting plants.

Xylella fastidiosa is a Gram-negative bacterium that causes diseases in several economically important crops, including Pierce's disease (PD) of grapevine, citrus variegated chlorosis, and almond leaf scorch. *X. fastidiosa* forms biofilms within the xylem vessels of plant hosts, which occludes vessels and impedes water flow within the vine (3). Symptoms of PD include marginal leaf necrosis, premature leaf abscission, fruit

desiccation, and ultimately plant death (3). *X. fastidiosa* is obligately transmitted by xylem-feeding insects primarily belonging to the hemipteran family Cicadellidae, subfamily Cicadellinae, termed sharpshooters (3). The association of *X. fastidiosa* with its insect vectors is unique, in that it is the only known insect-transmitted plant pathogen that is persistent but non-circulative (4). *X. fastidiosa* is semi-persistent in nymphs (i.e. the bacterium is lost after each vector molt) but persistent in adult vectors (which do not molt) (3, 4). Because *X. fastidiosa* is also propagative within vectors, the insects are able to inoculate the pathogen for months after acquisition from an infected plant (3). Transmission of *X. fastidiosa* consists of three main steps, namely, pathogen acquisition from an infected host plant, multiplication and retention of the pathogen within the vector, and inoculation of the pathogen into a susceptible plant host (5). Upon acquisition, *X. fastidiosa* colonizes the vector foregut by attaching to and forming robust biofilms within the cibarial and precibarial regions of the foregut (5, 6). Cells initially attach laterally and begin to colonize the foregut cuticle seemingly following the developmental steps of canonical biofilm formation, although the kinetics of biofilm development within vector foreguts are not well understood (6). Interestingly, in the later stages of biofilm formation, the cells become polarly attached to the foregut cuticle, presumably to allow for maximal surface area exposure to the nutrient-dilute xylem sap that is ingested by the insect (3). Several bacterial components, such as type I pili, hemagglutinin adhesins, and fimbriae, contribute (in various capacities) to different stages of *X. fastidiosa* colonization in sharpshooter vectors (3, 6). Killiny and Almeida examined the contribution of hemagglutinin adhesins HxfA and HxfB to the transmission

process and found that the adhesins were impaired in attachment to nitrocellulose coated with blue-green sharpshooter (BGSS) foregut extracts and transmission rates were low. Interestingly, *hxfA* and *hxfB* mutants multiplied to similar levels, compared with wild type, in vector foreguts. (6). In addition, overall transmission rates for a *fimA* knockout mutant (lacking the type I pilus) were lower than wild type rates (5). Exopolysaccharide (EPS) has also been implicated in the insect transmission of *X. fastidiosa* by the BGSS *Graphocephala atropunctata* (Signoret) (7). EPS^{-} mutants were transmitted at significantly lower rates than wild type *X. fastidiosa* but were not impaired in attachment to nitrocellulose coated with BGSS foregut extracts. This suggests that lack of EPS does not impair initial attachment to the insect foregut cuticle but may impair subsequent steps in the insect colonization process (6, 7). Interestingly, mutations in any of these fimbrial/afimbrial adhesins or changes in EPS production never fully compromised the transmissibility of the pathogen, indicating that vector transmission is a complex process that relies on many factors involved in the acquisition, retention, or inoculation of the pathogen. To date, little attention has been given to the predominant bacterial cell surface polysaccharide, i.e. lipopolysaccharide (LPS), and its role in this complex biological process, for any bacterial pathogen-vector relationship.

LPS is a tripartite macromolecule located in the outer membranes of all Gram-negative bacteria (8, 9). There are approximately 3.5 million LPS molecules on the bacterial outer membrane (10), occupying more than 75% of the bacterial cell surface (9, 11). LPS is comprised of three parts, i.e. lipid A, which anchors the molecule to the outer membrane, core oligosaccharide, and a terminal O antigen consisting of polysaccharide

chains (9, 12). While the lipid A and core portions of the molecule are highly conserved, the O antigen can vary greatly in composition and structure, even within strains of the same bacterial species (11, 13, 14). The O antigen is assembled in the cytoplasm and delivered independently to the periplasm, where it is ligated onto the lipid A-core complex and then translocated to the outer membrane (13). This process is mediated in part by the Wzy polymerase, which catalyzes polymerization of the individual O units that make up the O antigen chain (13). Our research group demonstrated previously that the O antigen of wild type *X. fastidiosa* is a high-molecular-weight polymer consisting of rhamnose-rich O units. In addition, targeted mutation of the Wzy polymerase resulted in a truncated O antigen that was primarily depleted of rhamnose. The *wzy* mutant strain was significantly impaired in production of the O antigen component of LPS, compared with wild type, which was clearly visible when purified LPS was analyzed on a discontinuous 12% Tricine-polyacrylamide electrophoretic gel (O antigen production was restored in the complemented *wzy/wzy+* strain) (15).

The location of the O antigen on the cell surface places it at the interface of the bacterium and its environment (13). Furthermore, the O antigen can extend as far as 30 nm into the surrounding milieu and exhibits some flexibility (12). Because of its prominence and extension into the environment, LPS (more specifically, the O antigen) has been implicated in various stages of microbial pathogenesis in both mammalian and plant systems (11, 14, 15). It can also play a protective role by acting as a barrier against antimicrobial substances and shielding the pathogen from host recognition (16, 17).

Furthermore, it acts as a key contributor to bacterial adhesion to host cells (i.e. plant and mammalian cells) or surfaces (10).

In general, bacterial cell surfaces are negatively charged; the magnitude of the charge depends on structures on the cell surface, including LPS (10, 18). In this study, we demonstrate that truncation of the *X. fastidiosa* O antigen causes the cell surface to become significantly more negatively charged than the wild type when cells were grown in defined *X. fastidiosa* medium (XFM) with 0.01% pectin. This change in charge was also observed in a previous study in which the cells were grown in rich PD3 medium (14, 15). In terms of relating O antigen structure and cell surface charge to function, truncation of the O antigen caused by a mutation in *wzy* led to a phenotype of hyperattachment to a glass surface *in vitro*. However, the *wzy* mutant was significantly compromised in the cell-cell aggregation phase of biofilm formation, which resulted in marked changes in the topography and roughness of the mature biofilm *in vitro*. The *wzy* mutant formed a thinner and rougher biofilm than did the wild type parent, indicating that it could initiate surface attachment but could not build on itself to form a mature biofilm. Consequently, the *wzy* mutant was severely defective in virulence in a susceptible grapevine host (15).

In this study, we demonstrate that the *wzy* mutant is significantly defective in attachment to the insect foregut cuticle, which is essentially the opposite of the hyper-attaching phenotype observed *in planta* and *in vitro*. This provides further evidence that the dynamics of biofilm formation are markedly different in the insect environment than in the plant environment, and we establish that the O antigen chain of LPS is a critical

modulator of *X. fastidiosa* attachment to the cuticular surface of the BGSS foregut. Furthermore, this defect in attachment halts biofilm formation in the foregut, thus compromising the overall acquisition and retention of *X. fastidiosa* by the BGSS. This highlights LPS as an important mediator of vector acquisition and as a potential target for disruption of *X. fastidiosa* transmission as a means of disease control.

RESULTS

O antigen chain length modulates vector acquisition of *X. fastidiosa*. After insects were fed on artificial diet sachets containing wild type bacteria, BGSS foreguts contained large flocculent microcolonies of bacteria. In *wzy* mutant-fed insects, however, bacterial aggregates were strikingly absent. A few sparse cells were observed throughout the foregut of *wzy* mutant-fed insects, but overall these insects showed almost no visible bacterial colonization in the cibarial and precibarial regions of the foregut and were nearly identical to insects that were exposed to the artificial diet solution control (Fig. 1.1 and 1.2).

Quantitatively, sharpshooters that were fed suspensions of the *wzy* mutant harbored significantly fewer ($F_{2, 39} = 18.29$, $P < 0.01$) cells than those that were fed wild type bacteria (Fig. 1.3). Numbers of bacterial cells were significantly different between insects fed wild type *X. fastidiosa* and those exposed to the *wzy* mutant or the artificial diet solution control; the latter two groups were not significantly different. We found that previously designed quantitative PCR (qPCR) primer sets were not able to detect the low *X. fastidiosa* titers within the insects at such an early time point after acquisition. This, in combination with the inhibitory effects of chitin, made initial attempts at *X. fastidiosa*

quantification unsuccessful. Therefore, we developed a new TaqMan-based protocol for this study that eliminated laborious removal of inhibitors from insect tissues; instead, we constructed our standard curve using a mixture of BGSS genomic DNA and *X. fastidiosa* genomic DNA to account for inhibitors inherent to the insect samples (see Fig. S1.1 in the supplemental material).

***In vivo* impaired attachment phenotype is mimicked *ex vivo* on BGSS hindwings.** The sharpshooter foregut is an internal structure, making it difficult to perform quantitative measurements on the physiochemical properties of the foregut cuticle. Several studies from other laboratories have deemed sharpshooter hindwings a suitable proxy for both qualitative and quantitative measures of *X. fastidiosa* interactions with the sharpshooter foregut (6, 19). Using BGSS hindwings, we quantified attachment of *X. fastidiosa* cell suspensions to wings by using qPCR. Both wild type and *wzy* mutant *X. fastidiosa* cells attached to the hindwings, but the *wzy* mutant was critically impaired in attachment. Significantly fewer (i.e., 10 times fewer) cells of the *wzy* mutant attached, compared with wild type cells; this phenotype was restored in the complemented *wzy/wzy+* strain ($F_{11,24} = 13.25$, $P < 0.0001$) (Fig. 1.4). Thus, the significant impairment that we observed both quantitatively and qualitatively *in vivo* was replicated *ex vivo* with BGSS hindwings, supporting the value of hindwings as a suitable proxy for the foregut cuticular surface (6,19).

Figure 1.1. Truncation of the O antigen compromises colonization of the cibarium

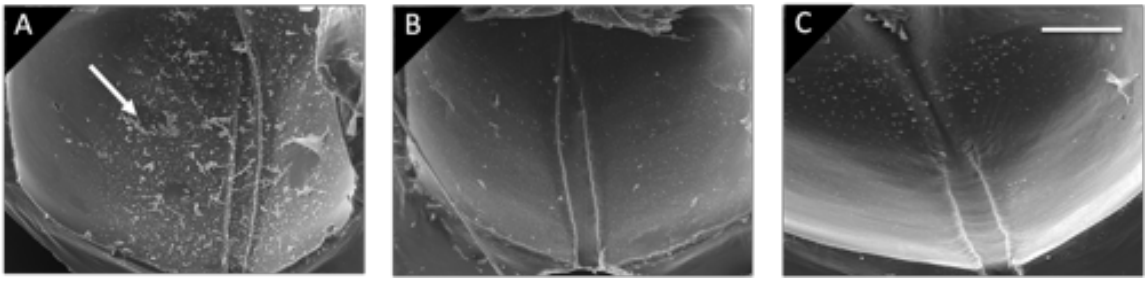

The *wzy* mutant had notably reduced ability to attach to the cibarium. Scanning electron micrographs of the hypopharyngeal surface of the cibarium of BGSS fed on artificial diets containing wild type *X. fastidiosa* (**A**)*, wzy* mutant (**B**), or artificial diet only (**C**) for 6 h are represented. Images are oriented so that the stylet food canal is at the bottom and the pharynx at the top; thus ingested fluid would flow inward from bottom to top. Images are representative of 30 total replicates per treatment. Arrow, bacterial aggregates. Diet-fed insects represent negative controls. Bar, 20 μm.

Figure 1.2. Truncation of the O antigen compromises colonization of the precibarium.

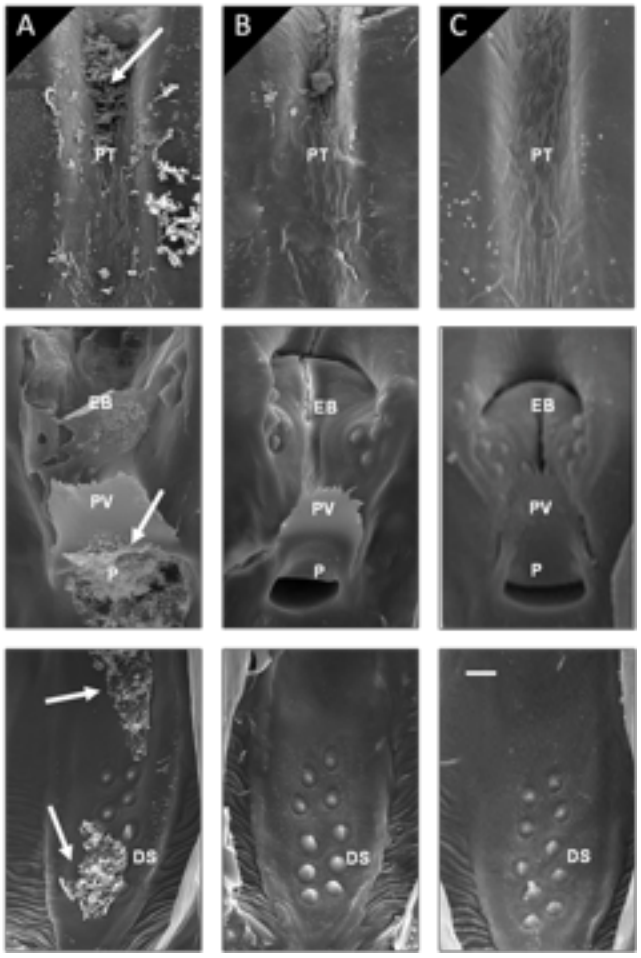

The *wzy* mutant had notably reduced ability to attach to all structures within the precibarium, including the distal sensilla, pit, precibarial valve, epipharyngeal basin, and precibarial trough. Scanning electron micrographs of the epipharyngeal surface of the precibarium of BGSS fed on artificial diets containing wild type *X. fastidiosa* (**A**)*, wzy* mutant (**B**), or artificial diet only (**C**) for 6 h are represented. The stylet food canal is oriented toward the bottom and the pharynx at the top; thus, ingested fluid would flow inward from bottom to top. Images are representative of 30 total replicates per treatment. Arrows, bacterial aggregates. Diet-fed insects represent negative controls. DS, distal sensilla; P, pit; PV, precibarial valve; EB, epipharyngeal basin; PT, precibarial trough. Bar, 5 μm.

Figure 1.3. O antigen chain length modulates acquisition by BGSS

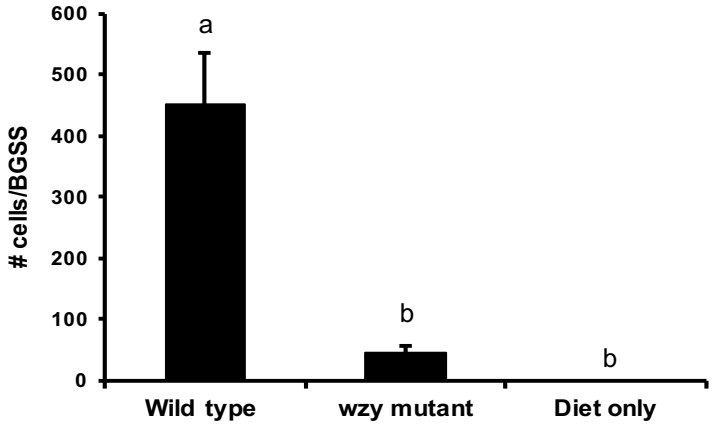

Sharpshooters that were fed on suspensions of the *wzy* mutant had significantly fewer cells adhering to the cuticle than did those that were fed on wild type bacteria. Inclusion of the BGSS DNA in the standards reduced standard amplification so that the sample amplification curves fell within the range of the standards. No *X. fastidiosa* cells were detected in insects fed solely on diet solution. Graph represents the means of 40, 36, and 33 insects for wild type, *wzy* mutant, and artificial diet treatments, respectively. Treatments with different letters over the bars were statistically different ($P < 0.01$).

Figure 1.4. The O antigen mutant is compromised in attachment to BGSS hindwings

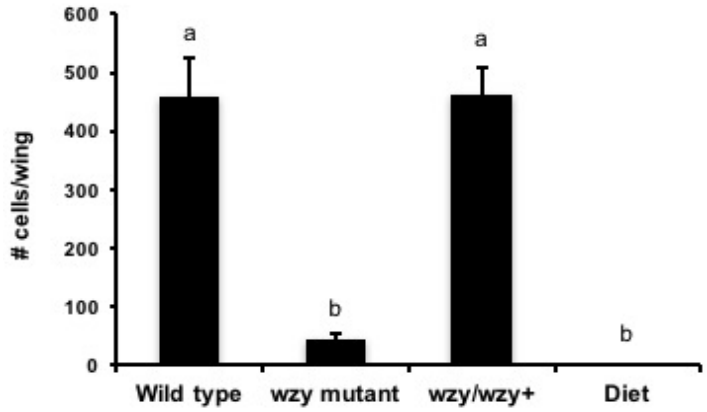

The *wzy* mutant cells attached 10-fold less to BGSS hindwings than did wild type cells. Wild type cells, *wzy* mutant cells, cells of the *wzy* complemented strain, or a negative control (insect diet solution) were incubated on individual hindwings for 6 h at 28°C. Attached bacterial cells were enumerated using qPCR. The graph represents the mean ± standard error of the mean of nine samples per treatment. Treatments with different letters over the bars were statistically different ($P < 0.0001$).

O antigen truncation alters the bacterial cell surface charge. The zeta potential, a measure of cell surface charge, indicated that the *wzy* mutant surface was significantly more negatively charged (-28.6 ± 1.6 mV) than the wild type surface (-20.6 ± 2.2 mV) ($P < 0.05$), when propagated in XFM with 0.01% pectin (Table 1.1), which follows the same trend observed in other growth media (15). The complemented *wzy/wzy+* strain had a surface charge (-22.9 ± 1.5 mV) similar to that of wild type *X. fastidiosa* (statistically insignificant, $P > 0.05$). Using classic Derjaguin – Landau – Verwey – Overbeek (DLVO) theory, which describes the force between charged surfaces interacting through a liquid medium, we estimated the attractive and repulsive forces between *X. fastidiosa* and the insect cuticle surface. For use in the construction of DLVO profiles, static contact angle (SCA) measurements of immobilized BGSS hindwings were obtained. The SCA of the hindwings was 134 ± 7°. Compared to SCA measurements of other hydrophobic surfaces, such as Teflon (SCA of 110°) (20), this indicated that the hindwing surface is extremely hydrophobic. We made several attempts to calculate the hydrophobicity of the *X. fastidiosa* cells, but their extremely aggregative nature made these experiments difficult to perform. Streaming potential measurements indicated that BGSS hindwings are also negatively charged (-27.4 ± 1.7 mV at pH 7.0) (Table 1.1). The energy barrier (repulsive force) experienced by *wzy* mutant cells (190.8 kT) was nearly double the barrier experienced by wild type cells (94.4 kT) (Fig. 1.5A). Secondary minimum depths (representing a dip in repulsive force) (Fig. 1.5B, arrow) and separation distances between BGSS hindwings and the different *X. fastidiosa* strains were calculated (Fig. 1.5C). The secondary energy minimum for wild type cells (-5.34 kT) was nearly a full 1

Table 1.1. Surface charge of *X. fastidiosa* strains and BGSS hindwings, as determined by zeta potential

Sample type	Zeta potential (mV)[a]
Wild type *X. fastidiosa*	-20.6 ± 2.20 A[b]
wzy mutant *X. fastidiosa*	-28.6 ± 1.64 B
wzy/wzy+ X. fastidiosa	-22.9 ± 1.50 A
BGSS hindwings	-27.4 ± 1.67

[a]Mobility values were determined by electrophoresis and converted to zeta potentials. All measurements were taken at pH 7. For bacterial strains, values represent the mean ± standard error of the mean for 15 samples per treatment. For BGSS hindwings, values represent the mean ± standard error of the mean for four biological replicates.

[b]Values followed by different letters are statistically different ($P < 0.01$).

Figure 1.5. DLVO profiles of wild type and *wzy* mutant *X. fastidiosa* strains

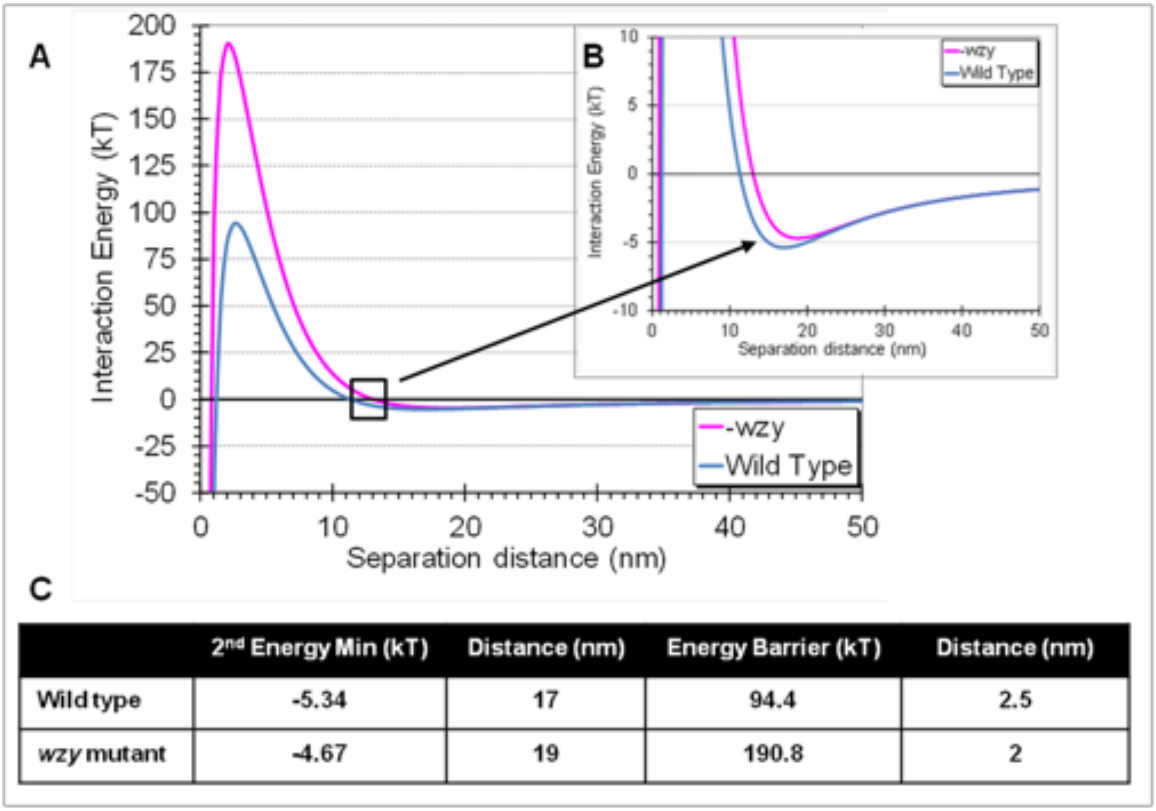

	2nd Energy Min (kT)	Distance (nm)	Energy Barrier (kT)	Distance (nm)
Wild type	-5.34	17	94.4	2.5
wzy mutant	-4.67	19	190.8	2

(**A and B**) Profiles display primary maximum curves (repulsive force) and secondary minimum curves (dip in the repulsive force) (boxed area in **A** and enlarged in **B**, indicated by the arrow) for wild type and *wzy* mutant cells. The energy barrier experienced by *wzy* mutant cells (190.8 kT) was nearly double the barrier experienced by wild type cells (94.4 kT). (**C**) Calculated secondary minimum depths and separation distances between BGSS hindwings and the different *X. fastidiosa* strains. The secondary energy minimum for wild type cells (-5.34 kT) was nearly a full 1 kT deeper than that for *wzy* mutant cells (-4.67 kT), indicating a stronger dip in repulsive force.

kT deeper than for *wzy* mutant cells (-4.67 kT) (Fig. 1.5C), indicating that the wild type cells have a higher propensity to stably attach to the vector foregut cuticular surface than do *wzy* mutant cells.

Comsol model of velocity magnitude in BGSS foreguts. During ingestion of xylem sap, the cibarial diaphragm (located at the posterior end of the foregut) exhibits a rhythmic motion, powering the piston-like cibarial pump. For convenience, we show the diaphragm in a semicontracted position within the cibarium (Fig. 1.6). Figure 6 represents a two-dimensional simulation of the fluid flow within the foregut. The bulk fluid flow of xylem sap through the precibarium is reported to exceed 100 to 500 mm/s during active ingestion, depending on the sharpshooter species (21-23). Here we show that the maximal velocity (V_{max}) within the precibarium of BGSS exceeds 70 mm/s, exhibiting significant shear force that reduces the probability of bacterial attachment. Due to the significant expansion within the cibarium, the V_{max} rapidly drops to nearly 5 mm/s. At 15 μm proximal to the opening of the cibarium, the shear rate decreases approximately 1,000-fold from that within the precibarium, indicating that the cibarium has areas of stagnation (Fig. 1.6, blue areas) that would favor initial bacterial attachment.

Areas of *X. fastidiosa* localization within the cibarium support predicted colonization sites determined by the Comsol model. Scanning electron micrographs of BGSS foreguts following artificial feeding of wild type *X. fastidiosa* and a 6-day clearing and multiplication period revealed the presence of robust *X. fastidiosa* biofilms localized

along the outer regions of the cibarium, which supports our Comsol model indicating that bacterial cells could more easily attach to the outer areas of the cibarium, compared to other regions of the foregut (Fig. 1.7).

Figure 1.6. Comsol model representing the hydrodynamics of xylem sap flow during ingestion

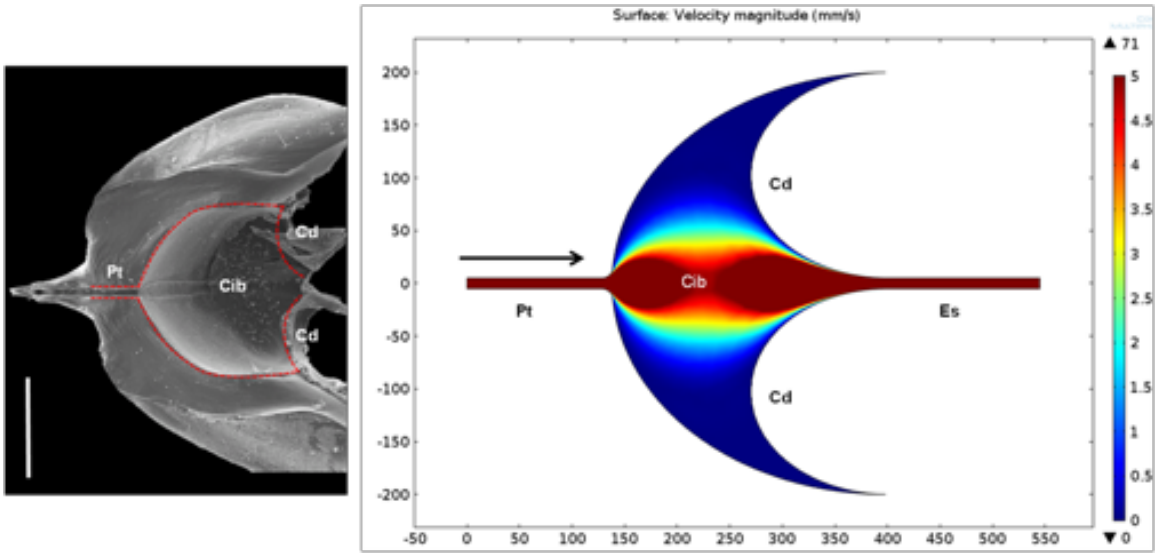

The precibarial trough and the central regions of the cibarium experience the greatest sheer hydrodynamic forces, as indicated by the gradient. Dark red areas, flow rates greater than 50 mm/s. Blue areas, areas of stagnation, occurring primarily in the outer regions of the cibarium. Arrow, direction of fluid flow. The figure represents a longitudinal section of the pharynges and is oriented so that the stylet food canal would be to the left and the esophagus to the right. The cibarial diaphragm is shown in a semicontracted position. The model focused specifically on the areas proximal to the epipharyngeal basin, as indicated by the dotted red outline in the left panel. Pt, precibarial trough; Cib, cibarium; Cd, cibarial diaphragm; Es, esophagus. Bar, 200 µm. The x and y-axes are in micrometers.

Figure 1.7. Localization of *X. fastidiosa* in the cibarium supports the Comsol model of predicted areas of colonization

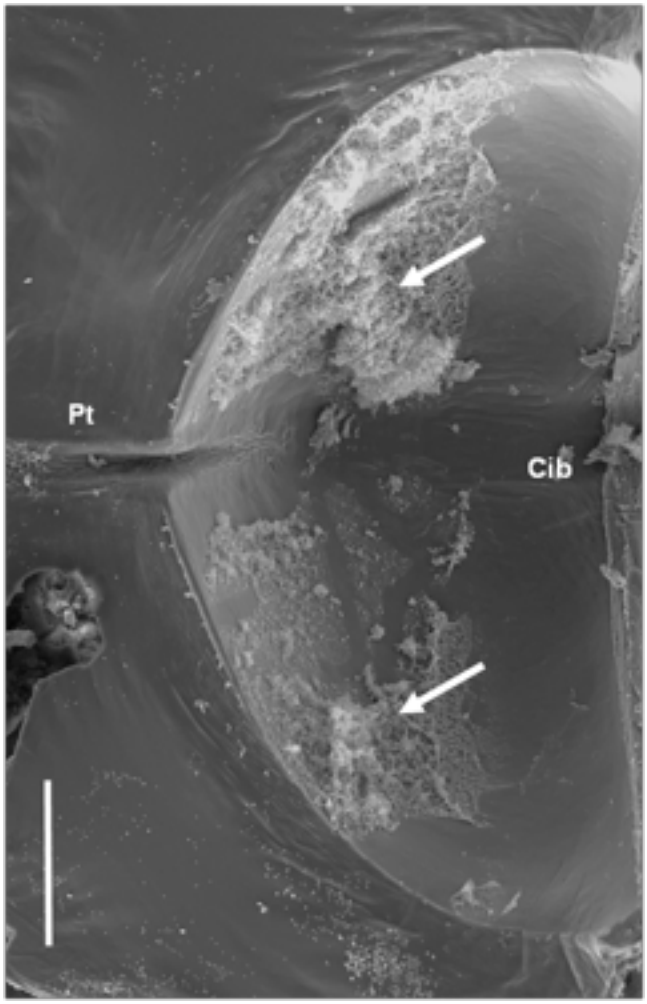

As indicated in the Comsol model, scanning electron micrographs confirm that the ultimate site of *X. fastidiosa* retention is in the cibarium, specifically in the outer regions where stagnation occurs. The figure represents a longitudinal section of the pharynges and is oriented so that the stylet food canal would be to the left and the esophagus to the right. The image is a representative of 15 total replicates. Arrows, wild type *X. fastidiosa* biofilm. Pt, precibarial trough; Cib, cibarium. Bar, 200μm.

DISCUSSION

Acquisition of bacteria by insect vectors depends heavily on the properties of the bacterial cell surface, because it is the first surface to interact with the surrounding environment and thus plays an important role in cell-cell and host-microbe interactions (10, 12). Bacteria have evolved surface-associated polysaccharides, namely LPS and EPS, that aid in attachment, protection, and survival under pressures exerted by specific host environments. In insect and plant hosts, *X. fastidiosa* seemingly follows the canonical steps involved in biofilm formation, i.e. initial attachment to the surface followed by aggregation/microcolony formation, macrocolony formation, and biofilm maturation. For *X. fastidiosa,* immunologically-based microscopy studies indicated that very sparse amounts of EPS are associated with the cells during the initial attachment phase, with the bulk of the EPS being produced during the late phase of biofilm maturation; substantial amounts can be seen intercalating the biofilm matrix of a mature biofilm (24). This effectively places LPS as the most prominently exposed polysaccharide during the early phases of biofilm formation (15). Therefore, LPS (more specifically, O antigen), likely functions as the first point of contact in attachment to a surface, effectively acting as a primary liaison between *X. fastidiosa* and its hosts. Thus, the structure of the O antigen can exert a powerful influence on the critical early stages of attachment. It is known that O antigen plays a role in plant and animal host colonization in bacterial pathosystems (15, 25-28). However, the role of O antigen in insect vector-pathogen interactions has been largely unexplored. In this study, we link O antigen

structure to function in the context of attachment to the foregut cuticle and insect acquisition in the *X. fastidiosa* pathosystem.

Our study focused on the role of the O antigen in the initial attachment steps of biofilm formation, which is crucial to the acquisition of *X. fastidiosa* by BGSSs. *In vivo*, wild type *X. fastidiosa* adhered to the foregut in titers of approximately 450 cells/BGSS, following a 6-h AAP on an artificial diet sachet and a 48-h multiplication and clearing period on basil plants (a non-*X. fastidiosa* host). In contrast, the *wzy* mutant was compromised in initial adherence to the insect foregut and was present with titers of approximately 45 cells/BGSS. Electron micrographs of the foreguts of BGSS fed on the artificial diet sachets indicated that the *wzy* mutant sparsely colonized both the cibarial and precibarial areas of the foregut, whereas, the wild type had thoroughly colonized both of these areas. Thus, based on both quantitative and qualitative data, we demonstrated that truncation of the O antigen results in poor adherence of the bacterium to insect foreguts during the early stages of the acquisition process. This defective attachment phenotype was also replicated on BGSS hindwings, which is an established tool used to mimic the *X. fastidiosa* binding sites within the insect foregut. Our findings corroborate data from other laboratories that have deemed sharpshooter hindwings a suitable proxy for both qualitative and quantitative measures of *X. fastidiosa* interactions with the sharpshooter foregut (6, 19, 29). In addition, Killiny and Almeida confirmed the specificity of the *X. fastidiosa*-sharpshooter hindwing interaction, because only *X. fastidiosa* was capable of binding to the hindwings and other Gram-negative bacterial

plant pathogens, such as *Pseudomonas syringae* pv. syringae, *Erwinia herbicola*, and *Xanthomonas campestris* pv. campestris did not attach to the hindwings (6).

Little is known about the influence of electrostatic interactions on bacterial attachment to vector surfaces. This prompted us to characterize both the *X. fastidiosa* cell surface and the insect cuticular surface. For *in vitro* attachment and electrokinetic studies, we used BGSS hindwings as a proxy system to determine how the wild type and the *wzy* mutant interact with the foregut cuticle. From those measurements, we extrapolated the electrostatic repulsive and attractive forces between those two entities using DLVO theory. By performing zeta potential and static contact angle measurements, we found that BGSS hindwings have an overall negative charge and are extremely hydrophobic (even more hydrophobic than Teflon). *X. fastidiosa* is negatively charged, as are most pathogenic bacteria (15). Interestingly, truncation of the *X. fastidiosa* O antigen significantly affected the zeta potential of the bacterial cell surface, in the XFM-pectin growth medium and caused the *wzy* mutant to become significantly more negatively charged than the wild type parent. In relation to the zeta potential of the hindwings (-27.4 mV), there is a stronger electrostatic repulsion between the *wzy* mutant (-28.6 mV) and the insect cuticle surface (due to the similarity in charge) than between wild type *X. fastidiosa* (-20.6 mV) and the insect cuticle. Therefore, on the basis of attractive electrostatic interactions, the wild type cells (containing a fully polymerized O antigen) have a greater propensity to attach to the cuticle.

Bacterial attachment to surfaces can be further modeled using classic DLVO theory, which serves to model particle (bacterial cell) stability (30). It describes the forces

between charged surfaces as they interact in a liquid environment (31). Specifically, the overall long-range interaction between two surfaces is composed of two additive forces, namely, electrostatic interactions and van der Waals attraction (31). The Hamaker constant was developed, as discussed previously, to account for the specific bacterium-water-insect cuticle interactions for our environmental conditions and interacting constituents. Hamaker constant calculations define the strength of the attractive van der Waals forces between a particle and a specific surface, and specific constants can be calculated based on the individual constituents of an interaction (32). Using these variables, the resulting DLVO profiles (presenting the magnitude of interaction energy [kT] between the surfaces, versus separation distance [nm]) for wild type and *wzy* mutant *X. fastidiosa* strains revealed the existence of a substantial energy barrier between the *wzy* mutant and the insect cuticle (190.8 kT), which was approximately double the energy barrier experienced between wild type *X. fastidiosa* and the insect cuticle (94.4 kT) (as indicated by the primary maxima curves in Figure 5A). This demonstrates that truncation of the O antigen notably increases the repulsion between the cell and the insect cuticular surface, indicating that *wzy* mutant cells would a greater challenge in overcoming this energy barrier to allow the attractive van der Waals forces to dominate for attachment to the foregut cuticle. Consequently, less force is also required to remove or dislodge these cells, compared with wild type, which supports our findings that *wzy* mutant cells have difficulty binding to the insect cuticle, both quantitatively and qualitatively.

Overall, the large energy barriers for both the wild type and *wzy* mutant strains suggest that bacterial attachment is unlikely in the primary maxima. Specifically, the

maximal height of the primary maximum curves indicates that *X. fastidiosa* cells, in general, have a considerable energy barrier to overcome to connect to and attach to the insect cuticular surface, yet they can still do this effectively. A closer inspection of the DLVO profiles indicated the presence of a substantial secondary energy minimum curve (Fig. 5B), representing a reversible dip in the repulsive force, for the wild type cells that was nearly a full 1 kT deeper than that for the *wzy* mutant cells (Fig. 5C). Bacterial cells can associate with and adhere to a surface while experiencing the relatively low-level interaction force within the secondary energy minimum (10). This dip in the overall repulsive force, although representing a weak interaction, likely allows the long-chain O antigen of wild type cells to approach and to interact with the insect surface and act as a tether, thereby facilitating stable deposition of the *X. fastidiosa* cell onto the cuticle. The strength of the interaction in this secondary energy minimum may be weak, but it is sufficiently stable to allow for initial attachment via the O antigen and subsequently for other proteinaceous bacterial adhesins and EPS to reinforce attachment to the foregut surface as the biofilm develops (10).

In order to understand more comprehensively the O antigen-modulated process of vector acquisition of *X. fastidiosa*, we combined information gleaned from the quantification of electrostatic interactions (and particle stability) with fluid flow throughout the BGSS foregut, using a Comsol model. Using this model, we estimated that the wall shear rate within the precibarium, or the rate at which progressive shearing deformation is applied to the fluid (measured in reciprocal seconds), can exceed 25,000 s^{-1} during active ingestion, with the maximum velocity exceeding 70 mm/s at a cross-flow

velocity of 5 mm/s. Because the velocity increases rapidly, the shear rate is high. Interestingly, the model predicted prominent areas of stagnation within the outer regions of the cibarium (Fig. 6, indicated in blue). During ingestion, the strong shear hydrodynamic forces occurring in the precibarium significantly reduce the initial probability that the cells will attach to the precibarium before they are washed away, during either swallowing (fluid flow through the precibarium and past the cibarium into the pharynx) or egestion (expulsion of fluid back out the stylets). Thus, in accordance with our model, the cibarium would be an easier site in which to attach initially (via the O antigen tether) and to remain attached within the foregut, in contrast with the precibarium, which is extremely turbulent.

We speculate that *X. fastidiosa* initially attaches to the cibarium, and as the bacteria multiply and migrate across the cibarial surface to form microcolonies and mature biofilms, the bacteria push into the precibarium, from which they can then become dislodged and inoculated into plants. The mechanism of migration from the cibarium to the precibarium is unknown but could be partially attributed to type IV pilus-driven twitching motility, which facilitates the migration of *X. fastidiosa* against fluid flow *in planta* (44). In research investigating spatial colonization patterns of *X. fastidiosa* over typical acquisition access periods, Backus and Morgan demonstrated that the initial site of colonization likely occurs in the cibarium, which then acts as a stable reservoir from which *X. fastidiosa* can load progressively into the distal portions of the precibarium (4). Indeed, the presence of *X. fastidiosa* in the precibarium is highly correlated with inoculation of grapevines 33). Our scanning electron micrographs (of BGSS foreguts fed

solely on wild type *X. fastidiosa*) further substantiated our model, because robust biofilms were more often associated with the outer regions of the cibarium, where less shear force is predicted to occur (Fig. 7). We acknowledge that this initial model is a simplified anatomical representation of the BGSS foregut, and the results presented here are representative of insects that have fed on artificial diets. In future studies, we will focus on fine-tuning the model to further our understanding of the fluid dynamics in the foregut. Expanding the studies to other sharpshooter species that serve as vectors for *X. fastidiosa,* as well as allowing insects to acquire directly from infected plants, is also warranted.

MATERIALS AND METHODS

Bacterial strains and growth conditions. We used wild type *X. fastidiosa* Temecula1 (34) and a *wzy* mutant strain (15). *X. fastidiosa* Temecula1 wild type and *wzy* mutant strains were grown for 7 days at 28°C on solid PD3 medium, with or without kanamycin at 5 μg/mL. For acquisition tests, strains were prepared as described previously (35), with slight modifications. In brief, wild type and *wzy* mutant *X. fastidiosa* cells were harvested from PD3 plates and suspended in liquid XFM medium. Bacterial cell suspensions were adjusted to OD_{600} of 0.25 (approximately 10^8 cells/mL); 20-μL aliquots of cell suspensions were striped onto XFM with 0.01% pectin. Cells were incubated at 28°C for an additional 7 days and suspended in artificial insect diet solution (containing 0.7 mM L-glutamine, 0.1 mM L-asparagine, and 1 mM sodium citrate [pH 6.4]) (35), and suspensions were adjusted to 10^8 cells/mL (OD_{600} 0.25).

Insect source and maintenance. Adult blue-green sharpshooters (BGSS), *Graphocephala atropunctata* (Signoret) (Hemiptera, Cicadellidae), were collected in Laguna Beach, CA. Insects were reared on sweet basil (*Ocimum basilicum* L.) under greenhouse conditions (22 ± 5°C). Prior to the assays, subsets of second-generation adults were tested using the quantitative PCR (qPCR) protocol described below, to confirm that the insects were free of *X. fastidiosa*. Only second-generation adults were used in the acquisition tests.

Insect acquisition experiments. Acquisition experiments using artificial diets were performed as described previously (35), with slight modifications. Insects were caged individually in artificial sachets constructed from the base of a 5-mL pipette tip and sealed with a moist cotton ball. Each replicate consisted of 35 µL of bacterial cell suspension loaded onto a layer of stretched Parafilm, with the drop later being covered with another layer of Parafilm. Insects were given a 6-h acquisition access period (AAP) at 20°C. To remove any unbound cells present in the ingested solutions, insects were transferred to healthy basil plants for a 48-h clearing and multiplication period. Immediately following the 48-h clearing and multiplication period at room temperature, 30 insect heads per treatment were placed in 4% glutaraldehyde fixative for scanning electron microscopy or whole insects were immediately stored at -20°C until DNA extraction and qPCR analysis. For qPCR analysis, 40 insects were exposed to the wild type bacteria, 36 were exposed to the *wzy* mutant, and 33 were exposed to diet only.

Quantification of *X. fastidiosa*. Following the 48-h clearing and multiplication period, insects were immediately stored at -20°C until further analysis. Genomic DNA extractions were performed on individual BGSS heads using the Qiagen DNeasy blood and tissue kit (Qiagen, Valencia, CA), with the addition of liquid nitrogen pretreatment. Using a disposable microtube pestle, individual heads were ground to a fine powder with liquid nitrogen. Samples were then processed according to the standard DNeasy protocol, and the resulting DNA was concentrated using a SpeedVac concentrator, prior to use in qPCR. For use in quantification of *X. fastidiosa* in the insect samples, standard curves

were created using a BGSS genomic DNA/*X. fastidiosa* genomic DNA concentration ratio of 2:1 (see Fig. S1 in the supplemental material). To prepare the DNA for determination of the insect sample standard curve, cultured *X. fastidiosa* cells were adjusted to an OD_{60} of 0.25, corresponding to approximately 1×10^8 cells/mL (1×10^5 cells/µL), and genomic DNA was extracted using the Qiagen DNeasy blood and tissue kit (Qiagen, Valencia, CA). The resulting DNA was mixed with insect DNA in a 2:1 concentration ratio. From this mixture, 10-fold serial dilutions were made to create a range of standards from 10,000 – 10 *X. fastidiosa* cells/µL (see Fig. S1 in the supplemental material). Quantitative PCR was performed using a C1000 thermal cycler fitted with a CFX96 real-time PCR detection system (Bio-Rad, Hercules, CA). TaqMan primers and probe targeting the ITS region of the *X. fastidiosa* Temecula1 genome were as follows: *Xf*ITSF6, 5' – GAGTATGGTGAATATAATTGTC – 3'; *Xf*ITSR6, 5' – C AACATAAACCCAAACCTAT – 3'; and *Xf*ITS6-probe1, 5' – 6 – FAM – CCAGGCGTCCTCACAAGTTA – black hole quencher 1 (BHQ1) – 6 – FAM – 3' (BHQ1 was obtained from Eurofins MWG Operon, Huntsville, AL. PCRs were performed in triplicate in a volume of 25 µL and contained 2.5 µL of 10x buffer mix (Qiagen, Valencia, CA), 2.5 µL of $MgCl_2$ buffer (Qiagen, Valencia, CA), 200 µM of each deoxynucleoside triphosphate (dNTP) (Qiagen, Valencia, CA), 400 nM of each primer, 250 nM probe, 1.25 units of *Taq* DNA polymerase, and 1 µL of sample or standard template. PCRs were performed using an initial denaturation step at 94°C for 5 min followed by 38 cycles of denaturation at 94°C for 20 s, primer annealing at 63°C for 30 s, and primer extension at 72°C for 30 s, with a final extension step at 72°C for 2 min.

Scanning electron microscopy. Using a series of ethanol dilutions, BGSS heads were dehydrated and critical point dried using the Tousimis Autosamdri-815B critical point dryer (Tousimis, Rockville, MD). Foreguts were gently dissected from insect heads and mounted onto copper tape attached to aluminum stubs. Samples were coated in a platinum – palladium mixture using the Cressington 108 Auto Sputter Coater (Cressington Scientific Instruments Ltd., Watford, England) and imaged using a Philips XL30 field emission gun (FEG) scanning electron microscope (FEI, Hillsboro, OR).

Hindwing attachment assay. The attachment assay was conducted according to previously established protocols (19), with slight modifications. Using BGSS adults from the same source colony, hindwings were removed and gently washed in distilled water. Wings were immobilized on water agar plates (1.5%; Becton, Dickinson, and Co., Franklin Lakes, NJ). *X. fastidiosa* wild type and *wzy* mutant strains were grown as described above. Suspensions were adjusted to OD_{600} of 0.25, and 2 μL of each suspension was loaded onto individual wings. Hindwings were incubated at 28°C for 6 h, after which suspensions were removed and wings were gently rinsed with distilled water. Each wing was used in a separate DNA extraction, using the Qiagen DNeasy blood and tissue kit (Qiagen, Valencia, CA), and bacterial titers were determined using the qPCR method described above. Experiments consisted of three independent assays with three replicates per strain, totaling nine insects per treatment.

Zeta Potential measurements of bacterial cells and sharpshooter hindwings. Zeta potential measurements on *X. fastidiosa* cells were determined using a ZetaPALS analyzer (Brookhaven Instruments Corporation, Holtsville, NY). Zeta potential measurements on *X. fastidiosa* cells were performed as described previously (15). All bacterial strains were grown on solid PD3 medium for 7 days, harvested, and suspended in liquid XFM (without filter-sterilized supplement containing L-asparagine, L-cysteine, L-glutamine, and bovine serum albumin). Cell suspensions were adjusted to an OD_{600} of 0.25 (approximately 10^8 cells/mL); 20-µL aliquots of cell suspensions were striped onto XFM with 0.01% pectin. Cells were incubated at 28°C for an additional 7 days, harvested, washed once with 10mM KCl, and resuspended in 10 mM KCl to a final OD_{600} of 0.2. The electrophoretic mobility of the bacterial cells was determined at 20°C using a ZetaPALS analyzer (Brookhaven Instruments Corporation, Holtsville, NY). Experiments consisted of three independent assays with five replicates per strain. Mobility values determined by electrophoresis were converted to zeta potential values (36).

To determine the relative surface charge of BGSS foreguts, streaming potential measurements were conducted on BGSS hindwings. A streaming potential analyzer (SurPASS, Anton Paar, Graz, Austria) with an adjustable gap cell was used to measure the electrokinetic properties of BGSS hindwings (in streaming current mode). Hindwings were immobilized on the sample supports (20 mm by 10 mm) within the cell, and the gap was adjusted to approximately 100 µm. Measurements were made at 25°C using 10 mM KCl (without initial pH adjustment), with a maximum pressure difference of 50 kPa. At

each pH increment, measurements were repeated four times. Acid titration (0.05 M HCl) was used to evaluate the surface charge at pH 7.

Hydrophobicity measurements of sharpshooter hindwings. Static contact angle (SCA) measurements of immobilized hindwings were performed using a drop shape analyzer (DSA25; KRÜSS, Hamburg, Germany). Average contact angles were obtained from measurements at four different points. Using the instrument software, SCA values were calculated using the tangential curve-fitting method, at 10 s after a drop of water (10 μL) had been dropped onto the surface.

DLVO profiles. The Derjaguin – Landau – Verwey – Overbeek (DLVO) theory was applied to further evaluate the relative contribution of electrostatic and van der Waals interactions between the foregut surface and bacteria within the insect (37-39). The van der Waals attraction is governed by a constant, i.e. the Hamaker constant (A), which depends on the material properties. The Hamaker constant used to evaluate the van der Waals interactions between chitin, water, and *X. fastidiosa* was A_{132} of 3 x 10^{-21}J. This constant (A_{132}) was calculated using the geometric mean (39) of known constants for water (39) and bacteria (40), and the Hamaker constant was determined using the contact angle of the BGSS hindwings (41, 42). Using this information, interaction profiles were developed assuming sphere-plate geometry (37-39, 43).

Comsol model. Using a commercial finite element package (Comsol Multiphysics v4.3), a computational model was developed to evaluate fluid flow through the sharpshooter foregut. The computational domain used was a two-dimensional longitudinal section through the pharynges. The two-dimensional model provides valuable insights into the dynamic process of sharpshooter feeding and fluid stagnation, which may promote bacterial attachment. However, it is representative of flow conditions only under steady-state laminar flow. The velocity field is described by the equations of motion for an incompressible fluid and the continuity equation. The following boundary conditions were imposed. At the inlet, a fully developed laminar velocity profile was specified, while the out flow boundary was set to constant (atmospheric) pressure. At the foregut surfaces (the upper and lower boundaries), the tangential velocity was set to zero (no-slip conditions). The computational domain was meshed using a structured, boundary-layer type mesh, with an increasing mesh density near the spacer and membranes surface. This enabled efficient computation while retaining accuracy where the largest concentration variations in the system were expected. Mesh refinement was carried out to ensure the independence of the solution on the mesh. In all simulations, the solution was assumed to be water, with fluid density and dynamic viscosity taken as 1000 kg/m^{-3} and 10^{-3} $Pa \cdot s$, respectively.

Statistical Tests. All experiments were analyzed by one-way analysis of variance (ANOVA), using PROC GLM (SAS Institute) to deal with unequal class sizes. Prior to the ANOVA, data were checked for normality and homogeneity of variance using PROC

UNIVARIATE (SAS Institute). All experiments met these criteria. Differences among treatment means were determined by Tukey's honestly significant difference (HSD) test at $P = 0.05$.

Supplemental Figure S1.1. Quantitative PCR standard curve for detection of *X. fastidiosa* in BGSS

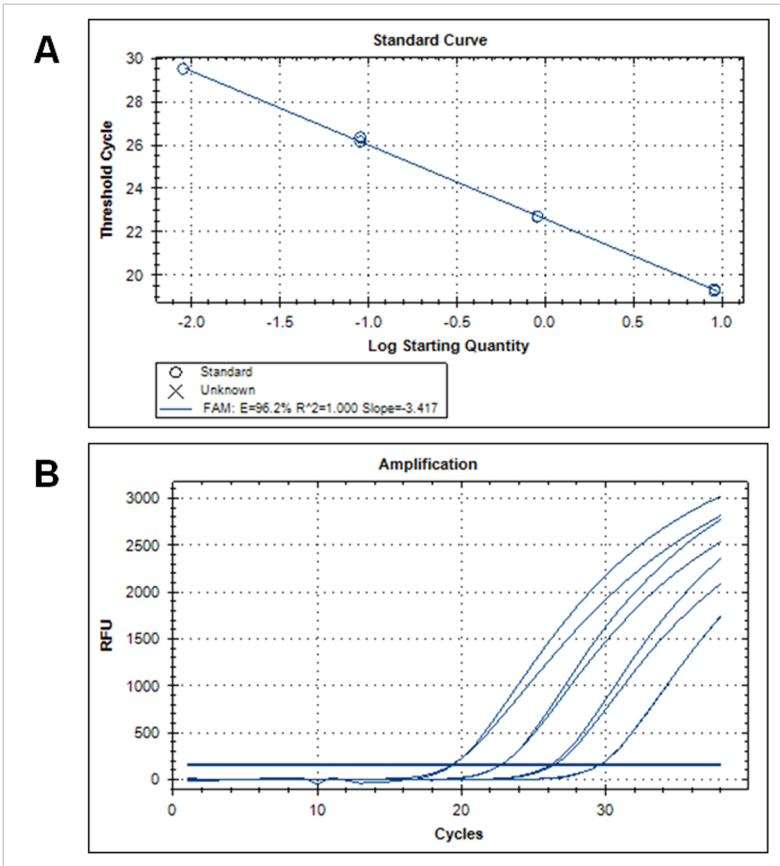

(**A**) Standard curve showing amplification efficiency of the qPCR assay. (**B**) Real-time amplification curves of standards. RFU, relative fluorescence unit. 1-4: 10-fold dilution series of a 2:1 mixture of BGSS genomic DNA and *X. fastidiosa* genomic DNA (1 = 10,000 cells, 2 = 1,000 cells, 3 = 100 cells, and 4 = 10 cells per 1µL of template). The specificity of the assay allowed for consistent and efficient detection of *X. fastidiosa* in sharpshooter foreguts, with a detection threshold of 10 cells.

LITERATURE CITED

1. **Lemon SM, Sparling PF, Hamburg MA, Relman DA, Choffnes ER, Mack A, Sparling F.** 2008. Vector-borne diseases: understanding the environmental, human health, and ecological connections. Workshop summary, p. *In* (ed), National Academies Press, Washington.

2. **Chen AYS, Walker GP, Carter D, Ng JCK.** 2011. A virus capsid component mediates virion retention and transmission by its insect vector. Proc. Natl. Acad. Sci. U.S.A. **108:**16777-16782.

3. **Chatterjee S, Almeida RPP, Lindow S.** 2008. Living in two worlds: The plant and insect lifestyles of *Xylella fastidiosa*. Annu. Rev. Phytopathol. **46:**243-271.

4. **Backus EA, Morgan DJW.** 2011. Spatiotemporal colonization of *Xylella fastidiosa* in its vector supports the role of egestion in the inoculation mechanism of foregut-borne plant pathogens. Phytopathology **101:**912-922.

5. **Killiny N, Almeida RPP.** 2014. Factors affecting the initial adhesion and retention of the plant pathogen *Xylella fastidiosa* in the foregut of an insect vector. Appl. Environ. Microbiol. **80:**420-426.

6. **Killiny N, Almeida RPP.** 2009. *Xylella fastidiosa* afimbrial adhesins mediate cell transmission to plants by leafhopper vectors. Appl. Environ. Microbiol. **75:**521-528.

7. **Killiny N, Martinez RH, Dumenyo CK, Cooksey DA, Almeida RPP.** 2013. The exopolysaccharide of *Xylella fastidiosa* is essential for biofilm formation, plant virulence, and vector transmission. Mol. Plant Microbe Interact. **26:**1044-1053.

8. **Dinglasan RR, Jacobs-Lorena M.** 2005. Insight into a conserved lifestyle: protein-carbohydrate adhesion strategies of vector-borne pathogens. Infect. Immun. **73:**7797-7807.

9. **Caroff M, Karibian D.** 2003. Structure of bacterial lipopolysaccharides. Carbohydr. Res. **338:**2431-2447.

10. **Walker SL, Redman JA, Elimelech M.** 2004. Role of cell surface lipopolysaccharides in *Escherichia coli* K12 adhesion and transport. Langmuir **20:**7736-7746.

11. **Lerouge I, Vanderleyden J.** 2002. O-antigen structural variation: mechanisms and possible roles in animal/plant–microbe interactions. FEMS Microbiol. Rev. **26:**17-47.

12. **Clements A, Gaboriaud F, Duval JFL, Farn JL, Jenney AW, Lithgow T, Wijburg OLC, Hartland EL, Strugnell RA.** 2008. The major surface-associated saccharides of *Klebsiella pneumoniae* contribute to host cell association. PLoS One **3:**e3817.

13. **Raetz CRH, Whitfield C.** 2002. Lipopolysaccharide endotoxins. Annu. Rev. Biochem. **71:**635.

14. **Zhang L, Radziejewska-Lebrecht J, Krajewska-Pietrasik D, Toivanen P, Skurnik M.** 1997. Molecular and chemical characterization of the lipopolysaccharide O-antigen and its role in the virulence of *Yersinia enterocolitica* serotype O:8. Mol. Microbiol. **23:**63-76.

15. **Clifford JC, Rapicavoli JN, Roper MC.** 2013. A Rhamnose-rich O-Antigen mediates ddhesion, virulence, and host colonization for the xylem-limited phytopathogen *Xylella fastidiosa*. Mol. Plant Microbe Interact. **26:**676-685.

16. **Pel MJC, Pieterse CMJ.** 2013. Microbial recognition and evasion of host immunity. J. Exp. Bot. **64:**1237-1248.

17. **Silipo A, Molinaro A, Sturiale L, Dow JM, Erbs G, Lanzetta R, Newman M-A, Parrilli M.** 2005. The elicitation of plant innate immunity by lipooligosaccharide of *Xanthomonas campestris*. J. Biol. Chem. **280:**33660-33668.

18. **Wilson WW, Wade MM, Holman SC, Champlin FR.** 2001. Status of methods for assessing bacterial cell surface charge properties based on zeta potential measurements. J. Microbiol. Methods **43:**153-164.

19. **Killiny N, Prado SS, Almeida RPP.** 2010. Chitin utilization by the insect-transmitted bacterium *Xylella fastidiosa*. Appl. Environ. Microbiol. **76:**6134-6140.

20. **Goswami S, Klaus S, Benziger J.** 2008. Wetting and absorption of water drops on Nafion films. Langmuir **24:**8627-8633.

21. **Purcell AH, Hopkins DL.** 1996. Fastidious xylem-limited bacterial plant pathogens. Annu. Rev. Phytopathol. **34:**131-151.

22. **Purcell AH, Finlay AH, McLean DL.** 1979. Pierce's disease bacterium: Mechanism of transmission by leafhopper vectors. Science **206:**839-841.

23. **Andersen PC, Brodbeck BV, Mizell RF.** 1992. Feeding by the leafhopper, *Homalodisca coagulata*, in relation to xylem fluid chemistry and tension. J. Insect Physiol. **38:**611-622.

24. **Roper MC, Greve LC, Labavitch JM, Kirkpatrick BC.** 2007. Detection and visualization of an exopolysaccharide produced by *Xylella fastidiosa* in Vitro and in planta. Appl. Environ. Microbiol. **73:**7252-7258.

25. **Petrocelli S, Tondo ML, Daurelio LD, Orellano EG.** 2012. Modifications of *Xanthomonas axonopodis* pv. citri lipopolysaccharide affect the basal response and the virulence process during citrus canker. PloS One **7:**e40051.

26. **Barak JD, Jahn CE, Gibson DL, Charkowski AO.** 2007. The role of cellulose and O-antigen capsule in the colonization of plants by *Salmonella enterica*. Mol. Plant Microbe Interact. **20:**1083-1091.

27. **Boyer RR, Sumner SS, Williams RC, Kniel KE, McKinney JM.** 2011. Role of O-antigen on the *Escherichia coli* O157: H7 cells hydrophobicity, charge and ability to attach to lettuce. Int. J. Food Microbiol. **147:**228-232.

28. **Bengoechea JA, Najdenski H, Skurnik M.** 2004. Lipopolysaccharide O-antigen status of *Yersinia enterocolitica* O: 8 is essential for virulence and absence of O-antigen affects the expression of other *Yersinia* virulence factors. Mol. Microbiol. **52:**451-469.

29. **Baccari C, Killiny N, Ionescu M, Almeida RPP, Lindow SE.** 2014. Diffusible signal factor-repressed extracellular traits enable attachment of *Xylella fastidiosa* to insect vectors and transmission. Phytopathology **104:**27-33.

30. **Fennema OR.** 1996. Food Chemistry, 3rd, p 115-116. New York, NY: Marcel-Dekker, Inc.

31. **Ravina L, Moramarco N.** 1993. Everything you want to know about Coagulation & Flocculation. Zeta-Meter, Inc.

32. **Hermansson M.** 1999. The DLVO theory in microbial adhesion. Colloids. Surf. B: Biointerfaces **14:**105-119.

33. **Almeida RPP, Purcell AH.** 2006. Patterns of *Xylella fastidiosa* colonization on the precibarium of sharpshooter vectors relative to transmission to plants. Ann. Entomol. Soc. Am. **99:**884-890.

34. **Guilhabert MR, Hoffman LM, Mills DA, Kirkpatrick BC.** 2001. Transposon mutagenesis of *Xylella fastidiosa* by electroporation of Tn5 synaptic complexes. Mol. Plant Microbe Interact. **14:**701-706.

35. **Killiny N, Almeida RPP.** 2009. Host structural carbohydrate induces vector transmission of a bacterial plant pathogen. Proc. Natl. Acad. Sci. U.S.A. **106:**22416-22420.

36. **O'Brien RW, White LR.** 1978. Electrophoretic mobility of a spherical colloidal particle. J. Chem. Soc., Faraday Transactions 2: Molecular and Chemical Physics **74:**1607-1626.

37. **Chowdhury I, Hong Y, Honda RJ, Walker SL.** 2011. Mechanisms of TiO 2 nanoparticle transport in porous media: role of solution chemistry, nanoparticle concentration, and flowrate. J. Colloid Interface Sci. **360:**548-555.

38. **Hong Y, Honda RJ, Myung NV, Walker SL.** 2009. Transport of iron-based nanoparticles: role of magnetic properties. Environ. Sci. Technol. **43:**8834-8839.

39. **Gregory J.** 2005. Particles in water: properties and processes. CRC Press.

40. **Redman JA, Walker SL, Elimelech M.** 2004. Bacterial adhesion and transport in porous media: Role of the secondary energy minimum. Environ. Sci. Technol. **38:**1777-1785.

41. **Janjaroen D, Ling F, Monroy G, Derlon N, Mogenroth E, Boppart SA, Liu W-T, Nguyen TH.** 2013. Roles of ionic strength and biofilm roughness on adhesion kinetics of *Escherichia coli* onto groundwater biofilm grown on PVC surfaces. Water Res. **47:**2531-2542.

42. **Van Oss CJ.** 1993. Acid—base interfacial interactions in aqueous media. Colloids. Surf. A: Physicochemical and Engineering Aspects **78:**1-49.

43. **Hogg R, Healy TW, Fuerstenau DW.** 1966. Mutual coagulation of colloidal dispersions. Trans. Faraday Soc. **62:**1638-1651.

44. **Meng Y, Li Y, Galvani CD, Hao G, Turner JN, Burr TJ, Hoch H.** 2005. Upstream migration of *Xylella fastidiosa* via pilus-driven twitching motility. J. Bacteriol. **187:**5560-5567.

CHAPTER II. O antigen acts as a shield to delay early plant immune recognition of the pathogenic bacterium *Xylella fastidiosa*

ABSTRACT

PAMP-triggered immunity (PTI) is the first line of plant defense against invading organisms. Initiated through the perception of conserved pathogen-associated molecular patterns (PAMPs), such as lipopolysaccharide or flagellin, PTI can provide early protection against a broad range of pathogens. Active suppression of PTI by microbial effector proteins, particularly those secreted by the Type III secretion system (T3SS), is a well-known strategy employed by bacterial plant pathogens that enables them to subvert PTI and successfully colonize their hosts. In this study, we demonstrate that the xylem-limited bacterium, *Xylella fastidiosa*, which lacks a T3SS, utilizes an alternative strategy to delay elicitation of innate immune responses. By decorating its LPS PAMP molecule with a high molecular weight O antigen, this bacterium physically masks itself from early recognition by the grapevine innate immune system. We have elucidated the chemical structure of the O antigen and found that it is primarily an α1,2-linked rhamnan polymer. *X. fastidiosa* cells lacking O antigen elicited hallmarks of PTI such as ROS production, specifically in the plant xylem tissue compartment, which is comprised primarily of non-living cells. By coupling histological and genome-wide transcriptional profiling, we demonstrate that *X. fastidiosa* lacking its O antigen shield activates defense related genes in grapevine. This includes a stronger and more prolonged oxidative burst at concentrations high enough to inhibit pathogen proliferation. To begin exploring translational applications of our findings, we also demonstrate that purified *X. fastidiosa*

LPS elicitor can prime grapevine defenses, thereby conferring host tolerance to subsequent challenge with *X. fastidiosa*.

INTRODUCTION

Plants are continuously faced with threats from pathogenic microbes. Unlike mammals, plants are sessile, unable to use mobility as a means to evade infection, and they lack mobile defender cells and an adaptive somatic immune system. Alternatively, they rely on the innate immunity of each individual cell and on intricate signal transduction pathways emanating from infection sites (1). The first tier of the immune system functions through recognition of pathogen- (or microbe-) associated molecular patterns (PAMPs/MAMPs) by extracellular pattern recognition receptors (PRRs). This results in PAMP-triggered immunity (PTI), also known as basal disease resistance, which aims to halt pathogen invasion (1). Activation of PRRs leads to intracellular signaling and transcriptional reprogramming, resulting in numerous pathogenesis-related changes that follow PAMP perception, such as rapid influxes of cytosolic Ca^{+2} and reactive oxygen species (ROS) (2). Additional downstream responses that occur within hours of PTI initiation are stomatal closure and cell wall modifications such as callose deposition (2). There has been great progress in elucidating the molecular mechanisms underlying PTI, but the focus has been primarily on foliar pathogens that enter through epiphytic means (e.g. *Pseudomonas syringae* pathovars and *Xanthomonas spp.*) (3). However, there is little information on the initiation of PTI in the vascular tissue, particularly in the xylem

where microorganisms come into contact with mostly non-living tissue that cannot mount a defense response on its own.

Vascular pathogens cause some of the most destructive diseases affecting commercial agriculture, in both annual and perennial crops (4). These pathogens colonize the xylem vessels where they proliferate and occlude the transportation of water and minerals throughout the plant (4). While many bacterial vascular pathogens enter host tissues passively (via wounds, cracks, or natural openings such as stomata and hydathodes) (4), some are delivered directly into the plant vascular system by insect vectors that feed on xylem sap (5-7). Plant hosts can deploy defense responses following infection with xylem-dwelling pathogens (4, 8-10). These responses comprise both physical (e.g. tyloses) and chemical defenses (e.g. ROS, phenolics, and antimicrobial compounds) that aim to halt pathogen spread or inhibit/kill pathogen growth, respectively. However, xylem cells undergo programmed cell death and are non-living at maturity and, thus, do not mount these defense responses on their own. Vascular pathogens are presumably recognized by receptors in the living parenchyma cells surrounding the xylem vessels (4, 11), which can undergo significant metabolic changes induced by infection. Perception of the xylem-dwelling bacterial pathogens *Xanthomonas oryzae* and *Ralstonia solanacearum* via receptor-mediated detection of secreted Type III effectors is well-documented (11), but the mechanisms of PAMP perception in the xylem, particularly in regards to PTI, are unclear. In addition to the xylem, these pathogens also have a leaf apoplastic phase as well, making it difficult to tease apart plant defense responses that are elicited strictly as a result of colonization of the xylem tissue.

Xylella fastidiosa is a Gram-negative, xylem-limited phytopathogen that is obligately transmitted by leafhopper vectors, mainly sharpshooters (6). In contrast with other vascular pathogens, which may simultaneously colonize xylem, phloem, and cambium tissue compartments, *X. fastidiosa* exclusively occupies the xylem, making it a robust model system for understanding xylem specific plant-microbe interactions (5). This destructive agricultural pathogen causes diseases in several economically important crops, namely Pierce's disease (PD) of grapevine, Citrus Variegated Chlorosis, and Almond Leaf Scorch and has recently been implicated in Olive Quick Decline Syndrome in Italy (12, 13). The bacteria form biofilms within the xylem vessels of plant hosts and elicits production of prolific host-derived xylem occlusions (i.e., tyloses) that reduce hydraulic conductivity of the plant (6, 14-16). In grapevine, symptoms of PD include marginal leaf necrosis, premature leaf abscission, fruit desiccation, and ultimately plant death (6), which all manifest at the very late stages of infection. In addition, there are significant transcriptional changes during the late stages of the infection process that include a pronounced impact on physiological responses to drought stress (17). However, details regarding the molecular basis of the *X. fastidiosa*-plant host interaction, including identification of specific PAMPs and the elicitation of basal defense responses in the very early phases of host infection, remain largely unknown. *X. fastidiosa* resides in many plant species as an endophytic commensal (18). However, there are numerous examples of specific *X. fastidiosa*-plant interactions where the bacterium behaves as a destructive pathogen. In either lifestyle, *X. fastidiosa* must actively overcome or avoid triggering initial host defense responses, such as PTI, to successfully colonize the plant. Many plant

and animal bacterial pathogens overcome PTI by secreting Type III effectors that disrupt or suppress PTI responses (19-21). Interestingly, genes encoding a Type III secretion system are strikingly absent in the *X. fastidiosa* genome (22, 23). Therefore, it must utilize another mechanism to avoid elicitation of PTI in its plant hosts.

Lipopolysaccharides (LPS) are structural components located in the outer membrane of all Gram-negative bacteria (24, 25). There are approximately 3.5 million LPS molecules on the bacterial outer membrane (26), making them the most dominant macromolecules on bacterial cell surfaces (25, 27). LPS are comprised of three parts: (i) lipid A that anchors the molecule to the outer membrane, (ii) a core oligosaccharide (OS), and (iii) a terminal O antigen consisting of polysaccharide chains (25, 28). The O antigen is the most surface-exposed portion of the LPS molecule and can extend up to 60 nm away from the surface of the bacterial cell (26, 29-31). While the lipid A and OS portions of the molecule are highly conserved, the O antigen can exhibit considerable structural variation (27, 29, 32). The O antigen is assembled in the cytoplasm and independently delivered to the periplasm, where it is ligated onto the lipid A/OS complex and then translocated to the outer membrane (29). This process is mediated, in part, by the Wzy polymerase, which catalyzes the polymerization of the individual O-units that make up the O antigen chain (29). Because of its prominence and extension into the environment, LPS, and more specifically the outermost exposed O antigen, have pleiotropic roles in bacterial pathogenesis in both mammalian and plant systems (e.g. adhesion and promotion of biofilm), which relate to bacterial fitness *in vivo* (27, 32-34).

LPS are also well-characterized PAMPs that are perceived by a wide range of plant species and initiate PTI (20, 35). Purified LPS from diverse bacterial pathogens induce a rapid burst of nitric oxide, a hallmark of the elicitation of PTI, in suspension cultures and leaves of *Arabidopsis thaliana* (36). In addition, Desaki et al (2006) demonstrated that LPS from various plant and animal pathogens can induce defense responses in rice cells, which suggests that the machinery recognizing LPS is evolutionarily conserved (37). Plant host perception of LPS can also induce callose deposition and up-regulation of PR gene expression (38, 39). We hypothesize that during the interaction between *X. fastidiosa* and a susceptible grapevine host, the bacterium's long chain, rhamnose-rich O antigen shields the conserved lipid A and OS regions of the LPS molecule, and likely additional PAMPs located on the cell surface, from being recognized by the plant immune system, providing an opportunity for *X. fastidiosa* to avoid early elicitation of defense responses and establish itself in the host. A similar scenario occurs in *Escherichia coli*, where truncation of the O antigen caused an increased sensitivity to serum, suggesting the full length O antigen provides a masking effect towards the host immune system (40). *Salmonella enterica* subsp. *enterica* sv. (*S.*) Typhimurium also possesses an O antigen that aids in evasion of the murine immune system (41).

In previous studies, we have demonstrated that truncation of the O antigen compromised *X. fastidiosa's* ability to colonize the grapevine xylem and elicit PD symptoms (33). Here we demonstrate that altering the molecular architecture of the *X. fastidiosa* cell surface by truncating the O antigen also drastically affects plant host

recognition of the pathogen at both the genetic and phenotypic levels. Interestingly, wild type *X. fastidiosa*-initiated gene expression cascades associated primarily with responses to abiotic stresses, such as decreases in hydraulic conductivity beginning very early in the infection process, while cells lacking the O antigen shield elicited a significant up-regulation of genes enriched in ROS production and defense-related genes. Although transcriptional profiles of wild type-inoculated plants eventually displayed immune-related responses as compared to the *wzy*-inoculated plants, this effective delay in recognition allowed wild type cells to establish a compatible interaction and cause disease. Based on these data, we establish that O antigen serves as a shield to delay recognition of *X. fastidiosa* by the plant innate immune system.

RESULTS

PD symptoms are attenuated in grapevines primed with purified LPS. Pre-treatment of plants with LPS can prime the defense system, resulting in an enhanced response to subsequent pathogen attacks. This defense-related "memory" stimulates the plant to initiate a faster and/or stronger response against future invading pathogens (42). In grapevine (*Vitis vinifera*), previous studies have demonstrated defense priming for the protection against the foliar pathogens *Botrytis cinerea* and *Plasmopara viticola*, which have markedly different lifestyles and infection routes than *X. fastidiosa* (43-46). We sought to establish if purified LPS could be used to prime grapevines against subsequent challenge with the vascular pathogen, *X. fastidiosa*. LPS can prime plant defense responses in as little as 4-24 h post-treatment. Therefore, we verified if the innate

immune response in grapevine follows similar kinetics observed in previous studies (47, 48). Grapevines that were pre-treated with either form of LPS (wild type or *wzy* mutant) prior to *X. fastidiosa* challenge exhibited significantly fewer PD symptoms over the course of the experiment. However, grapevines that were pre-treated for 4 h showed the most significantly attenuated symptoms. Even after 12 weeks post-inoculation, symptoms of these LPS-treated plants rated a 1 on the PD rating scale, reflecting only 1 or 2 leaves just beginning to show marginal necrosis (49). Buffer pre-treated controls were fully symptomatic, rating around 3 on the PD rating scale (49) (Fig. 2.1). This indicated that a 4 h and 24 h pre-treatment with purified LPS from either wild type or the *wzy* mutant confers tolerance to PD. The priming effect appears to be transient because plants pre-treated with LPS 24 h prior to challenge showed a slight increase in the severity of PD symptoms, but they were still significantly attenuated compared with buffer pre-treated control vines.

LPS induces an oxidative burst in grapevine. Because of the significant decrease in PD symptom development following pre-treatment with both forms of LPS, we proceeded to compare the activity of wild type and *wzy* mutant LPS elicitor. Treatment of plants with purified LPS induces an oxidative burst in both monocots and dicots (20, 35, 37, 50). Using a luminol-based assay, both wild type and *wzy* mutant purified LPS induced an oxidative burst of similar amplitude in grapevine leaf discs (Fig. 2.2A), and total ROS production (expressed as area under the curve) was not significantly different between the

Figure 2.1. Pierce's Disease symptom severity in grapevines primed with purified *X. fastidiosa* LPS

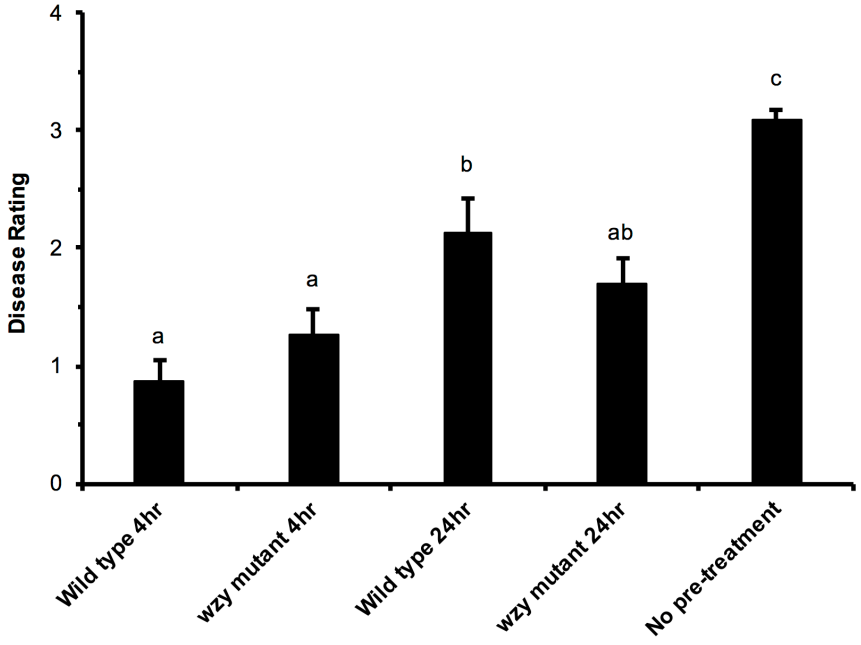

Average disease ratings of *V. vinifera* 'Cabernet Sauvignon' grapevines pre-treated with wild type or *wzy* mutant LPS (50µg/mL), then challenged at 4 h or 24 h post-LPS treatment with live *X. fastidiosa* cells. Disease ratings were taken at 12 weeks post-challenge. The LPS pre-treated plants are significantly attenuated in symptom development, compared with plants that did not receive pre-treatment. Graph represents the mean of 24 samples per treatment. Bars indicate standard error of the mean. Treatments with different letters over the bars are statistically different ($P < 0.05$).

treatments (Fig. 2.2B). It's possible that the potent elicitor is actually the conserved lipid A-core portions of the LPS molecule, which would be equally exposed in both wild type and *wzy* purified LPS. This likely explains why wild type and *wzy* purified LPS elicited similar responses in terms of an oxidative burst. In the context of whole cells, however, these conserved regions would likely be shielded by the O antigen in wild type cells.

Structural characterization of the LPS O antigen shield. DOC-PAGE analysis of purified LPS indicated a severe change in the electrophoretic profile of *wzy* mutant LPS, compared with the wild type LPS (Fig 2.3A lanes 1 and 2). Silver staining indicated the presence of a high molecular weight O antigen in wild type LPS (Fig. 2.3A lane 1, arrow) that was notably absent in *wzy* mutant LPS (Fig. 2.3A lane 2). In addition, staining intensity of the wild type LPS bands at the bottom of the gel was weaker compared to that of the *wzy* mutant. In *wzy* mutant LPS, the O antigen band was absent, and the lower bands on the gel were more pronounced, which is indicative of reduced or no O antigen production. This observation was supported by comparative chemical analysis and subsequent structural studies. In wild type LPS, we observed the presence of Rhamnose (Rha), Xylose (Xyl), Mannose (Man), Glucose (Glc), Galacturonic Acid (GalA), 3-deoxy-D-*manno*-2-octulosonic acid (Kdo), methylated deoxy hexose, N-acetylglucosamine (GlcNAc), and hydroxyl fatty acids 10:0(3OH), 10:0(2OH) and 12:0(3OH), 12:0(2OH) characteristic for lipid A of LPS (Table S2.1). Interestingly, in the

Figure 2.2. Purified LPS-induced ROS production *ex vivo*

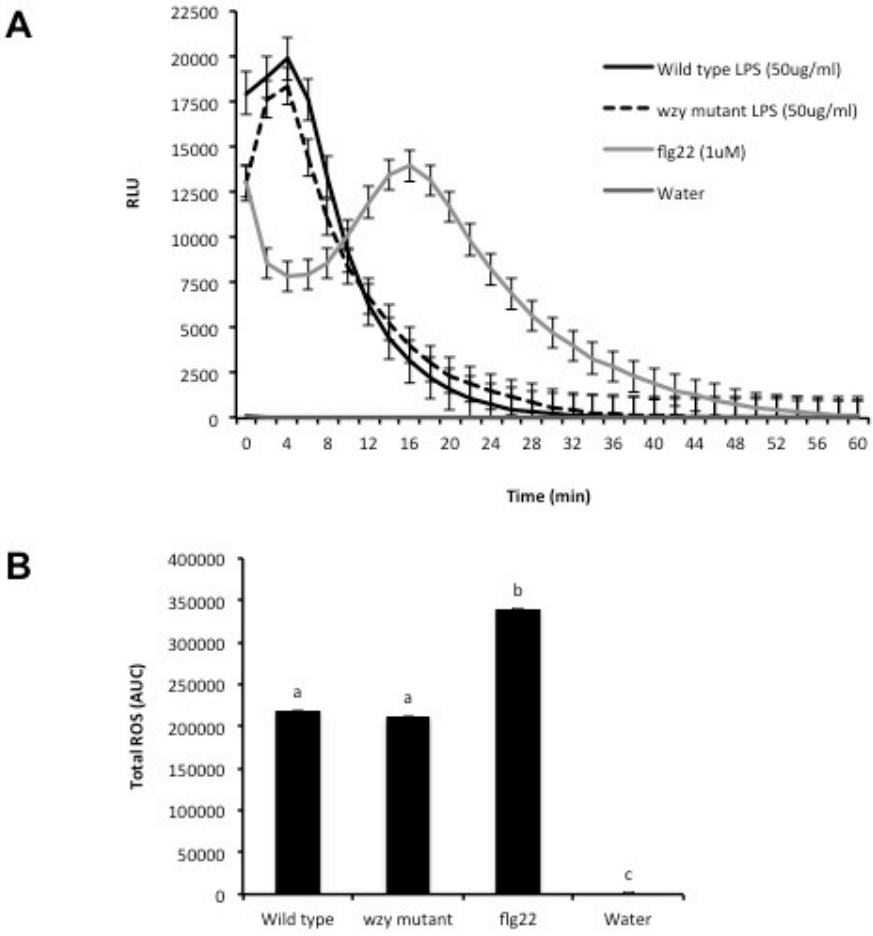

Discs of *V. vinifera* 'Cabernet Sauvignon' leaves were treated with 20µL of purified LPS (50µg/mL) from *X. fastidiosa* wild type or *wzy* mutant cells, or a water negative control. **(A)** The amplitude of ROS production remained similar for both wild type and *wzy* mutant LPS, reaching max production at approximately 4 minutes, and plateaued starting around 30 minutes. **(B)** Total ROS production is reported as area under the curve (AUC) for plot of luminescence intensity over time. Treatments with different letters over the bars are statistically different ($P < 0.05$).

wzy mutant, we observed a reduction in the amounts of Rha and Xyl, relative to the other glycosyl constituents and to the content of hydroxyl fatty acids. These data, combined with DOC-PAGE observation, indicated that the wild type O antigen polymer is composed predominantly of rhamnose and xylose, while the *wzy* mutant is likely producing LPS with a severely truncated O antigen polymer. The remainder of identified glycosyl residues likely originated from core oligosaccharide and lipid A moieties.

In order to describe structural properties of O antigen in wild type and *wzy* mutant LPS, the polysaccharide moiety (O antigen + core) was liberated from lipid A and resolved based on molecular size (Fig. 2.3B). Comparative analysis of SEC profiles indicated different distributions of polysaccharides in both strains. In the wild type strain, a majority of polysaccharide (40.8% total column load) was eluted in Fraction III (average molecular mass of approximately 10-20kD) and a remainder (24.8% of total column load) in Fraction IV. In contrast, a majority of *wzy* polysaccharide (55.0% total PS column load) was eluted in Fraction IV (average molecular mass below 10kDa), which was only present in low quantity in the wild type parent. This fraction likely represented different molecular size forms of core oligosaccharide or truncated core-O antigen polysaccharide. Fraction I that was eluted in void (Vo) column was due to traces of unhydrolyzed, intact LPS.

Monosaccharide analysis, including the determination of absolute configurations of O antigen polysaccharides from the wild type strain (SEC fraction III), confirmed the presence of L-rhamnose and D-xylose in an 8:1 molar ratio. Methylation analysis demonstrated the presence of terminal Xyl*p*, 2-substituted Rha*p*, 3-substituted Rha*p*, 2,3-

disubstituted Rha*p*. ^{1}H and ^{13}C NMR analysis demonstrated two series of anomeric signals with a ratio of integral intensities ~ 4:1, indicative of at least two different polysaccharide chains. These results suggest that isolated fraction III consisted of at least two different polysaccharide chains. The 1D ^{1}H NMR spectrum showed six minor anomeric signals of equal intensity in the anomeric region (δ 4.4-5.2), named from **A** to **G**, according to decreasing chemical shifts values, and one major signal named **H** (Table S2.2). The δ values of residues **A**, **B**, **C**, **D**, **E** and **H** suggest the presence of α-configurations (singlets), and the δ values of residues of **F** and **G** indicate the occurrence of β-configurations (broadened doublets, $J_{1,2}$ ~8). The spectrum presented one broad high-filed signal at ~ δ 1.30, arising from the methyl groups of Rha residues. The complete assignments of the ^{1}H and ^{13}C chemical shifts of the OPS were possible based on 2D TOCSY (mixing times, 30-150 ms), NOESY (200 ms), and HSQC experiments (Table S2.2). Comparison of TOCSY spectra with increasing mixing time allowed the assignments of sequential order of the chemical shifts belonging to the same spin system. Residues **A**, **B**, **C**, **D**, **E** and **H**, with short H-1 tracks (only H-2 is seen) and the typical H-6 signals for 6-deoxyhexoses, represent the Rha residues. The complete spin system of residues **F** and **G** was indicative of a *xylo*-configuration. In addition, the 2D TOCSY (150 ms), NOESY (200 ms) and ^{1}H-^{13}C HSQC spectra showed the predominant signals for **H** residue (Fig. S2.1A). The TOCSY **H** H-1 track (δ 5.10) showed cross-peak with **H** H-2, whereas the resonances for **H** H-2,3,4,CH_3 were found via H-2 track. The ^{13}C NMR data demonstrated a downfield position of **H** C-2 at δ 79.3, suggesting 2-substituted α-Rha*p* (51). The NOESY inter-residue cross-peak of **H** H-1, with another **H** H-2, indicated a

H(1-2)**H** linkage. Based on methylation analysis and 1D/2D NMR data, the major polysaccharide present in fraction III is a linear α1-2 linked rhamnan (Fig. 2.3C1).

In addition to homopolymer (**H**) NMR signals, five minor anomeric signals belonging to α-Rha*p* (residues **A**-**E**) and β-Xyl*p* (residues **F** and **G**) were identified. Residues **A** and **C** were assigned to 2-substitituted α-Rha*p* (downfield shift of **A** C-2 at δ 79.3 and **C** C-2 δ 79.6), and the residue **D** was identified as 3-substitituted α-Rha*p* (downfield shift of **D** C-3 at δ 76.2). The signals for C-2 (δ 79.6) and C-3 (δ 76.2) of residues **B** and **E** were both shifted downfield indicating the presence of 2,3-disubstituted α-Rha*p*. ^{13}C chemical shifts of residues **G** and **F** were consistent with terminal β-Xyl*p* (51). The 2D NOESY inter-residue cross-peaks (Fig. S2.1B) allowed assignment of the glycosyl sequence of second polymer. In particular, 2-substitution of **A** and **C** residues was reflected by **D** H-1/**A** H-2 and **E** H-1/**C** H-2, cross-peaks, respectively. Furthermore, NOE cross-peaks between **C** H-1/ **B** H-3, **A**1 H-1/**B** H3, **G** H-1/**B** H-2 and **B** H-1/ **E** H-3, **F** H-1/**E** H-2 provided information about the location of branching positions of residues **B** and **E**. The 3-substitution of residue **D** was observed by the inter-residue connectivity of **B** H-1/**D** H-3. The absence of downfield glycosylation shift at C-2 carbon of residue **D** (δ 69.7) supports the occurrence of 3-substituted residue **D**. Combining all analytical data, a repeat unit of the second polymer consists of -α-L-rhamnan backbone substituted with either two or one β-D-Xyl residues (Fig. 2.3C2 and C3). This penta-/tetra-repeat lacks the strict regularity owning to nonstoichiometric substitution with a side terminal Xyl.

Figure 2.3. O antigen composition and structure analysis

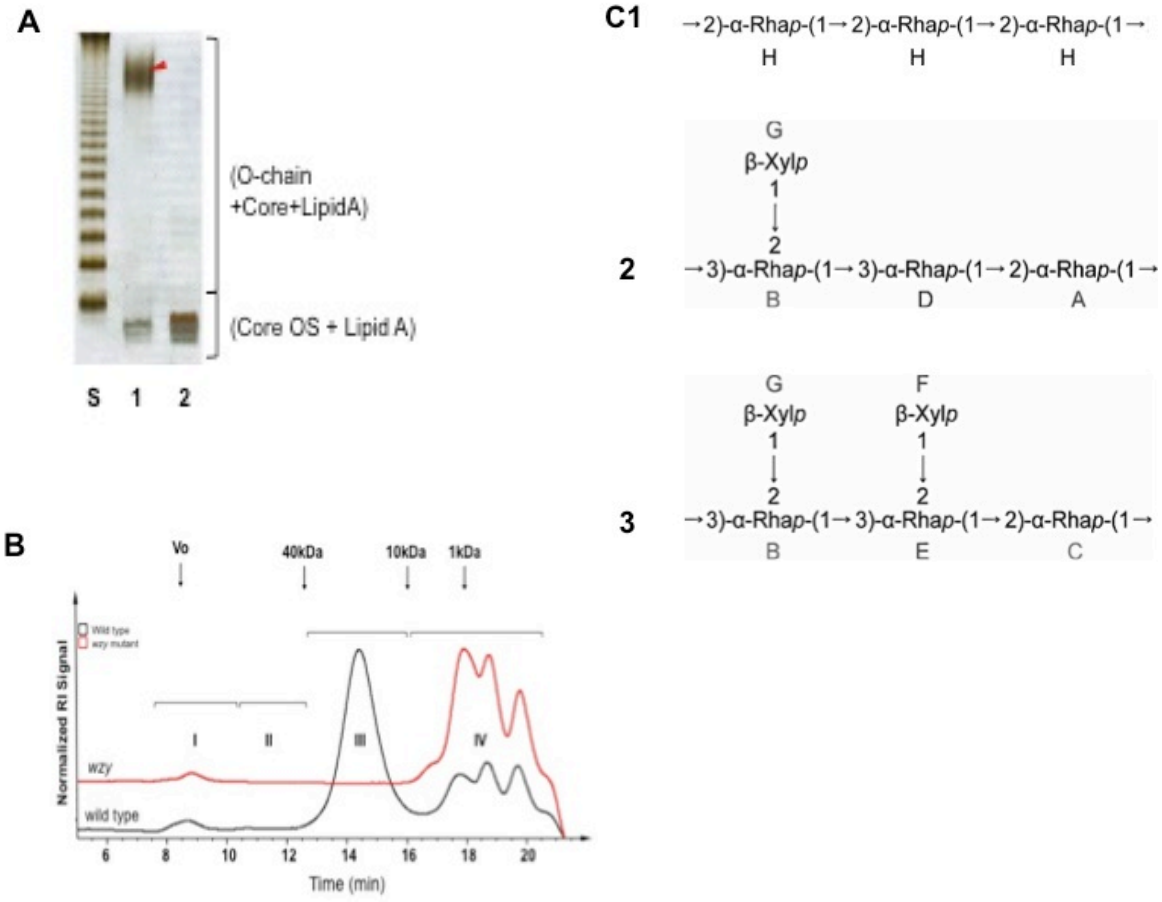

(A) DOC-PAGE analysis of LPS isolated from *X. fastidiosa* wild type and *wzy* mutant. Lane S = *Salmonella enterica* s. Typhimurium, smooth LPS; Lane 1 = Wild type; Lane 2 = *wzy* mutant. Red arrow indicates the presence of high molecular weight O antigen that is not observed in the *wzy* mutant LPS. **(B)** SEC chromatograms of polysaccharides liberated from LPS of *X. fastidiosa* wild type (black) and *wzy* mutant (red). Standard dextrans of 40,000, 10,000 and 1,000 Da were used for calibration of the Superose 12. **(C1)** The structure of *X. fastidiosa* wild type O antigen polymer is composed primarily of a linear α1-2 linked rhamnan. A repeat unit of the second polymer consists of -α-L-rhamnan backbone substituted with either one **(C2)** or two **(C3)** β-D-Xyl residues. O antigen from the *wzy* mutant is predicted to contain a single rhamnose residue.

O antigen structural alterations modulate the intensity of the oxidative burst. In the intact bacterial cells, much of the lipid A-core complex is embedded in the outer membrane. Thus, to explore the effects of O antigen structural alterations on the elicitation of PTI in the biological context of intact cells, we evaluated *X. fastidiosa* cell-induced production of ROS in grapevine leaves *ex vivo*. Although both wild type and *wzy* mutant cells induced oxidative bursts in the leaf discs, the mutant triggered a more intense oxidative burst, with ROS production peaking around 10 min and persisting nearly 80 min (Fig. 2.4A). The wild type bacteria failed to produce a sharp peak of ROS as compared to the *wzy* bacteria, and production plateaued around 60 min. In addition, total ROS production (expressed as area under the curve) was significantly larger in response to *wzy* mutant cells as compared with wild type (Fig. 2.4B). This result substantiates our hypothesis that lack of the O antigen shield modifies perception of *X. fastidiosa* cells upon introduction into the host, resulting in swifter and more intense PTI responses.

The O antigen-modulated oxidative burst is largely localized within xylem vessels *in vivo*. To determine where ROS production was localized *in situ*, we performed DAB (3,3*'*-diaminobenzidine)-mediated tissue printing of grapevine petioles that were inoculated with wild type *X. fastidiosa*, *wzy* mutant, or 1X PBS buffer as a control. DAB reacts with H_2O_2, which is the major ROS associated with the oxidative burst in plants (52), to produce a reddish-brown color. Grapevines inoculated with the *wzy* mutant exhibited more intense H_2O_2 production prominently localized in the xylem vessels (Fig.

2.5A), indicating that these vines are actively responding to the changes occurring in the xylem. Further quantitative comparison of staining intensity amongst the treatments, using ImageJ, indicated that, indeed, *wzy* elicits more intense production of ROS in the xylem than does the wild type *X. fastidiosa* (Fig. 2.5B).

Because the intensity of the *wzy*-induced ROS burst in the xylem may have a direct antimicrobial activity against *X. fastidiosa*, we performed an H_2O_2 survival assay. We chose a final concentration of 100μM H_2O_2 based on the lower threshold of ROS detected by the DAB staining method (DAB staining detects H_2O_2 in the range of 100μM – 10mM) (53). In addition, to mirror the kinetics of peak ROS production seen *in vivo*, we exposed the cells to H_2O_2 for ten minutes. Both wild type and *wzy* mutant cells were affected by treatment with hydrogen peroxide, but significantly fewer *wzy* mutant cells survived (10.1%), compared with wild type cells (50.2%) (Fig. 2.5C).

Tylose formation in response to wild type and *wzy* mutant infection. Tyloses are vascular occlusions that are outgrowths of the xylem parenchyma cell into the vessel lumen. These are commonly initiated by *X. fastidiosa* infection. Tylose formation occurs later in the infection process, and the abundant tyloses observed in PD-infected vines exacerbates symptoms (15). We examined PD symptoms and tylose formation in grapevines at 18 weeks post-inoculation with wild type or *wzy* mutant *X. fastidiosa* cells, compared with 1X PBS control vines. *Wzy* mutant-inoculated vines rated a 2 or below, representing a few leaves exhibiting marginal necrosis; wild type-inoculated vines rated over 3, representing over half of the vine exhibiting foliar necrosis; and 1X PBS controls

Figure 2.4. O antigen-modulated ROS production *ex vivo* by intact bacterial cells

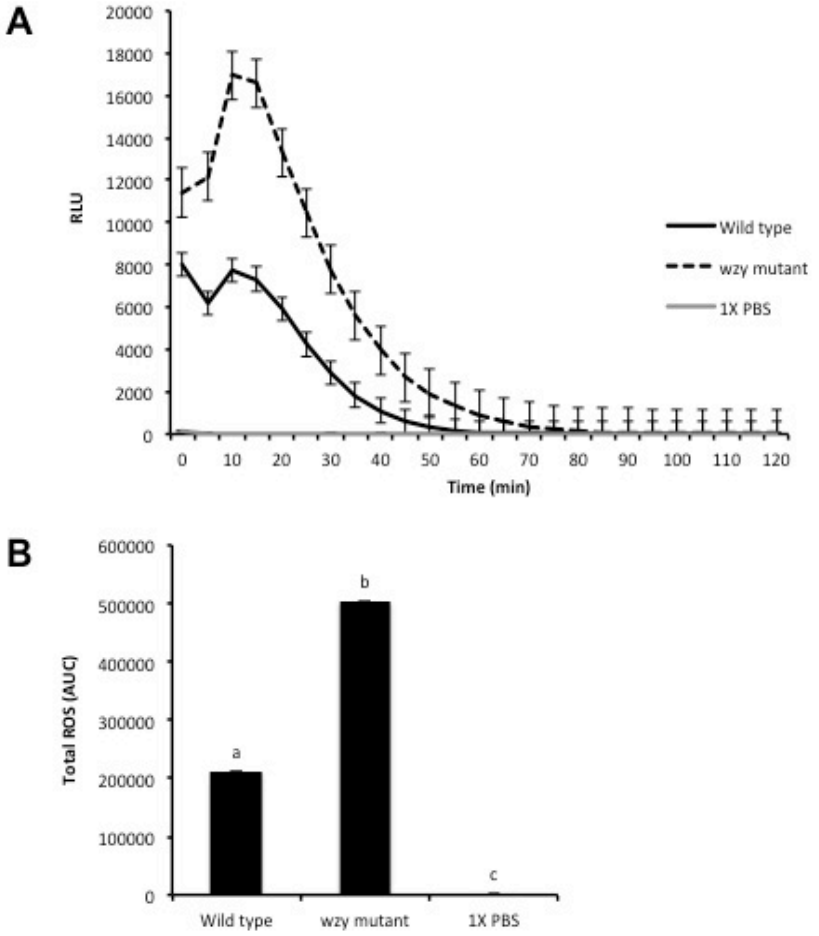

Discs of *V. vinifera* 'Cabernet Sauvignon' leaves were treated with 20µL of a 10^8 CFU/mL suspension of *X. fastidiosa* wild type or *wzy* mutant cells, or a 1X PBS control. **(A)** *Wzy* mutant cells induced a significantly stronger oxidative burst that persisted nearly 20 minutes longer than leaves inoculated with wild type bacteria (which contained fully polymerized O antigens). Graph represents the mean of 24 replicates per treatment ± standard error of the mean. **(B)** Total ROS production is reported as area under the curve (AUC) for plot of luminescence intensity over time. Treatments with different letters over the bars are statistically different ($P < 0.05$).

Figure 2.5. *In situ* localization of O antigen-modulated ROS production in the xylem

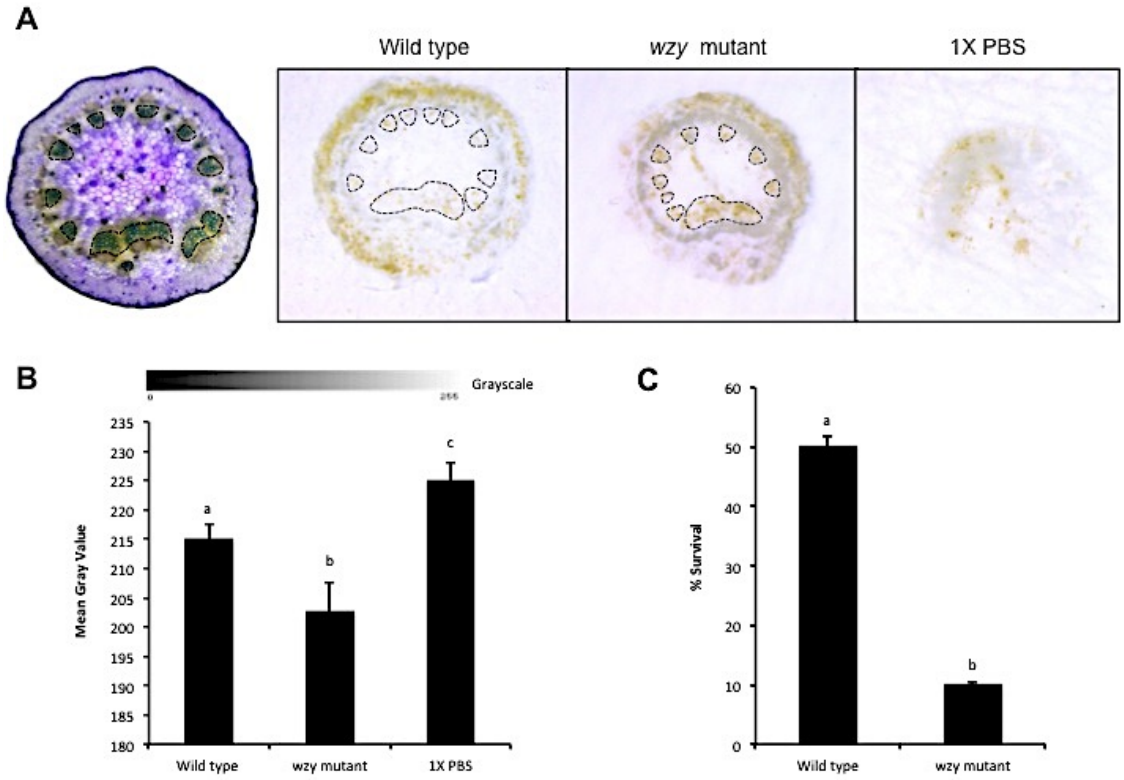

(A) DAB-mediated tissue printing at 15 minutes post-inoculation revealed a strong production of H_2O_2 specifically in the xylem vessels of grapevines inoculated with *wzy* mutant cells. Vines inoculated with wild type *X. fastidiosa* exhibited H_2O_2 production predominantly in peripheral collenchyma tissue, with some production in the xylem vessels. Vines inoculated with 1X PBS buffer served as negative controls. **(B)** Mean gray value of DAB-stained images, representing differences in staining intensity. Grayscale intensities vary from 0 to 255; 0 = black, 255 = white, and the values in between are shades of gray. The mean gray value of DAB-stained images from *wzy* mutant-inoculated plants is significantly lower than wild type or 1X PBS-inoculated plants, indicating a darker, or more intense stain, and thus higher amounts of H_2O_2. Treatments with different letters over the bars are statistically different ($P < 0.05$). **(C)** Suspensions of *X. fastidiosa* wild type or *wzy* mutant cells were incubated with 100µM H_2O_2 for 10 min, followed by dilution plating and enumeration. Survival percentages of *wzy* mutant cells were significantly lower than *X. fastidiosa* wild type cells ($P < 0.0001$). Following treatment with H_2O_2, 10.1% and 50.2% of *wzy* and wild type cells survived, respectively. Data are means of three biological replications.

rated 0, showing no PD symptoms (Fig. 2.6 panel A). We observed marked differences in the abundance of tyloses in response to wild type vs *wzy* mutant-inoculated plants. In wild type-inoculated vines, tyloses were present in nearly all xylem vessels (Fig. 2.6 panel B), and vessels were often completely occluded with multiple tyloses (Fig. 2.6 panel C). In contrast, *wzy* mutant-inoculated vines contained very few tyloses. In the case where a tylose was present, it was often one large tylose that only partially occluded the vessel. All control vines, inoculated with 1X PBS, were free of occlusions.

Callose and suberin deposition in response to wild type and *wzy* mutant infection. In addition to tyloses, the plant vascular tissue can initiate additional reinforcement of the cell walls to limit bacterial growth in infected plants. This includes callose and suberin deposition (54). Light microscopy of infected stems revealed widespread deposition of callose in the phloem tissue of *X. fastidiosa* wild type-infected plants (Fig. 2.7, arrow), suggesting communication between the xylem and phloem regarding the presence of *X. fastidiosa*. In addition, there was a pronounced deposition of suberin associated specifically with tylose-occluded vessels (Fig. 2.7*). In contrast, *wzy* mutant-infected plants showed little to no evidence of either callose or suberin deposition in the vascular tissue, and these plants looked similar to 1X PBS control plants.

Figure 2.6. Tylose development in PD-infected grapevines

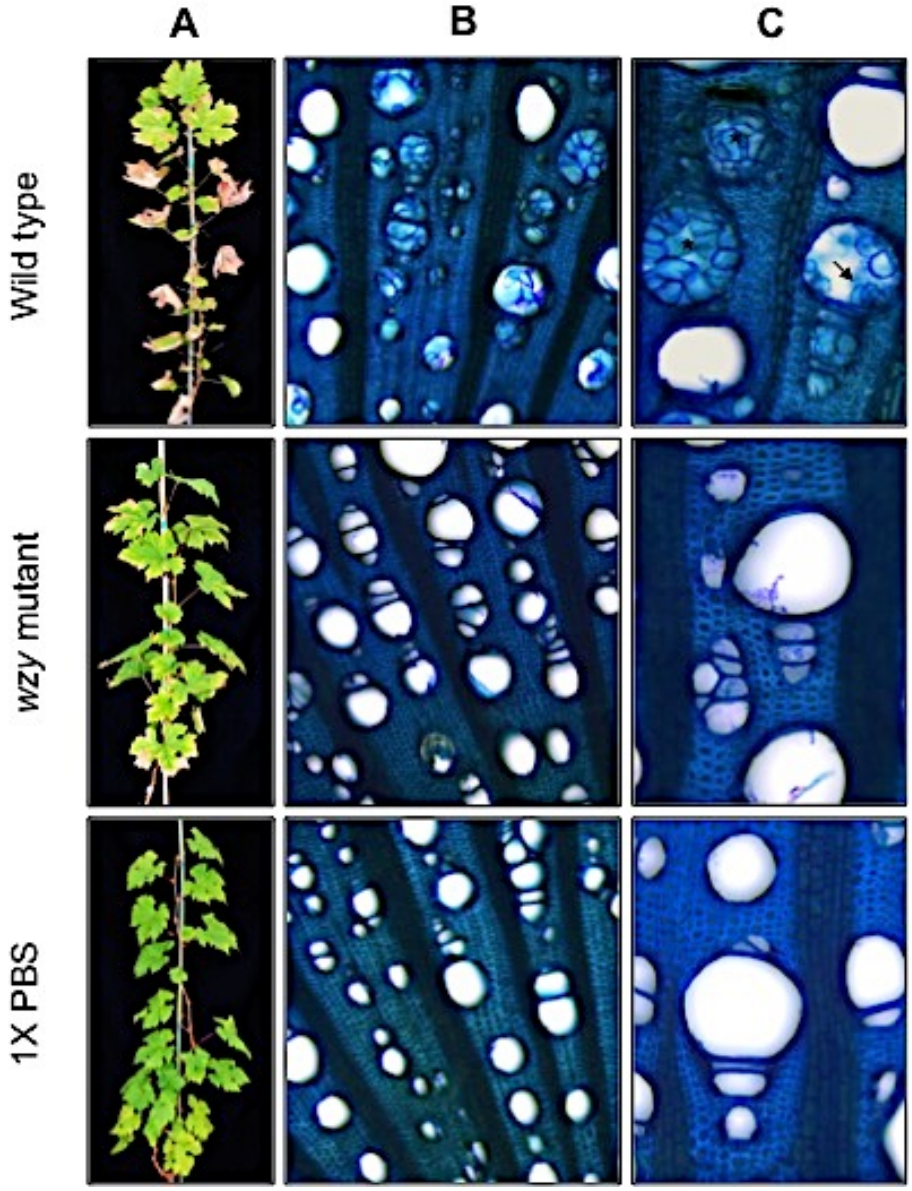

Images represent grapevines at 18 weeks post-inoculation, inoculated with wild type *X. fastidiosa* cells, *wzy* mutant cells, or 1X PBS buffer. **(A)** Representative images of PD progress prior to histological examination. **(B)** Micrograph showing tylose production in cross sections of grapevine xylem (brightfield stained with Toluidine Blue O). **(C)** Close-up of xylem vessels showing complete occlusion with multiple tyloses (*) in wild type-inoculated vines. A few small tyloses also occurred in these vines (closed arrowheads). Tyloses were largely absent in the xylem vessels of *wzy* mutant-inoculated vines. No tyloses were present in the stems of 1X PBS-inoculated vines.

Figure 2.7. Callose and suberin deposition are more prevalent in wild type-infected vines

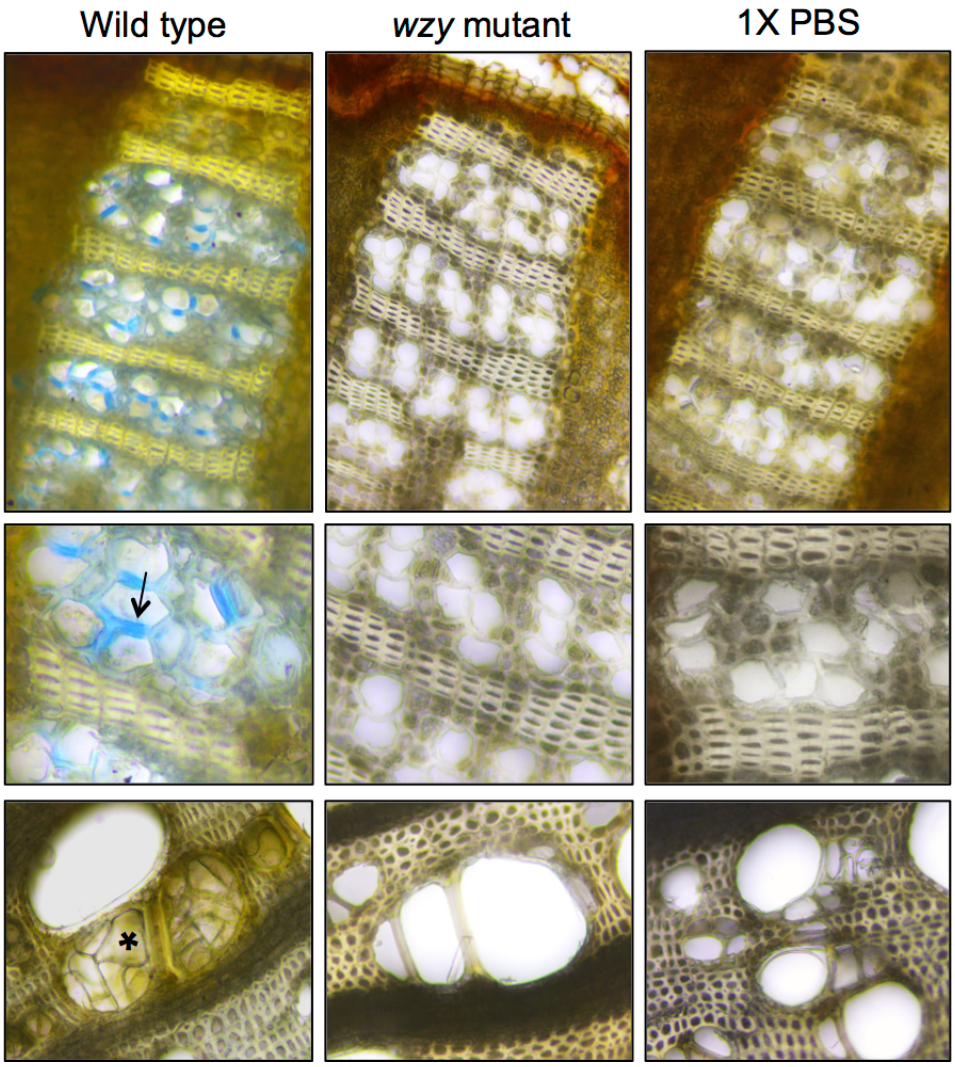

Images represent grapevines at 18 weeks post-inoculation, inoculated with wild type *X. fastidiosa* cells, *wzy* mutant cells, or 1X PBS buffer. Wild type-inoculated plants exhibited widespread callose deposition in the phloem tissue (appears as blue color, indicated by arrow). In addition, there was pronounced deposition of suberin in xylem vessels (indicated by gold color), especially in vessels with multiple tyloses (*). No callose or suberin was present in the stems of *wzy* or 1X PBS-inoculated vines.

Transcriptomic analyses of early grapevine responses to *X. fastidiosa* wild type and *wzy* mutant strains. To elucidate the early plant immune responses to *X. fastidiosa* at the transcriptional level, we performed an RNAseq experiment on grapevines inoculated with wild type, *wzy* mutant, or 1X PBS buffer (controls). Our initial priming study indicated that the O antigen-modulated response was most active at 4 h post-inoculation and tapered at 24 h post-inoculation. Previous studies investigating laminarin-induced defense genes in grapevine demonstrated that transcript accumulation of specific PR genes was not detectable until 10 h post-treatment, with some genes not reaching peak expression until 20 h post-treatment (46). Thus, in an effort to encompass a range of potential grapevine defense responses, RNAseq analyses were conducted using petioles collected at 8 h and 24 h post-inoculation. A total of 4,559 grape genes presented significant differential expression (DE, $P < 0.05$) as a result of *X. fastidiosa* challenge, when their expression in *X. fastidiosa*-inoculated vines (i.e. wild type or *wzy* mutant) was compared against that in the 1X PBS controls. DE genes that represent up-regulations were further classified into groups I to IX according to their patterns of expression (Fig. 2.8A). Significant correlation ($r = 0.71$, $P = 1.37\times10^{-06}$) between RNAseq and qRT-PCR data was detected when we examined the expression of a subset of genes from all groups that showed up-regulation in response to wild type and *wzy* mutant cells (Table S2.3). Functional pathways induced as a result of inoculations with wild type or *wzy* mutant cells were determined by enrichment analysis ($P < 0.05$) of functional categories in the groups of up-regulated genes (Fig. 2.8B,C).

Group I corresponded to 200 genes significantly up-regulated only in response to the *wzy* mutant at 8 h post-inoculation, but not to inoculation with wild type cells. Notably, genes associated with plant responses to biotic stresses were predominantly enriched in this group. This included the enhanced expression of several pathogenesis related (PR) genes, including two *PR-1* precursors (*VIT_03s0088g00700, VIT_03s0088g00710*), β-1,3 glucanase (*PR-2*) (*VIT_08s0007g06040*), a class 4 chitinase (*PR-3*) (*VIT_05s0094g00330*), *PR-4* (chitinase) (*VIT_14s0081g00030*), *PR-10* (*VIT_05s0077g01530*) and *PR-10.3* (*VIT_05s0077g01530*) (55). Additional *PR* genes included three genes involved with the production of thaumatin and a polygalacturonase-inhibiting protein, *PGIP 1* (*VIT_13s0064g01370*). The expression of genes performing antioxidant functions (e.g., thioredoxins and glutaredoxins) and ROS-scavenging enzymes (e.g., peroxidases and catalases) were also induced early in response to *wzy*. Specifically, there were three Class III peroxidases (*VIT_18s0001g06840*; *VIT_18s0001g06850*; *VIT_18s0001g06890*). These enzymes are among the enzymes that accumulate in abundance in xylem sap during colonization by vascular pathogens (4, 56). Their functions include specific roles in defense against pathogen infection, such as enhanced production of ROS (as signal mediators and antimicrobial agents) and enhanced production of phytoalexins (57). Most importantly, the up-regulation of these peroxidase genes corroborates our phenotypic data of an enhanced and dynamically different production of ROS in *wzy*-inoculated plants. Group I was also enriched in plant secondary metabolic pathways, which produce a variety of antioxidants and/or phytoalexins. There was an increase in the expression of enzymes contributing to

phenylpropanoid biosynthesis, such as a stilbene synthase (*VIT_16s0100g01200*) and a chalcone reductase (*VIT_05s0077g02150*) connected with production of flavonoids. Genes associated with Salicylic Acid (SA)-mediated defense pathways were enriched, indicating that the *wzy* mutant is activating distinct phytohormone signaling pathways beginning at 8 h post-inoculation. In addition, the up-regulation of *PR-1* genes (which are known markers of SA) further supports the role of SA in activating defenses against *X. fastidiosa* attack. These enriched pathways were strikingly absent in wild type-inoculated vines at this time point (Fig. 2.8B).

There were over 800 genes in group IV, which corresponded to transcripts specifically up-regulated at 8 h post-inoculation in response to wild type *X. fastidiosa* cells. Interestingly, these genes were enriched ($P < 0.05$) primarily in responses to abiotic or general stresses (i.e., drought, oxidative, temperature, and wounding stresses) rather than biotic stresses and were not directly related to immune responses, as was observed in the *wzy* mutant-inoculated plants. Group IV included numerous genes functioning in plant cell wall modification and metabolism, including pectinesterases, polygalacturonases (PGs), expansins, and a xyloglucan endotransglucosylase/hydrolase (XTH). The up-regulation of a PG-coding gene (*VIT_01s0127g00400*) at 8 h post-inoculation with the wild type strain was further validated by qRT-PCR (Table S2.3). XTH enzymes have been implicated in the early events of abiotic stress responses, including induction by drought and in response to the stress hormone ethylene, whereas PGs have been shown to be involved in tylose formation (58). Enrichment of genes associated with ethylene biosynthesis and signaling as well as numerous ethylene-

responsive transcription factors (ERF1, ERF003, ERF011, ERF related to APETALA2) were also observed in wild type-inoculated plants 8 h post-inoculation. In the context of PD, ethylene has also been linked to tylose production, which requires extensive reorganization of plant cell walls (59). Up-regulation of these genes supports our phenotypic data indicating an increase in tylose formation in wild type-inoculated plants. The concomitant up-regulation of cell wall modification enzymes and ethylene biosynthetic genes indicates that the transcriptional cascade leading to tylose production likely initiates very early in the infection process, while phenotypic evidence of abundant tylose production occurs later in the infection process (60). There was also an enrichment of genes encoding components of the lignin (e.g. laccases) and suberin biosynthetic pathways that were unique to wild type-inoculated plants at this time point. Both lignin and suberin are important for wound healing and fortification of the xylem walls. Suberization can also help prevent unnecessary water loss during drought stress (61). Up-regulation of these genes supports our phenotypic data indicating an increase in suberin deposition in wild type-inoculated plants. There were also genes enriched in general stress responses and responses related to dehydration, indicating that the plant is, in part, initially perceiving wild type *X. fastidiosa* infection as water stress (abiotic) rather than pathogen (biotic) stress (17).

At 24 h post-inoculation, 164 genes were significantly up-regulated specifically in response to the *wzy* mutant (Group II), and there were 746 genes that showed significant up-regulation in response to wild type cells at this time point (Group V). Grapevines inoculated with wild type cells continued to express a number of genes related to plant

cell wall modification/metabolism, including pectinesterases and expansins. Interestingly, enrichment of polysaccharide metabolism pathways included 2 genes functioning specifically in callose biosynthesis (callose synthase, *VIT_13s0156g00210* and 1,3-beta-glucan synthase, *VIT_19s0138g00120*). This demonstrates that the production of callose is initiated very early in the infection process and supports our phenotypic data indicating a pronounced deposition of callose in the phloem of wild type-inoculated plants heavily infected with PD. In addition to continued responses to abiotic stress, there were a large number of genes enriched in responses to biotic stress at this time point, indicating that at this later time point of 24 hr, grapevines are now perceiving and responding to *X. fastidiosa* as a biotic invader, as opposed to solely an abiotic stress. Enriched pathways included those specific to plant-pathogen interactions, i.e. NBS-LRR superfamily genes. An abundance of genes enriched in secondary metabolic pathways, such as phenylpropanoid and flavonoid biosynthesis pathways, were also present at this time point. There was consistent enrichment of genes belonging to ethylene-mediated signaling pathways, in addition to JA, auxin, and ABA signaling pathways. All of these pathways, including those related to biotic and abiotic stress, were distinctly enriched in wild type-inoculated vines and were not enriched in *wzy*-inoculated vines at the 24 hr time point (Fig. 2.8C).

These data indicate that grapevines differentially perceive *wzy* mutant cells compared to wild type cells. Perception of the *wzy* mutant activates early defense networks associated with biotic stresses involved in the swift activation of PTI responses,

in particular a robust production of ROS and downstream SA-mediated defense pathways that were not observed in plants inoculated with wild type *X. fastidiosa*.

Temporal dynamics of transcriptional responses to *X. fastidiosa* wild type or *wzy* mutant strains in local and systemic tissue. To characterize trends of gene expression over time, and in local (POI) and systemic tissue following infection by wild type and *wzy* bacteria, we performed additional RNAseq analyses on petioles collected at 48 h, 1 week, and 4 weeks post-inoculation, in addition to 1X PBS controls. Grape genes with significant DE ($P < 0.05$) at distinct time points post-inoculation were determined by pair-wise comparisons between each type of inoculation, time point, and tissue type (local or systemic) against the respective PBS-inoculated control. We then defined 26 clusters based on the patterns of expression of the DE grape genes across the three time points (Fig. 2.9A). For example, C05 (Cluster 5) contains DE genes that are up-regulated at 48 hours post-inoculation, but then have steady expression at 1 week and 4 weeks post-inoculation as compared to the 1X PBS negative control. By performing enrichment analysis in the gene clusters ($P < 0.05$), we identified over-represented functions related to plant immune responses that were distinct to each inoculation and tissue types (Fig. 2.9A,B).

Genes encoding key facets of SA-mediated signaling pathways (*Enhanced disease susceptibility 1* (*EDS1*) genes, *VIT_17s0000g07370* and *VIT_17s0000g07420*) were uniquely expressed in local tissue of *wzy*-inoculated plants; these genes had steady

Figure 2.8. Grapevine responses to early infection by *wzy* mutant or wild type *X. fastidiosa*

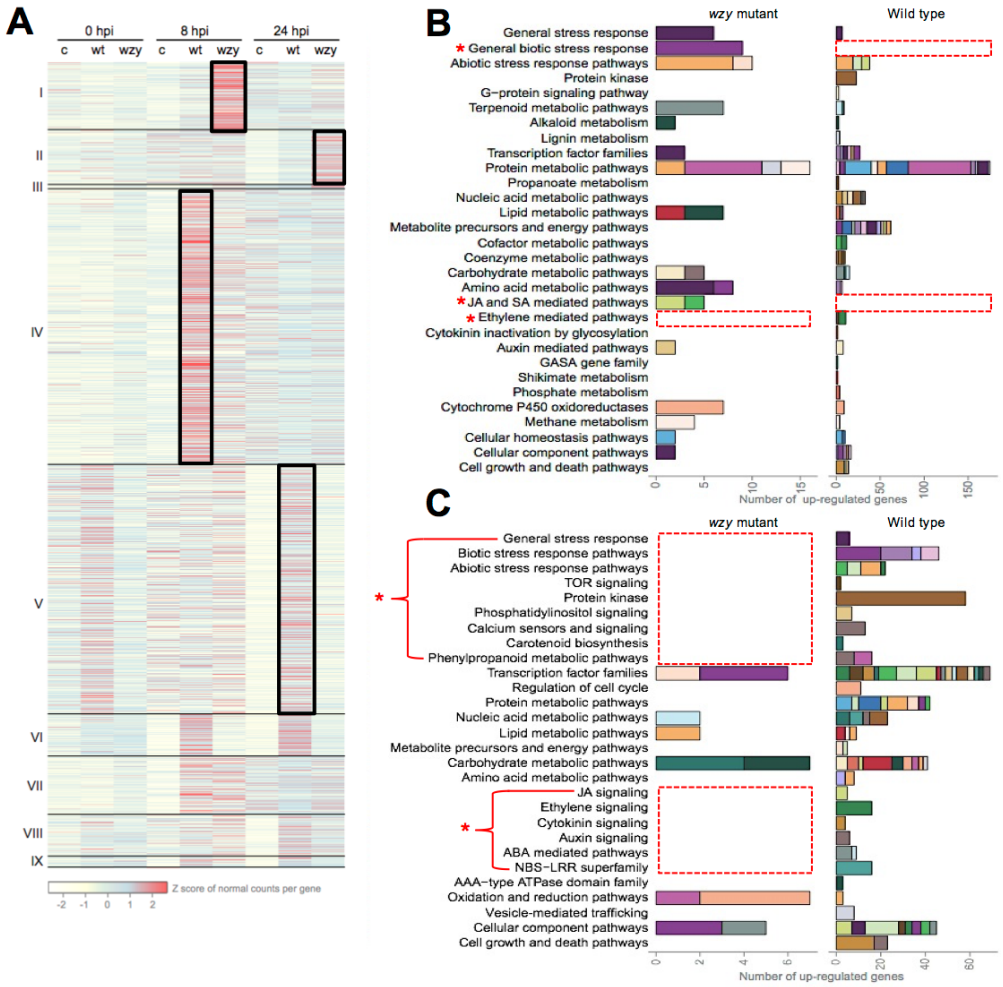

(A) Up-regulated grape genes ($P < 0.05$) in response to *wzy* mutant (wzy) or wild type (wt) bacteria at 8 and 24 hours post-inoculation (hpi) when compared to 1X PBS controls (c). Genes are classified into nine groups (I - IX) based on their expression pattern. The colors in the heat map represent the Z score of the normal counts per gene, and black boxes represent gene groups distinctly up-regulated in response to each treatment and time point. **(B)** Enriched grape functional pathways ($P < 0.05$) among genes up-regulated during wzy (Group I) or wt (Group IV) infections at 8 hpi. **(C)** Enriched grape functional subcategories ($P < 0.05$) among genes up-regulated during wzy (Group II) or wt (Group V) infections at 24 hpi. Colored stacked bars represent individual pathways. Red boxes highlight functions of interest (*) that are enriched in one treatment, but not enriched in the other at each time point.

expression at 48 h and 1 week post-inoculation and then were up-regulated at 4 weeks post-inoculation (C25). EDS genes encode proteins associated with the SA pathway and have been implicated in grapevine defenses against powdery mildew (62). Furthermore, a *PR-1* gene (*VIT_11s0052g01620*) was up-regulated at 48 h post-inoculation and then steadily expressed in systemic tissue. Consistent up-regulation of SA-associated genes in both local and systemic tissues at these later time points of inoculation with the *wzy* mutant, as well as very early time points (8 h) as described above, suggests that induction of SA-mediated pathways is not only maintained over time, but also systemically activated throughout the plant in response to *X. fastidiosa* lacking its O antigen shield. Systemic induction of the SA-mediated defense pathways was not evident in wild type inoculated plants. Instead, wild type cells induced genes associated with JA-mediated defense pathways in local tissue. This included 9 genes encoding proteins functioning in the metabolism of alpha-linolenic acid, which serves as an important precursor in the biosynthesis of JA (63). These genes had steady expression at 48 h and 1 week post-inoculation and then were up-regulated at 4 week post-inoculation (C25).

Enrichment analyses of *wzy*-responsive genes that were unique to systemic tissues revealed genes associated with drought stress response pathways, namely 14 genes enriched in ABA signaling (C05). Genes enriched in lignin metabolism exhibited peak expression levels at 1 week post-inoculation with *wzy* mutant, but remained steady at 4 weeks post-inoculation (C20). Lignin metabolism has been linked to coping with drought stress (64). This is in contrast with what was observed in wild type-inoculated vines where drought stress-related and lignin metabolism pathways were up-regulated much

earlier in the infection process (8 h post-inoculation). This suggests that perception of the abiotic stresses that accompany *X. fastidiosa* infection occur much later in plants inoculated with the *wzy* mutant.

Enrichment analysis of wild type-responsive genes in systemic tissue revealed genes encoding ERF transcription factors that were up-regulated at 4 weeks post-inoculation (C25), demonstrating that activation of ethylene-mediated signaling occurs throughout the infection process (early at 8 hpi and also later time points) in both local and systemic tissue. Similar to the trend seen with SA in response to *wzy* mutant cells, this consistent up-regulation of ethylene-related genes in response to wild type cells suggests that induction of ethylene-mediated signaling pathways is not only maintained over time, but also systemically activated throughout the plant in response to *X. fastidiosa* containing its O antigen shield. Stimulation of ethylene-mediated signaling may promote the prolific production of tyloses formed in wild type-inoculated vines (Fig. 2.6) (15, 65). At 1 week post-inoculation, genes enriched in JA-mediated signaling pathways were uniquely up-regulated in systemic tissue of wild type-inoculated vines, and expression continued to increase at 4 weeks post-inoculation (C19). This consistent enrichment and up-regulation provides further support for the role of JA in grapevine responses to wild type *X. fastidiosa* (17). Our findings established that this phytohormone pathway is initiated within the first 24 h of the infection process and that stimulation of the JA pathway is consistently maintained in both local and systemic tissues of wild type inoculated plants. In addition, 7 genes enriched in callose biosynthesis were uniquely up-regulated at 1 week post-inoculation with wild type cells (C20), and expression remained

steady at 48h and 4 weeks post-inoculation. This is over half of the total callose-related genes in the genome. These results confirmed our phenotypic data indicating that callose deposition in the phloem occurs late in the infection process (Fig. 2.7).

Fig 2.9. Temporal dynamics of transcriptional responses to *X. fastidiosa* wild type or *wzy* mutant strains in local and systemic tissue

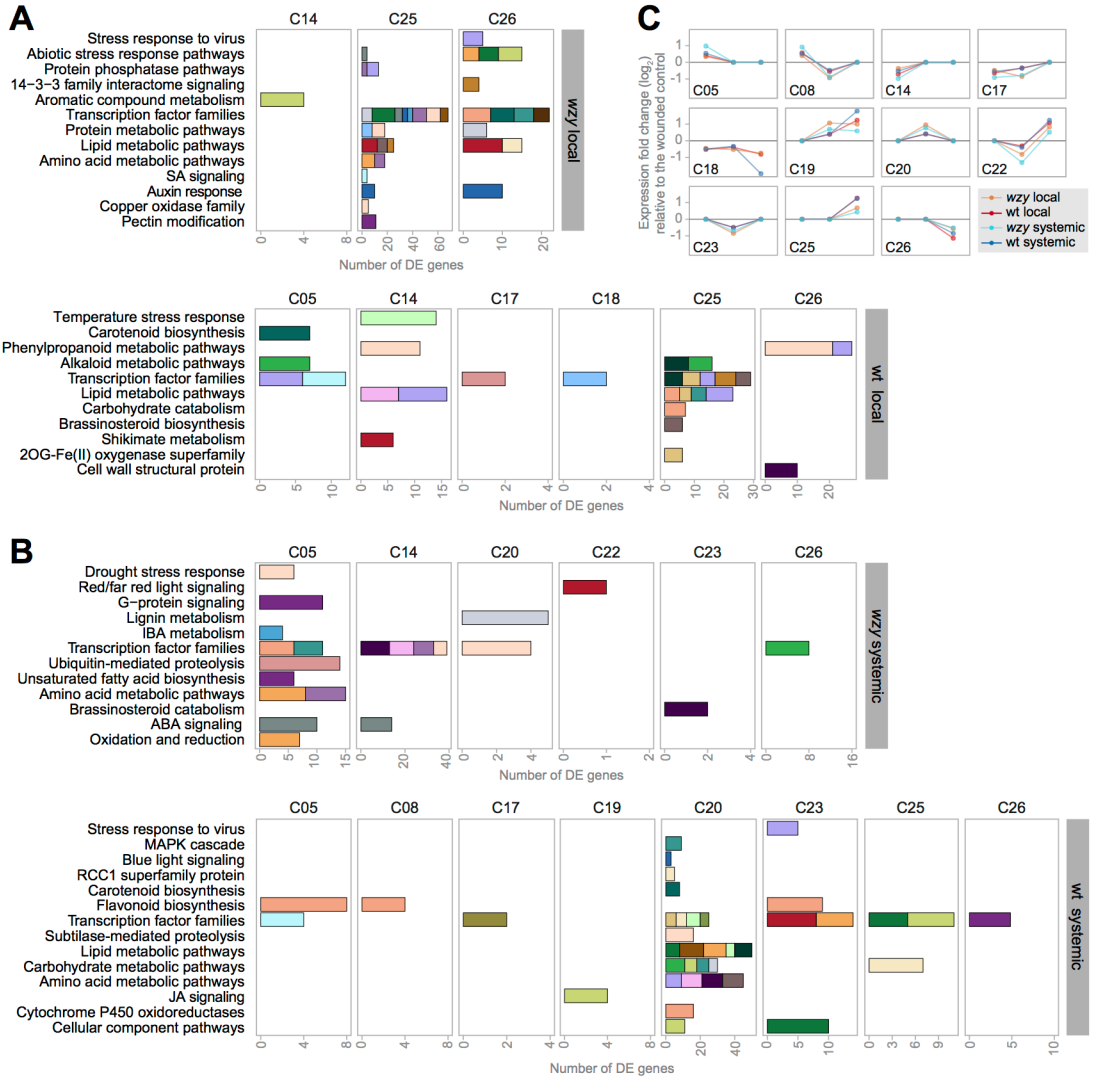

Enriched grape functional pathways ($P < 0.05$) in differentially expressed (DE) gene clusters representing local **(A)** or systemic **(B)** responses to *X. fastidiosa* inoculation. Only enriched pathways related to grapevine immune responses and that were unique to wild type (wt) or *wzy* mutant inoculations are depicted. Colored stacked bars represent individual pathways. **(C)** Patterns of expression of gene clusters enriched in functional pathways with biological relevance. Lines represent the medoids for each cluster. Dots represent expression fold changes of each medoid (log2) at a given time point post-inoculation (in order: 48 h, 1 week, and 4 weeks) when compared to 1X PBS controls.

DISCUSSION

Xylem-limited pathogens occupy a highly specialized ecological niche. For *X. fastidiosa*, this specialization is further compounded by the fact it resides solely in two unique environments: in its plant hosts and in the mouthparts of its insect vectors. Therefore, it utilizes distinct mechanisms to maintain its dual lifestyle. Successful pathogens must contend with the plant immune system, and despite the fact that *X. fastidiosa* lacks Type III-secreted effectors to combat plant basal defense responses, it succeeds in causing several destructive diseases in commercial agriculture. However, the molecular basis of this has yet to be explored. Plants have evolved to recognize the molecular architecture of the bacterial cell surface, specifically through the perception of conserved PAMPs. Alterations in these conserved microbial signatures, and thus alterations in the structure and composition of the bacterial cell surface, can significantly alter plant host perception of pathogens. LPS is the most dominant macromolecule on the surface of Gram-negative bacteria. Due to its abundance, it has been implicated in many bacteria-host interactions. Previous studies have demonstrated the role of LPS, and more specifically O antigen, in bacterial evasion of innate immune responses in mammals (66, 67), but this mechanism is rarely observed in the context of plant pathogens. In this study, we demonstrate that O antigen is a novel mechanism used by *X. fastidiosa* to delay immune recognition in a susceptible grapevine host, thus contributing to the establishment of a compatible interaction and pathogenesis.

Structural analysis of the *X. fastidiosa* O antigen in wild type cells revealed that it is a linear α1-2 linked L-rhamnan polymer. The production of this polymer was abolished

in *wzy* mutant cells. Although mutations in LPS can often affect the production of other cell surface polysaccharides, namely exopolysaccharide (EPS), we did not observe any differences in EPS production between the *wzy* mutant and wild type *X. fastidiosa*. Thus, we are confident that we can attribute the observed phenotypes solely to presence or lack of O antigen. Many phytopathogenic bacteria display O antigens that consist primarily of oligorhamnans, which can vary in D or L configuration (68). However, the heterogeneous population of O antigen, demonstrated by the presence of additional minor polymers containing ß-D-xylose substitutions on the main α-L-rhamanan backbone in wild type cells, was unexpected. Some mammalian bacterial pathogens, namely *Pseudomonas aeruginosa*, are able to concomitantly synthesize two types of O antigen, termed A and B band, which serve different functions for the cell. The A band consists of a conserved homopolymer, while B band structure varies among the several different serotypes of *P. aeruginosa* (69, 70). Further analysis is currently underway to determine if these polymers are autonomous on the cell surface (i.e. attached to separate lipid A-core) or if they are attached to the same core as the primary α-L-rhamanan backbone.

The oxidative burst is a critical, early plant response to pathogen infection (52) and contributes to resistance by inhibiting bacterial growth. It consists of a rapid, intense production of ROS (e.g. superoxide anions and H_2O_2), which are toxic compounds with antimicrobial properties (52). In response to cells lacking the O antigen, grapevines induced a robust oxidative burst that was prominently localized within the xylem tissue compartment, while wild type cells (containing a long chain O antigen) elicited a significantly muted oxidative burst. We reason that wild type *X. fastidiosa* has evolved

this long chain O antigen to successfully shield itself (namely PAMPs on the cell surface) from the grape innate immune system, thus attenuating these responses. The production of ROS localized specifically in the xylem was very striking.

Xylem vessels are non-living at maturity. Therefore, the oxidative burst is presumably originating from the adjacent living, metabolically active, parenchyma cells that are sensing the changes in the xylem vessels (9, 71). To obtain quantitative and temporal data regarding the kinetics of the oxidative burst elicited by the mutant, we conducted an *ex vivo* luminol-based assay using whole cells. The data mirrored those from the *in vivo* DAB staining assay; specifically, the cells of the *wzy* mutant induced a significantly stronger and more prolonged burst of ROS from leaf discs than those from the wild type strain. In addition, total ROS production was significantly larger in response to the mutant, compared with the wild type parent. The detection threshold for DAB stain is 100μM H_2O_2, thus, giving a rough estimate of the lower limit of H_2O_2 present in the xylem vessels of vines inoculated with the *wzy* mutant. Remarkably, 90% of *wzy* mutant cells did not survive treatment with 100μM H_2O_2, indicating that the production of ROS induced by the O antigen mutant is at a concentration high enough to significantly reduce bacterial populations *in planta*. The *wzy* mutant is compromised in xylem colonization and is more sensitive to exogenous oxidative stress than wild type. However, these cells still reach a population threshold to be isolated from local tissue (not systemic) (33). Taken together with the transcriptomic and phenotypic data from the study presented here, we establish that elicitation of a robust oxidative burst plays a critical role in killing large numbers of invading *wzy* bacteria that are lacking the

camouflage of the long chain O antigen. We hypothesize that this, combined with the production of additional defense responses and the activation of specific phytohormone signaling pathways (which can initiate resistance in systemic tissues), significantly impairs colonization attempts by these mutant cells. Conversely, the weak production of ROS shown during the compatible wild type *X. fastidiosa*-grapevine interaction is ineffective at preventing pathogen ingress.

Grapevines responded very differently to wild type *X. fastidiosa* cells during the early stages on infection. Rather than eliciting hallmarks of responses to biotic stresses as the *wzy* mutant did, wild type cells elicited physiological responses related to abiotic stresses, namely drought stress. Specifically, there was induction of a wide range of genes whose products are known to function in drought stress tolerance, including the induction of genes associated with the biosynthesis of abscisic acid (ABA), an important mediator of water-stress adaptation (72). Choi et al (2013) demonstrated the upregulation of ABA-associated genes in grapevines at 4 weeks post-inoculation with *X. fastidiosa*, prior to the onset of PD symptoms (17). Our results further corroborate their hypothesis that *X. fastidiosa* has a strong impact on physiological parameters related to drought stress, and we demonstrate that these transcriptional changes are initiated within 8 h post-introduction. Furthermore, beginning at 8 h post-inoculation, wild type-inoculated vines induced a range of transcripts related to plant cell wall modification, including the production of numerous cell wall-degrading enzymes such as polygalacturonases (PGs), expansins, and a xyloglucan endotransglucosylase/ hydrolase (XTH). XTH enzymes have been implicated in the early events of abiotic stress responses, and in addition to

expansins, their expression has been shown to be strongly enhanced by ethylene (73, 74). Perez-Donoso et al (2007) established that PD-infected vines produce more ethylene than healthy vines, and exposing grapevines to ethylene mimicked some of the hallmark plant responses associated with *X. fastidiosa* infection (59). These included host-derived vascular occlusions, such as tyloses, the formation of which requires extensive plasticity and reorganization of the plant cell wall. It has been hypothesized that *X. fastidiosa*-induced ethylene plays a role in the signaling process that initiates the formation of host-derived vascular occlusions, which are implicated in exacerbating PD symptoms (59). Tyloses are the predominant type of occlusion that forms in grapevines with differing PD resistances. Sun et al (2013) demonstrated that tyloses formed throughout PD-susceptible grapevines, with over 60% of vessels becoming fully occluded, whereas tyloses occurred in less than 20% of vessels in PD-resistant vines (15). Histological examination of tylose formation in wild type and *wzy* mutant treatments further confirmed this observation, with the majority of xylem vessels in the susceptible, wild type-inoculated vines exhibiting complete occlusion with multiple tyloses. In contrast, *wzy* mutant-inoculated vines, which exhibited fewer PD symptoms, contained very few tyloses, which only partially occluded vessels.

We observed the formation of additional physical defenses in response to wild type cells, which were not present in *wzy* mutant-inoculated vines, such as a pronounced deposition of suberin in vessels occluded with multiple tyloses. Suberin deposition is an established plant defense response to vascular wilt pathogens (75). Interestingly, this is the first evidence of suberin deposition associated with the *X. fastidiosa*-grapevine

interaction. The primary role of suberization is linked to water retention (76). This is based on knowledge that (i) suberization involves the deposition of a significant amount of waxes (the removal of which results in an increase in water permeability) (77, 78) and (ii) that suberization occurs primarily in tissues that do not form a cuticle (79, 80). Beginning at 8 h post-inoculation, *X. fastidiosa* wild type-inoculated vines expressed numerous APETELA2-domain and ethylene response element binding proteins, which have been shown to influence wax levels and permeability (61). Suberin has also been implicated specifically in antimicrobial defenses, preventing lateral colonization of other vascular pathogens such as *Verticillium spp*. (81). Therefore, in the context of PD development, it is likely that suberization serves to mitigate unnecessary water loss from the xylem and may act as an additional physical barrier, attempting to block systemic spread of *X. fastidiosa*.

We also present the first visual evidence of callose deposition associated with the *X. fastidiosa*-grapevine interaction. Interestingly, callose deposition was observed in the phloem, indicating there is likely communication between the xylem and phloem in the context of a xylem-limited *X. fastidiosa* infection. In addition to tyloses and lignin, callose is an important defense mechanism in plants. One callose synthase (*VIT_13s0156g00210*) was upregulated at 24 h post-inoculation, in response to wild type *X. fastidiosa.* As the infection progressed, we observed nearly 60% of the total callose-related genes in the genome uniquely up-regulated in systemic tissue in response to wild type cells. The resulting differences in deposition between the treatments were further confirmed histologically. Callose deposition has been documented in grapevine in

response to foliar pathogens, such as powdery mildew (*Erysiphe necator*) (82), but has not been demonstrated to be part of the grapevine's response to *X. fastidiosa* infection. It has long been hypothesized that sharpshooter discrimination against PD-infected, symptomatic vines is due largely to vector preference: that is, sharpshooters perceive symptomatic vines as poor quality hosts (83). Because sharpshooters must process enormous amounts of xylem sap to meet their nutritional needs, it has been speculated that sharpshooters associate PD symptoms with increased xylem tension and disruption in hydraulic conductivity, which impinges on their ability to effectively pump xylem sap. Indeed, Daugherty et al. demonstrated that sharpshooters do not discriminate between healthy and infected (asymptomatic) vines, which would likely contain low populations of *X. fastidiosa*. However, sharpshooters were less likely to alight on vines exhibiting PD symptoms (83). Our results demonstrate the presence of callose when wild type-inoculated vines exhibited significant levels of leaf scorching. Therefore, we speculate that callose deposition also contributes to sharpshooter discrimination against symptomatic vines, because they would encounter additional obstructions during stylet penetration. Although many additional experiments would need to be performed to confirm this event, this may contribute to the model of *X. fastidiosa* vector preference.

Overall, the RNAseq data indicated that grapevines readily perceive *wzy* mutant cells lacking the O antigen shield as a biotic stress to the system and activate specific defense responses (primarily those contributing to ROS production, phytoalexin biosynthesis, and *PR* gene induction) within 8 hours upon recognition. These responses were not observed in response to wild type cells at this time point. In contrast, grapevines

responded to wild type *X. fastidiosa* cells containing the long chain O antigen as a general or abiotic stress as early as 8 h post-inoculation, particularly related to a disruption in hydraulic conductivity. This suggests that even at these very early stages of infection, the plant perceives vascular invasion by wild type *X. fastidiosa* as a threat to hydraulic function and is preparing itself for drought stress. This is further supported by the deposition of suberin later in the infection process. Notably, at 24 h post-inoculation, grapevines began responding to wild type cells as a biotic threat and initiated defense responses such as the production of phytoalexins and other antimicrobial compounds. Furthermore, these vines were actively trying to prevent systemic spread of the pathogen through the production of structural barriers, such as tyloses and callose. This indicates that *wzy* infection fails to elicit the sectors of the immune system related to initiation of tylose formation as compared to wild type *X. fastidiosa*. We speculate that this occurs because the *wzy* mutant is arrested during the early infection stages via a PTI-mediated mechanism and, thus, does not proliferate within the xylem as successfully as wild type *X. fastidiosa*. In fact, *wzy* populations are significantly lower (2.3×10^5 CFU/g tissue) than wild type populations at 14 weeks post-inoculation (33). Therefore, the biological kinetics of disease progress are altered in *wzy*-infected plants, providing the plant an opportunity to reduce bacterial titer. We propose that in wild type cells, O antigen shields the underlying PAMPs located on the cell surface, therefore altering early plant host recognition of *X. fastidiosa* and thus avoiding the production of a potentially lethal oxidative burst. This, combined with the ability of cell surface polysaccharides to act as a

permeability barrier (preventing the entry of toxic ROS into the cell) (84), allows the wild type bacteria to colonize to high population levels without detrimental impediment.

Vascular pathogens live deep in the interior of their host plants, studies into their biology are complicated. However, understanding the biology of vascular pathogens and the molecular mechanisms underlying plant defense against these pathogens is crucial for the design of novel management strategies. Plant defenses are triggered by a variety of elicitors (85, 86), and pre-treatment of plants with purified LPS elicitor can potentiate the defense system resulting in an enhanced response to subsequent pathogen attack (20, 47, 87). This defense-related memory is called defense priming and stimulates the plant to initiate a faster and/or more aggressive response against future invading pathogens (42). Priming often results in an oxidative burst, nitric oxide synthesis and expression of defense-related genes, which resemble the induced defenses we observed in plants treated with the *wzy* mutant (35, 87). An LPS PAMP has been specifically implicated in priming in the *X. campestris* pv. *vesicatoria* pathosystem. Pepper leaves pre-treated with the LPS isolated from an incompatible (non-virulent) xanthomonad had enhanced expression of several PR proteins after being challenged with virulent *X. campestris* pv. *vesicatoria* (35). The rapid release of H_2O_2 is generally assumed to be a key event in the orchestration of various cellular defense responses and is a well-described response of plant cell suspensions to molecules with eliciting activities (88). In our study, pre-treatment of vines with either *wzy* or wild type LPS primed grapevines to be more tolerant to *X. fastidiosa*. We employed a ROS assay to further examine the activity of the elicitor. When LPS was liberated from wild type and *wzy* mutant cells and purified, there

was little difference in the degree of elicitation of the oxidative burst between the treatments, which could explain why the priming results were similar. It is possible that the potent elicitor is actually the lipid A-core portions of the molecule, which would be exposed in both wild type and *wzy* mutant LPS in this situation, as the molecule has been liberated from the cells. However, in the context of intact cells, O antigen would serve to shield these portions in wild type cells. In the context of perennial plants such as grapevines, a primed state can persist across multiple growing seasons, which is commonly referred to as delayed induced resistance (89, 90). In grapevine, the LPS-mediated primed state is transient and appears to be lost following 24 h pre-treatment. We plan to explore repeated applications of LPS to determine if we can extend the primed state. Through understanding the molecular basis of innate immune resistance, we are exploiting the power of ROS induction by the LPS elicitor to reveal novel therapeutic targets for the creation of more sustainable methods of PD protection. Genetic resistance is the best strategy for controlling vascular wilt pathogens (4). This study has provided the starting point from which we can begin to unravel the mechanisms that contribute to the primed state, and identifying these defense genes could be an important step towards obtaining grapevine resistant varieties through breeding or genetic engineering.

MATERIALS AND METHODS

Bacterial strains and growth conditions. We used the wild type *X. fastidiosa* strain Temecula1 (91) and a *wzy* mutant strain (33). *X. fastidiosa* wild type and *wzy* mutant strains were grown for 7 days at 28°C on solid PD3 medium without or with kanamycin at 5μg/mL, respectively.

Isolation and purification of LPS and core-O-specific polysaccharide. Crude LPSs were isolated from *X. fastidiosa* wild type and *wzy* mutant bacterial cell pellets via the hot phenol-water extraction procedure (92). Dialyzed phenol and water phases (3500 MWCO) were freeze-dried and washed with 9:1 (v/v) ethanol in water at 4°C. Nucleic acids and proteins were removed by overnight treatment with RNase and DNase (37°C), followed by overnight incubation with Proteinase K (37°C) and dialysis (2000 MWCO) at 4ºC against several exchanges of dH_2O. Dialysate of LPS was ultracentrifuged at 100,000 × *g* at 4ºC for 18 h and recovered from the pellet. Intact LPS was dissolved in 0.1M EDTA H4/ 0.3M TEA (pH7) and resolved on Superose 12 10/300 GL (GE Healthcare Life Sciences) FPLC column assembled with AKTA system (Amersham Biosciences) with 50 mM ammonium acetate buffer (pH6.7) used as eluent with 0.5 ml/min flow. Eluted fractions were recorded with a refractive index (RID-10A, Shimadzu) and multiple wavelength (λ=210, 254 and 280 nm; AKTA system) detectors, respectively. LPS fractions were LPS was resolved on 18% acrylamide using deoxycholic acid (DOC) detergent (93), followed by silver staining using the Bio-Rad Silver Staining Kit (Bio-Rad). Optionally, gel was stained with alcian blue (94), followed by silver

staining. Void volume LPS fraction was used for O-chain separation and comparative chemical and structural studies. Carbohydrate moiety of LPS was liberated from lipid A by 1.5 hour mild hydrolysis in 1% HOAc (v/v) at 100°C and recovered from supernatant after 20min centrifugation at 5000×*g*, at 30°C. Similarly to LPS, free O antigen moiety was dissolved in 50 mM ammonium acetate buffer (pH6.7) and chromatographed on Superose 12 10/300 GL (see description above). Fractions were collected based on response from refractive index detector.

Glycosyl composition of LPS and linkage analysis of O-chain polysaccharides (OPS). The glycosyl and fatty acid composition of the LPS was determined by the preparation of trimethylsilyl (TMS) methylglycosides after methanolysis with 1M methanolic HCl at 80 ºC for 18 h, in the presence of an internal standard of inositol and analyzed by GLC-MS (95, 96). Obtained derivatives were analyzed on Hewlett-Packard HP5890 gas chromatograph equipped with mass selective detector 5970 MSD using EC-1 fused silica capillary column (30m × 0.25 mm I.D.) and the following temperature program: 80ºC for 2 min, then increased to 160ºC at 20ºC/min, and to 200ºC at 2ºC/min followed by an increase to 250 °C at 10°C/min with an 11 min hold.

OPS polysaccharides were hydrolyzed with 2M TFA (120°C, 2 h) and converted to alditol acetates (AAs) by conventional methods (97) . Glycosyl linkage of OPS was determined after hydrolysis with 2M TFA at 121ºC, overnight reduction with $NaBD_4$ and conversion to partially methylated alditol acetates (PMAA) (97, 98). GLC-MS analysis was performed on an HP-5890 GC interfaced to a mass selective detector 5970 MSD

using a Supelco SP2330 (30m× 0.25 mm ID) capillary column with temperature program: 80ºC for 2 min, then increased to 170ºC at 30ºC/min, and to 235ºC at 4ºC/min with a 20 min hold. Absolute configuration of O-chain monosaccharides were determined by comparative GLC analysis of the trimethylsilylated (-)-2-butyl glycosides with that of authentic monosaccharide standards (99, 100) using an Equity-1 fused silica capillary column and GC-MS condition similar with analysis of TMS methyl glycosides.

1D and 2D nuclear magnetic resonance spectroscopy. Polysaccharide samples were exchanged twice with 99.9% D_2O and finally dissolved in 100% D_2O (Cambridge Isotope Laboratories, Andover, MA) to a final concentration of approximately 2.5 mg/mL (for main recovered fractions from wild type and *wzy* mutant). 1D proton and 2D (^{1}H -^{1}H TOCSY, ^{1}H-^{13}C-HSQC, -HMBC) spectra were acquired at 25°C with standard "Presat" solvent signal suppression on a Varian 600 MHz spectrometer equipped with a 3 mm cold probe (Varian, Inova Palo Alto, CA) . The NMR acquisitions were processed using MNova software (Mestrelab Research, Santiago de Compostela, Spain). The spectra were referenced relative to the DSS signal (δ_H=0 ppm; δ_C=0 ppm).

LPS extractions for ROS assays and plant defense priming. LPS extractions were performed based on the method of Marolda et al. (101), with some modification. Briefly, *X. fastidiosa* cells were grown on solid PD3 medium for 7 days at 28°C. Following incubation, cells were harvested with 1X PBS buffer and spun down to form dense pellets. Cell pellets were stored at -80°C until LPS extractions. Prior to LPS extractions,

cell pellets were washed 2x with 1X PBS buffer and suspended in 300µL Solution A (0.05M Na_2HPO_4 x $7H_2O$, 0.005M EDTA; pH 7) + 40µL Proteinase K (Qiagen #19131). Suspensions were incubated overnight at room temperature. LPS was extracted from cell pellets using a hot phenol/water method and resulting LPS was further purified using dialysis (MWCO 1 kD). Following purification, LPS was quantified using the Purpald Assay (102).

ROS assays. Leaf discs (1/8") were punched from *Vitis vinifera* 'Cabernet Sauvignon' grapevines. Discs were placed into individual wells of a 96-well microtiter plate (Costar; Fisher Scientific, catalog #3912), with each well containing 200µL H_2O. Discs were allowed to sit overnight at room temperature, in the dark. The following day, 200µL reactions were performed within each well and contained 2µL of a 100nM stock of luminol and 20µL of a 10^8 CFU/mL suspension of *X. fastidiosa* cells or 20µL of purified LPS (50µg/mL final concentration). Water or 1X PBS negative controls were used for LPS or cell suspensions, respectively. Reactions were initiated by the addition of 1µL of 1mg/100µL stock of horseradish peroxidase, and relative luminescence was measured in a Tecan Infinite F200 plate reader. Assay was performed in triplicate. Total ROS production was determined by calculating the area under the curve for each treatment, and data was analyzed using the Kruskal-Wallis test for nonparametric one-way ANOVA. Prior to the test, data were checked for normality and homogeneity of variance and did not meet these criteria. Post hoc comparisons amongst the treatments used Mann-Whitney U tests at $P = 0.05$.

***In situ* localization of *X. fastidiosa*-induced H_2O_2.** This procedure was adapted from the methods of Liu et al. (103). Briefly, nitrocellulose membrane (0.45µm in pore size) was soaked in 5mg/mL DAB-HCL solution (pH 3.8) and then dried at room temperature for 30 min in the dark. Tissue printing was performed at ~20°C. At 15 min post-inoculation with wild type *X. fastidiosa, wzy* mutant cells (40µL of 10^8 CFU/mL suspension), or a 1X PBS buffer control, petioles were removed, and freehand sections were made of approximately 1mm thickness using a razor blade (completed within 5 sec). The sections were gently pressed onto the impregnated nitrocellulose membrane for 10 sec. The membrane was washed with 100% EtOH to remove any possible inhibitors and photographed under a stereomicroscope (M165C, Leica Microsystems CMS GmbH, Wetzlar, Germany) after 5 min at room temperature. Image analysis was conducted using the NIH program, ImageJ, according to the methods of Bunderson, et al (2004) (104). Briefly, the DAB stained images were converted to grayscale and then minimum and maximum threshold values were established to remove background staining. Finally, mean gray values for each treatment were calculated and analyzed by one-way ANOVA. Prior to the test, data were checked for normality and homogeneity of variance and met these criteria. Post hoc comparisons amongst the treatments used Tukey's honestly significant difference (HSD) test at $P = 0.05$.

H_2O_2 survival assay. *X. fastidiosa* wild type or *wzy* mutant cells were grown on solid PD3 medium, without or with kanamycin at 5µg/mL, for 7 days at 28°C. Following incubation, cells were harvested with 1X PBS buffer and adjusted to OD_{600} 0.25 (10^8

CFU/mL). Treatments consisted of 500µL of cell suspension and 500µL of 1X PBS, with or without the addition of 5µL of 100µM H_2O_2 (final concentration). Suspensions were incubated at 28ºC at 100rpm for 10 min and then immediately placed on ice. The resulting suspension was diluted and plated onto solid PD3 medium according to standard methods. Percent survival was determined as the number of CFU/mL in treated cells divided by the number of CFU/mL in untreated cells (without H_2O_2), multiplied by 100. Prior to the test, data were checked for normality and homogeneity of variance and did not meet these criteria. Comparisons amongst the treatments used Mann-Whitney U tests at $P = 0.05$.

Histology

Tylose development in PD-infected grapevines. Stem sections of *Vitis vinifera* 'Cabernet Sauvignon' were harvested at 18 weeks post-inoculation with *X. fastidiosa* wild type, *wzy* mutant culture, or a 1X PBS negative control. Tissue was fixed in 80% ethanol prior to histological examination. Freehand sections were made of approximately 100µm, stained with Toluidine Blue O (0.05%), and observed using a brightfield microscope (DM4000, Leica Microsystems CMS GmbH, Wetzlar, Germany).

Suberin and callose deposition in PD-infected grapevines. Stem sections of *Vitis vinifera* 'Cabernet Sauvignon' were harvested at 18 weeks post-inoculation with *X. fastidiosa* wild type, *wzy* mutant culture, or a 1X PBS negative control. Tissue was fixed in 80% ethanol prior to histological examination. Freehand sections were made of

approximately 100μm and stained with Sudan III (0.2%), followed by Aniline Blue (0.05%), and observed using a brightfield microscope (DM4000, Leica Microsystems CMS GmbH, Wetzlar, Germany).

Plant inoculations. *Vitis vinifera* 'Cabernet Sauvignon' vines were needle-inoculated (105) with either *X. fastidiosa* wild type, *wzy* mutant, or 1X PBS buffer control. Cells of *X. fastidiosa* strains were harvested from plates of PD3 media in 1X PBS buffer, and suspensions were adjusted to OD_{600} 0.25. Each vine was inoculated twice (with a 20μL drop) on the main stem. For RNAseq experiments, petioles were harvested at each time point and then immediately placed into liquid nitrogen. Petioles were stored at -80°C, and before RNA extraction, the frozen tissue was ground to a fine powder using stainless steel beads in a TissueLyser II (QIAGEN Inc., USA) for 30 s at a frequency of 30/s.

RNA extraction and sequencing. Total RNA was extracted from 0.1g of ground tissue per sample. The frozen tissue was homogenized by inversion in 500 μl of extraction buffer (PureLink Plant RNA Reagent, Ambion cat# 12322-012) for 5 min at room temperature. After homogenization, 100μl of Plant RNA isolation Aid (Ambion cat# AM9690) was added to the suspension and mixed by inversion for 5 min at room temperature. Samples were centrifuged at top speed for 5 min at room temperature to pellet insoluble debris and other contaminants. The supernatant was transferred to a new tube and then 100μl of 5M NaCl and 300μl chloroform were added and mixed for 5 min by inversion. Samples were centrifuged at 12,000 xg for 10 min at 4^{o}C to separate the

phases, and the upper aqueous phase was transferred to a new tube. Samples were treated with DNase RNase-free (5 U) and incubated for 20 min at 37^{o}C. After DNase treatment, 500µl of chloroform was added and mixed for 5 min as described above. To separate the phases, the samples were centrifuged again at 12,000 xg for 10 min at 4^{o}C, and the upper aqueous phase was transferred to a new tube. An equal volume of isopropyl alcohol was added, after the samples were mixed by inversion and incubated at room temperature for 10 min. Precipitated RNA was centrifuged at 12,000 xg for 10 min at 4^{o}C, and the supernatant was discarded. The RNA pellets were washed with 1mL of 80 % ethanol and centrifuged at 12,000 xg for 2 min at room temperature. Then the pellets were air-dried at room temperature and re-suspended in 30µl RNase-free water. RNA quality was evaluated by gel electrophoresis, and quantity was determined using the Qubit fluorometer.

cDNA libraries were generated from mRNA and sequenced using an Illumina HiSeq 3000 platform. The sequencing of four HiSeq lanes generated a total of 763 million 50 bp single-end reads. Reads were trimmed and filtered to retain high-quality sequence information only (Q > 20). An average of 24.5 ± 3 millions of reads per sample (87.6±1.7% of the total) were unambiguously mapped on the reference PN40024 transcriptome. Counts were normalized to control for technical variation using DESeq2 (106), which was also used for statistical testing. Functional annotations and biological processes associated to the differentially expressed grape genes were obtained from VitisNet (https://www.sdstate.edu/ps/research/vitis/pathways.cfm) (107). The differentially expressed genes were classified according to inferred biological process and

molecular function, using the terminology and hierarchical relationships of the Gene Ontology (GO) consortium. Eighteen different GO categories were sufficient to describe our results. Enrichment analyses of grape biological processes were performed in R using a hypergeometric test with a significant cut-off of $P < 0.05$.

Quantitative reverse transcription PCR (qRT-PCR). cDNA was synthetized from 500ng of total RNA using M-MLV Reverse Transcriptase (Promega). qRT-PCR was performed on a StepOnePlus PCR System using Fast SYBR Green Master Mix (Applied Biosystems). The qRT-PCR conditions were as follows: 95°C for 10 min, followed by 40 cycles of 95°C for 3 s and 60°C for 30 s. *VvActin* (*VIT_04s0044g00580)* (108), was selected as reference gene to linearize the transcript levels for all genes of interest using the formula $2^{(\text{Reference gene CT} - \text{Gene of interest CT})}$ (109). Three biological replicates were tested per inoculated *X. fastidiosa* strain (wild type and *wzy* mutant) and each of the time points. The specificity was confirmed by analyzing the melting curves at temperatures ranging from 60-95 °C.

Supplemental Figure S2.1. 1D and 2D nuclear magnetic resonance spectroscopy

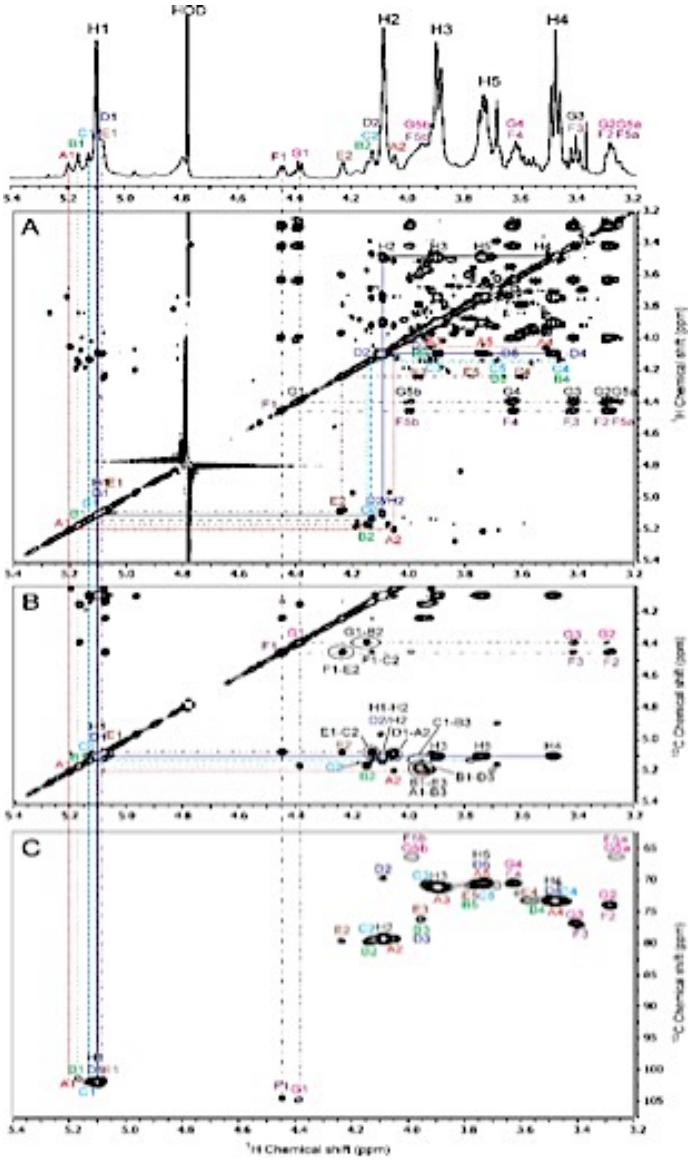

The 1D ^{1}H NMR and 2D TOCSY-150 ms (A), NOESY-200 ms (B) and HSQC spectra (C) of OPS, recorded in D_2O at 25°C. The CH_3 signals were observed at ~ δ 1.30, but were not included in the figure. Cross-peaks belonging to the same scalar-coupling network are indicated near dotted lines starting from the corresponding diagonal peaks.

Supplemental Table S2.1. Composition analysis of LPS isolated from wild type and *wzy* mutant *X. fastidiosa* cells

	Glycosyl Residues (Mol %)										
	Rib	Rha	Xyl	Man	Glc	GalA	GlcNAc (GlcN)	Kdo*	O-Me-CHO*	10:0(3OH) 10:0(2OH)*	12:0(3OH) 12:0(2OH)*
Wild type	-	82.2	12.0	1.5	1.6	2.3	0.3	+	+	+	+
wzy mutant	-	19.0	1.0	4.1	15.1	52.6	8.2	+	nd/tr	+	+

Not all glycosyl residues were quantified due to lack of unique standard. *Identified but not quantified; tr = trace; nd = non detected

Supplemental Table S2.2. ^{1}H and ^{13}C NMR chemical shifts of the O-polysaccharides, recorded in D_2O, at 25°C

	Residue	^{1}H / ^{13}C chemical shifts (δ)					
		1	2	3	4	5	6
A	→2)-α-L-Rha-(1→	5.20	4.05	3.92	3.51	3.74	1.31
		102.0	79.3	71.0	73.3	70.5	18.0
B	→2,3)-α-L-Rha-(1→	5.16	4.15	3.95	3.55	3.78	1.29
		101.2	79.6	76.2	73.2	70.5	18.0
C	→2)-α-L-Rha-(1→	5.13	4.13	3.92	3.46	3.71	1.28
		102.0	79.6	70.7	70.7	70.5	18.0
D	→3)-α-L-Rha-(1→	5.10	4.08	3.95	3.48	3.74	1.30
		102.0	69.7	76.2	73.3	70.5	18.0
E	→2,3)-α-L-Rha-(1→	5.08	4.23	3.96	3.58	3.78	1.29
		102.0	79.6	76.2	73.2	70.8	18.0
F	β-D-Xyl-(1→	4.45	3.28	3.40	3.62	3.98/3.26	-
		104.5	74.0	76.9	70.4	66.3	
G	β-D-Xyl-(1→	4.38	3.28	3.40	3.62	3.98/3.26	-
		104.7	74.0	76.9	70.4	66.3	
H	→2)-α-L-Rha-(1→	5.10	4.09	3.90	3.48	3.74	1.28
		103.2	79.3	71.1	73.3	70.5	18.0

Supplemental Table S2.3. Quantitative reverse transcription PCR (qRT-PCR) validation of RNAseq data

Group	Gene	Annotation	Comparison	Timepoint	RNAseq		qPCR	
					Fold change (log_2)	*P*	Fold change (log_2)	*P*
I	VIT_11s0052g01780	1-deoxy-D-xylulose-5-phosphate synthase	wt/Control	8 h	0.23	5.41E-01	0.16	7.09E-01
I	VIT_11s0052g01780	1-deoxy-D-xylulose-5-phosphate synthase	wzy/Control	8 h	1.64	9.79E-04	1.78	2.29E-01
I	VIT_11s0052g01780	1-deoxy-D-xylulose-5-phosphate synthase	wt/Control	24 h	0.05	8.30E-01	0.30	3.09E-01
I	VIT_11s0052g01780	1-deoxy-D-xylulose-5-phosphate synthase	wzy/Control	24 h	0.36	2.00E-01	0.33	1.95E-01
II	VIT_00s0253g00040	Monocopper oxidase SKS17 (SKU5 Similar 17)	wt/Control	8 h	0.42	5.01E-02	0.16	5.83E-01
II	VIT_00s0253g00040	Monocopper oxidase SKS17 (SKU5 Similar 17)	wzy/Control	8 h	0.16	5.17E-01	-0.17	8.14E-01
II	VIT_00s0253g00040	Monocopper oxidase SKS17 (SKU5 Similar 17)	wt/Control	24 h	0.35	1.53E-01	-0.35	1.21E-01
II	VIT_00s0253g00040	Monocopper oxidase SKS17 (SKU5 Similar 17)	wzy/Control	24 h	0.53	9.84E-03	0.06	8.70E-01
III	VIT_08s0040g02200	Peroxidase ATP2a	wt/Control	8 h	0.34	2.92E-01	-0.24	7.12E-01
III	VIT_08s0040g02200	Peroxidase ATP2a	wzy/Control	8 h	0.83	9.22E-01	0.78	4.03E-01
III	VIT_08s0040g02200	Peroxidase ATP2a	wt/Control	24 h	-0.07	3.93E-02	-0.87	3.06E-01
III	VIT_08s0040g02200	Peroxidase ATP2a	wzy/Control	24 h	0.76	2.02E-03	-0.46	3.26E-01
IV	VIT_01s0127g00400	Polygalacturonase GH28	wt/Control	8 h	5.33	3.41E-07	2.77	3.68E-02
IV	VIT_01s0127g00400	Polygalacturonase GH28	wzy/Control	8 h	2.48	6.83E-02	0.78	3.16E-01
IV	VIT_01s0127g00400	Polygalacturonase GH28	wt/Control	24 h	2.19	5.50E-02	2.50	1.62E-01
IV	VIT_01s0127g00400	Polygalacturonase GH28	wzy/Control	24 h	0.36	3.66E-01	0.94	1.19E-01
V	VIT_14s0060g00480	S-adenosylmethionine synthetase 1 (SAM1)	wt/Control	8 h	-0.51	2.35E-03	-1.01	1.12E-01
V	VIT_14s0060g00480	S-adenosylmethionine synthetase 1 (SAM1)	wzy/Control	8 h	-0.09	5.91E-01	-0.78	1.91E-01
V	VIT_14s0060g00480	S-adenosylmethionine synthetase 1 (SAM1)	wt/Control	24 h	0.25	5.00E-02	0.21	4.14E-02
V	VIT_14s0060g00480	S-adenosylmethionine synthetase 1 (SAM1)	wzy/Control	24 h	0.02	8.21E-01	0.12	7.01E-01
VI	VIT_13s0067g02360	Peroxidase, class III	wt/Control	8 h	1.75	7.37E-11	1.53	8.26E-02
VI	VIT_13s0067g02360	Peroxidase, class III	wzy/Control	8 h	1.25	2.02E-02	1.37	2.31E-01
VI	VIT_13s0067g02360	Peroxidase, class III	wt/Control	24 h	1.64	4.55E-03	0.62	1.78E-01
VI	VIT_13s0067g02360	Peroxidase, class III	wzy/Control	24 h	0.61	6.08E-02	0.34	4.45E-01
VII	VIT_11s0052g01650	Pathogenesis-related protein 1 precursor (PRP 1)	wt/Control	8 h	2.56	7.47E-11	1.77	1.13E-01
VII	VIT_11s0052g01650	Pathogenesis-related protein 1 precursor (PRP 1)	wzy/Control	8 h	1.39	9.12E-03	1.51	3.35E-01
VII	VIT_11s0052g01650	Pathogenesis-related protein 1 precursor (PRP 1)	wt/Control	24 h	-0.04	9.45E-01	0.23	5.56E-01
VII	VIT_11s0052g01650	Pathogenesis-related protein 1 precursor (PRP 1)	wzy/Control	24 h	-0.03	9.74E-01	0.66	5.90E-02
VIII	VIT_04s0008g00420	Clavata1 receptor kinase (CLV1)	wt/Control	8 h	0.19	5.95E-01	1.50	2.25E-01
VIII	VIT_04s0008g00420	Clavata1 receptor kinase (CLV1)	wzy/Control	8 h	0.05	9.15E-01	0.63	4.58E-01
VIII	VIT_04s0008g00420	Clavata1 receptor kinase (CLV1)	wt/Control	24 h	0.97	1.44E-08	1.82	1.59E-01
VIII	VIT_04s0008g00420	Clavata1 receptor kinase (CLV1)	wzy/Control	24 h	0.79	9.98E-06	1.12	1.38E-01
IX	VIT_11s0052g01150	Nicotianamine synthase	wt/Control	8 h	1.99	1.84E-07	0.40	3.78E-01
IX	VIT_11s0052g01150	Nicotianamine synthase	wzy/Control	8 h	1.22	8.84E-03	0.10	8.90E-01
IX	VIT_11s0052g01150	Nicotianamine synthase	wt/Control	24 h	1.77	1.03E-08	0.72	1.83E-01
IX	VIT_11s0052g01150	Nicotianamine synthase	wzy/Control	24 h	1.15	5.83E-03	0.14	7.91E-01

qRT-PCR validation of a subset of genes from the RNAseq study on early grapevine responses to wild type and *wzy* mutant *X. fastidiosa*. The results are shown as fold changes (log2), and the corresponding *P* values are provided.

LITERATURE CITED

1. **Jones JDG, Dangl JL.** 2006. The plant immune system. Nature **444:**323-329.

2. **Schwessinger B, Zipfel C.** 2008. News from the frontline: recent insights into PAMP-triggered immunity in plants. Current Opinion in Plant Biology **11:**389-395.

3. **Abramovitch RB, Anderson JC, Martin GB.** 2006. Bacterial elicitation and evasion of plant innate immunity. Nat Rev Mol Cell Biol **7:**601-611.

4. **Yadeta KA, Thomma BPHJ.** 2013. The xylem as battleground for plant hosts and vascular wilt pathogens. Frontiers in Plant Science **4**.

5. **Purcell AH, Hopkins DL.** 1996. Fastidious xylem-limited bacterial plant pathogens. Annual Review of Phytopathology **34:**131-151.

6. **Chatterjee S, Almeida RPP, Lindow S.** 2008. Living in two Worlds: The Plant and Insect Lifestyles of *Xylella fastidiosa*. Annual Review of Phytopathology **46:**243-271.

7. **Roper MC.** 2011. *Pantoea stewartii* subsp. *stewartii*: lessons learned from a xylem-dwelling pathogen of sweet corn. Molecular Plant Pathology **12:**628-637.

8. **Beckman CH.** 1964. Host responses to vascular infection. Annual Review of Phytopathology **2:**231-252.

9. **Hilaire E, Young SA, Willard LH, McGee JD, Sweat T, Chittoor J, Guikema JA, Leach JE.** 2001. Vascular defense responses in rice: peroxidase accumulation in xylem parenchyma cells and xylem wall thickening. Molecular Plant-Microbe Interactions **14:**1411-1419.

10. **Rep M, Dekker HL, Vossen JH, de Boer AD, Houterman PM, Speijer D, Back JW, de Koster CG, Cornelissen BJ.** 2002. Mass spectrometric identification of isoforms of PR proteins in xylem sap of fungus-infected tomato. Plant Physiology **130:**904-917.

11. **Berne S, Javornik B.** 2016. Signalling Crosstalk of Plant Defence Responses to Xylem-invading Pathogens.

12. **Saponari M, Boscia D, Nigro F, Martelli G.** 2013. Identification of DNA sequences related to *Xylella fastidiosa* in oleander, almond and olive trees exhibiting leaf scorch symptoms in Apulia (Southern Italy). Journal of Plant Pathology **95**.

13. **Hopkins D, Purcell A.** 2002. *Xylella fastidiosa*: cause of Pierce's disease of grapevine and other emergent diseases. Plant disease **86:**1056-1066.

14. **Janse JD, Obradovic A.** 2010. *Xylella fastidiosa*: its biology, diagnosis, control and risks. Journal of Plant Pathology **92:**S1. 35-S31. 48.

15. **Sun Q, Sun Y, Walker MA, Labavitch JM.** 2013. Vascular occlusions in grapevines with Pierce's disease make disease symptom development worse. Plant Physiology **161:**1529-1541.

16. **Choat B, Gambetta GA, Wada H, Shackel KA, Matthews MA.** 2009. The effects of Pierce's disease on leaf and petiole hydraulic conductance in *Vitis vinifera* cv. Chardonnay. Physiologia Plantarum **136:**384-394.

17. **Choi H-K, Iandolino A, da Silva FG, Cook DR.** 2013. Water deficit modulates the response of *Vitis vinifera* to the Pierce's disease pathogen *Xylella fastidiosa*. Molecular Plant-Microbe Interactions **26:**643-657.

18. **Hill B, Purcell A.** 1995. Multiplication and movement of *Xylella fastidiosa* within grapevine and four other plants. Phytopathology **85:**1368-1372.

19. **Zipfel C.** 2009. Early molecular events in PAMP-triggered immunity. Current Opinion in Plant Biology **12:**414-420.

20. **Newman M-A, Dow JM, Molinaro A, Parrilli M.** 2007. Invited review: Priming, induction and modulation of plant defence responses by bacterial lipopolysaccharides. Journal of Endotoxin Research **13:**69-84.

21. **Chisholm ST, Coaker G, Day B, Staskawicz BJ.** 2006. Host-microbe interactions: shaping the evolution of the plant immune response. Cell **124:**803-814.

22. **Lambais MR, Goldman MH, Camargo LE, Goldman GH.** 2000. A genomic approach to the understanding of *Xylella fastidiosa* pathogenicity. Current Opinion in Microbiology **3:**459-462.

23. **Simpson AJG, Reinach FC, Arruda P, Abreu FA, Acencio M, Alvarenga R, Alves LMC, Araya JE, Baia GS, Baptista CS, Barros MH, Bonaccorsi ED, Bordin S, Bove JM, Briones MRS, Bueno MRP, Camargo AA, Camargo LEA, Carraro DM, Carrer H, Colauto NB, Colombo C, Costa FF, Costa MCR, Costa-Neto CM, Coutinho LL, Cristofani M, Dias-Neto E, Docena C, El-Dorry H, Facincani AP, Ferreira AJS, Ferreira VCA, Ferro JA, Fraga JS, Franca SC, Franco MC, Frohme M, Furlan LR, Garnier M, Goldman GH, Goldman MHS, Gomes SL, Gruber A, Ho PL, Hoheisel JD, Junqueira ML,**

Kemper EL, Kitajima JP, Krieger JE, et al. 2000. The genome sequence of the plant pathogen *Xylella fastidiosa*. Nature **406:**151-157.

24. **Dinglasan RR, Jacobs-Lorena M.** 2005. Insight into a conserved lifestyle: protein-carbohydrate adhesion strategies of vector-borne pathogens. Infection and Immunity **73:**7797-7807.

25. **Caroff M, Karibian D.** 2003. Structure of bacterial lipopolysaccharides. Carbohydrate Research **338:**2431-2447.

26. **Walker SL, Redman JA, Elimelech M.** 2004. Role of Cell Surface Lipopolysaccharides in Escherichia coli K12 Adhesion and Transport. Langmuir **20:**7736-7746.

27. **Lerouge I, Vanderleyden J.** 2002. O-antigen structural variation: mechanisms and possible roles in animal/plant–microbe interactions. FEMS Microbiology Reviews **26:**17-47.

28. **Clements A, Gaboriaud F, Duval JFL, Farn JL, Jenney AW, Lithgow T, Wijburg OLC, Hartland EL, Strugnell RA.** 2008. The major surface-associated saccharides of *Klebsiella pneumoniae* contribute to host cell association. PLoS One **3:**e3817.

29. **Raetz CRH, Whitfield C.** 2002. Lipopolysaccharide endotoxins. Annual review of Biochemistry **71:**635.

30. **Ivanov IE, Kintz EN, Porter LA, Goldberg JB, Burnham NA, Camesano TA.** 2011. Relating the physical properties of *Pseudomonas aeruginosa* lipopolysaccharides to virulence by atomic force microscopy. Journal of Bacteriology **193:**1259-1266.

31. **Kotra LP, Golemi D, Amro NA, Liu G-Y, Mobashery S.** 1999. Dynamics of the Lipopolysaccharide Assembly on the Surface of *Escherichia coli*. Journal of the American Chemical Society **121:**8707-8711.

32. **Zhang L, Radziejewska-Lebrecht J, Krajewska-Pietrasik D, Toivanen P, Skurnik M.** 1997. Molecular and chemical characterization of the lipopolysaccharide O-antigen and its role in the virulence of *Yersinia enterocolitica* serotype O:8. Molecular Microbiology **23:**63-76.

33. **Clifford JC, Rapicavoli JN, Roper MC.** 2013. A Rhamnose-Rich O-Antigen Mediates Adhesion, Virulence, and Host Colonization for the Xylem-Limited Phytopathogen *Xylella fastidiosa*. Molecular Plant-Microbe Interactions **26:**676-685.

34. **Rapicavoli JN, Kinsinger N, Perring TM, Backus EA, Shugart HJ, Walker S, Roper MC.** 2015. O-antigen Modulates Insect Vector Acquisition of the Bacterial Plant Pathogen, *Xylella fastidiosa*. Applied and Environmental Microbiology **81:**8145-8154.

35. **Dow M, Newman M-A, von Roepenack E.** 2000. The induction and modulation of plant defense responses by bacterial lipopolysaccharides. Annual Review of Phytopathology **38:**241-261.

36. **Erbs G, Newman M-A.** 2011. Lipopolysaccharide and Its Interactions with Plants. Springer.

37. **Desaki Y, Miya A, Venkatesh B, Tsuyumu S, Yamane H, Kaku H, Minami E, Shibuya N.** 2006. Bacterial Lipopolysaccharides Induce Defense Responses Associated with Programmed Cell Death in Rice Cells. Plant and Cell Physiology **47:**1530-1540.

38. **Silipo A, Molinaro A, Sturiale L, Dow JM, Erbs G, Lanzetta R, Newman M-A, Parrilli M.** 2005. The elicitation of plant innate immunity by lipooligosaccharide of *Xanthomonas campestris*. Journal of Biological Chemistry **280:**33660-33668.

39. **Zeidler D, Zähringer U, Gerber I, Dubery I, Hartung T, Bors W, Hutzler P, Durner J.** 2004. Innate immunity in Arabidopsis thaliana: lipopolysaccharides activate nitric oxide synthase (NOS) and induce defense genes. Proceedings of the National Academy of Sciences of the United States of America **101:**15811-15816.

40. **Guo H, Yi W, Shao J, Lu Y, Zhang W, Song J, Wang PG.** 2005. Molecular analysis of the O-antigen gene cluster of *Escherichia coli* O86: B7 and characterization of the chain length determinant gene (*wzz*). Applied and Environmental Microbiology **71:**7995-8001.

41. **Duerr CU, Zenk SF, Chassin C, Pott J, Gütle D, Hensel M, Hornef MW.** 2009. O-antigen delays lipopolysaccharide recognition and impairs antibacterial host defense in murine intestinal epithelial cells. PLoS Pathogens **5:**e1000567.

42. **Conrath U.** 2011. Molecular aspects of defence priming. Trends in Plant Science **16:**524-531.

43. **Verhagen BW, Trotel-Aziz P, Couderchet M, Höfte M, Aziz A.** 2009. *Pseudomonas spp.*-induced systemic resistance to *Botrytis cinerea* is associated with induction and priming of defence responses in grapevine. Journal of Experimental Botany**:**erp295.

44. **Verhagen B, Trotel-Aziz P, Jeandet P, Baillieul F, Aziz A.** 2011. Improved resistance against *Botrytis cinerea* by grapevine-associated bacteria that induce a prime oxidative burst and phytoalexin production. Phytopathology **101:**768-777.

45. **Varnier A-L, Sanchez L, Vatsa P, Boudesocque L, Garcia-Brugger A, Rabenoelina F, Sorokin A, Renault J-H, Kauffmann S, Pugin A, Clement C, Baillieul F, Dorey S.** 2009. Bacterial rhamnolipids are novel MAMPs conferring resistance to *Botrytis cinerea* in grapevine. Plant, Cell & Environment **32:**178-193.

46. **Aziz A, Poinssot B, Daire X, Adrian M, Bézier A, Lambert B, Joubert J-M, Pugin A.** 2003. Laminarin elicits defense responses in grapevine and induces protection against *Botrytis cinerea* and *Plasmopara viticola*. Molecular Plant-Microbe Interactions **16:**1118-1128.

47. **Newman M-A, Von Roepenack-Lahaye E, Parr A, Daniels MJ, Dow JM.** 2002. Prior exposure to lipopolysaccharide potentiates expression of plant defenses in response to bacteria. The Plant Journal **29:**487-495.

48. **Conrath U, Beckers GJ, Flors V, García-Agustín P, Jakab G, Mauch F, Newman M-A, Pieterse CM, Poinssot B, Pozo MJ.** 2006. Priming: getting ready for battle. Molecular Plant-Microbe Interactions **19:**1062-1071.

49. **Guilhabert MR, Kirkpatrick BC.** 2005. Identification of *Xylella fastidiosa* antivirulence genes: hemagglutinin adhesins contribute to *X. fastidiosa* biofilm maturation and colonization and attenuate virulence. Molecular Plant-Microbe interactions **18:**856-868.

50. **Newman M-A, Daniels MJ, Dow JM.** 1995. Lipopolysaccharide from *Xanthomonas campestris* induces defense-related gene expression in *Brassica campestris*. Molecular Plant-Microbe Interactions **8:**778-780.

51. **Senchenkova SN, Shashkov AS, Laux P, Knirel YA, Rudolph K.** 1999. The O-chain polysaccharide of the lipopolysaccharide of *Xanthomonas campestris* pv. *begoniae* GSPB 525 is a partially L-xylosylated L-rhamnan. Carbohydrate Research **319:**148-153.

52. **Wojtaszek P.** 1997. Oxidative burst: an early plant response to pathogen infection. Biochemical Journal **322:**681.

53. **Thordal‐Christensen H, Zhang Z, Wei Y, Collinge DB.** 1997. Subcellular localization of H2O2 in plants. H2O2 accumulation in papillae and hypersensitive response during the barley—powdery mildew interaction. The Plant Journal **11:**1187-1194.

54. **Senthil-Kumar M, Mysore KS.** 2013. Nonhost resistance against bacterial pathogens: retrospectives and prospects. Annual Review of Phytopathology **51:**407-427.

55. **Dufour MC, Lambert C, Bouscaut J, Mérillon JM, Corio-Costet MF.** 2013. Benzothiadiazole-primed defence responses and enhanced differential expression of defence genes in *Vitis vinifera* infected with biotrophic pathogens *Erysiphe necator* and *Plasmopara viticola*. Plant Pathology **62:**370-382.

56. **Chakraborty S, Nascimento R, Zaini PA, Gouran H, Rao BJ, Goulart LR, Dandekar AM.** 2016. Sequence/structural analysis of xylem proteome emphasizes pathogenesis-related proteins, chitinases and β-1, 3-glucanases as key players in grapevine defense against *Xylella fastidiosa*. PeerJ **4:**e2007.

57. **Hiraga S, Sasaki K, Ito H, Ohashi Y, Matsui H.** 2001. A large family of class III plant peroxidases. Plant and Cell Physiology **42:**462-468.

58. **Sun Q, Rost TL, Matthews MA.** 2008. Wound-induced vascular occlusions in *Vitis vinifera* (Vitaceae): Tyloses in summer and gels in winter1. American Journal of Botany **95:**1498-1505.

59. **Pérez-Donoso AG, Greve LC, Walton JH, Shackel KA, Labavitch JM.** 2007. *Xylella fastidiosa* infection and ethylene exposure result in xylem and water movement disruption in grapevine shoots. Plant Physiology **143:**1024-1036.

60. **Stevenson JF, Matthews MA, Greve LC, Labavitch JM, Rost TL.** 2004. Grapevine susceptibility to Pierce's disease II: progression of anatomical symptoms. American Journal of Enology and Viticulture **55:**238-245.

61. **Pollard M, Beisson F, Li Y, Ohlrogge JB.** 2008. Building lipid barriers: biosynthesis of cutin and suberin. Trends in Plant Science **13:**236-246.

62. **Gao F, Dai R, Pike SM, Qiu W, Gassmann W.** 2014. Functions of EDS1-like and PAD4 genes in grapevine defenses against powdery mildew. Plant Molecular Biology **86:**381-393.

63. **Blée E.** 2002. Impact of phyto-oxylipins in plant defense. Trends in Plant Science **7:**315-322.

64. **Baxter HL, Stewart Jr CN.** 2013. Effects of altered lignin biosynthesis on phenylpropanoid metabolism and plant stress. Biofuels **4:**635-650.

65. **Sun Q, Rost TL, Reid MS, Matthews MA.** 2007. Ethylene and not embolism is required for wound-induced tylose development in stems of grapevines. Plant Physiology **145:**1629-1636.

66. **Billips BK, Schaeffer AJ, Klumpp DJ.** 2008. Molecular basis of uropathogenic Escherichia coli evasion of the innate immune response in the bladder. Infection and Immunity **76:**3891-3900.

67. **Van der Ley P, De Graaff P, Tommassen J.** 1986. Shielding of *Escherichia coli* outer membrane proteins as receptors for bacteriophages and colicins by O-antigenic chains of lipopolysaccharide. Journal of Bacteriology **168:**449-451.

68. **Bedini E, De Castro C, Erbs G, Mangoni L, Dow JM, Newman M-A, Parrilli M, Unverzagt C.** 2005. Structure-dependent modulation of a pathogen response in plants by synthetic O-antigen polysaccharides. Journal of the American Chemical Society **127:**2414-2416.

69. **Rocchetta H, Burrows L, Lam J.** 1999. Genetics of O-antigen biosynthesis in *Pseudomonas aeruginosa*. Microbiology and Molecular Biology Reviews **63:**523-553.

70. **Kocharova N.** 1995. Structure and properties of the common polysaccharide antigen of *Pseudomonas aeruginosa* bacteria (review). Biokhimiia (Moscow, Russia) **60:**1964.

71. **Barnett JR.** 2006. Cell-cell communication in wood, p 135-147, Cell-cell channels. Springer.

72. **Bonetta D, McCourt P.** 1998. Genetic analysis of ABA signal transduction pathways. Trends in Plant Science **3:**231-235.

73. **Cho SK, Kim JE, Park J-A, Eom TJ, Kim WT.** 2006. Constitutive expression of abiotic stress-inducible hot pepper CaXTH3, which encodes a xyloglucan endotransglucosylase/hydrolase homolog, improves drought and salt tolerance in transgenic Arabidopsis plants. FEBS letters **580:**3136-3144.

74. **Ookawara R, Satoh S, Yoshioka T, Ishizawa K.** 2005. Expression of α-expansin and xyloglucan endotransglucosylase/hydrolase genes associated with shoot elongation enhanced by anoxia, ethylene and carbon dioxide in arrowhead (*Sagittaria pygmaea* Miq.) tubers. Annals of Botany **96:**693-702.

75. **Pearce R, Holloway P.** 1984. Suberin in the sapwood of oak (*Quercus robur* L.): its composition from a compartmentalization barrier and its occurrence in tyloses in undecayed wood. Physiological Plant Pathology **24:**71-81.

76. **Bernards MA.** 2002. Demystifying suberin. Canadian Journal of Botany **80:**227-240.

77. **Soliday C, Kolattukudy P, Davis R.** 1979. Chemical and ultrastructural evidence that waxes associated with the suberin polymer constitute the major diffusion barrier to water vapor in potato tuber (*Solanum tuberosum* L.). Planta **146:**607-614.

78. **Vogt E, Schönherr J, Schmidt H.** 1983. Water permeability of periderm membranes isolated enzymatically from potato tubers (*Solanum tuberosum* L.). Planta **158:**294-301.

79. **Esau K.** 1977. Anatomy of seed plants-2.

80. **Matzke K, Riederer M.** 1991. A comparative study into the chemical constitution of cutins and suberins from *Picea abies* (L.) Karst., *Quercus robur* L., and *Fagus sylvatica* L. Planta **185:**233-245.

81. **Robb J, Powell D, Street P.** 1989. Vascular coating: a barrier to colonization by the pathogen in Verticillium wilt of tomato. Canadian Journal of Botany **67:**600-607.

82. **Gindro K, Pezet R, Viret O.** 2003. Histological study of the responses of two *Vitis vinifera* cultivars (resistant and susceptible) to *Plasmopara viticola* infections. Plant Physiology and Biochemistry **41:**846-853.

83. **Daugherty MP, Rashed A, Almeida RPP, Perring TM.** 2011. Vector preference for hosts differing in infection status: sharpshooter movement and *Xylella fastidiosa* transmission. Ecological Entomology **36:**654-662.

84. **D'Haeze W, Holsters M.** 2004. Surface polysaccharides enable bacteria to evade plant immunity. Trends in Microbiology **12:**555-561.

85. **Ebel J, Cosio EG.** 1994. Elicitors of plant defense responses. International Review of Cytology **148:**1-36.

86. **Montesano M, Brader G, Palva ET.** 2003. Pathogen derived elicitors: searching for receptors in plants. Molecular Plant Pathology **4:**73-79.

87. **Erbs G, Newman M-A.** 2003. The role of lipopolysaccharides in induction of plant defence responses. Molecular Plant Pathology **4:**421-425.

88. **Zhang Y, Yang X, Liu Q, Qiu D, Zhang Y, Zeng H, Yuan J, Mao J.** 2010. Purification of novel protein elicitor from *Botrytis cinerea* that induces disease resistance and drought tolerance in plants. Microbiological Research **165:**142-151.

89. **Haukioja E, Suomela J, Neuvonen S.** 1985. Long-term inducible resistance in birch foliage: triggering cues and efficacy on a defoliator. Oecologia **65:**363-369.

90. **Zvereva EL, Kozlov MV, Niemelä P, Haukioja E.** 1997. Delayed induced resistance and increase in leaf fluctuating asymmetry as responses of *Salix borealis* to insect herbivory. Oecologia **109:**368-373.

91. **Guilhabert MR, Hoffman LM, Mills DA, Kirkpatrick BC.** 2001. Transposon Mutagenesis of *Xylella fastidiosa* by Electroporation of Tn5 Synaptic Complexes. Molecular Plant-Microbe Interactions **14:**701-706.

92. **Westphal O, Jann K.** 1965. Bacterial lipopolysaccharides. Meth. Carbohydr. Chem. **5:**83-91.

93. **Krauss JH, Weckesser J, Mayer H.** 1988. Electrophoretic analysis of lipopolysaccharides of purple non-sulfur bacteria. International Journal of Systematic Bacteriology **38:**157-163.

94. **Corzo J, Perez-Galdona R, Leon-Barrios M, Gutierrez-Navarro AM.** 1991. Alcian blue fixation allows silver staining of the isolated polysaccharide component of bacterial lipopolysaccharides in polyacrylamide gels. Electrophoresis **12:**439-441.

95. **York WS, Darvill, A. G., McNeil, M., Stevenson, T. T., and Albersheim, P.** 1986. Isolation and Characterization of Plant-Cell Walls and Cell-Wall Components. Methods in Enzymology **118:**3-40.

96. **Bhat UR, Forsberg LS, Carlson RW.** 1994. Structure of lipid A component of *Rhizobium leguminosarum* bv. phaseoli lipopolysaccharide. Unique nonphosphorylated lipid A containing 2-amino-2-deoxygluconate, galacturonate, and glucosamine. Journal of Biological Chemistry **269:**14402-14410.

97. **Lindberg B, Lonngren J.** 1978. Methylation analysis of complex carbohydrates: general procedure and application for sequence analysis. Methods Enzymol. **50:**3-33.

98. **Ciucanu I, Kerek F.** 1984. A simple and rapid method for the permethylation of carbohydrates. Carbohydrate Research **131:**209-217.

99. **Gerwig GJ, Kamerling JP, Vliegenthart JFG.** 1978. Carbohydrate Research **62:**349-357.

100. **Gerwig GJ, Kamerling JP, Vliegenthart JFG.** 1979. Determination of the absolute configuration of monosaccharides in complex carbohydrates by capillary G.L.C. Carbohydrate Research **77:**1-7.

101. **Marolda CL, Lahiry P, Vinés E, Salidías S, Valvano MA.** 2006. Micromethods for the characterization of lipid A-core and O-antigen lipopolysaccharide. *In* Brockhausen I (ed), Methods in Molecular Biology, vol 347. Humana Press, Inc., Totowa, NJ.

102. **Lee C-H, Tsai C-M.** 1999. Quantification of Bacterial Lipopolysaccharides by the Purpald Assay: Measuring Formaldehyde Generated from 2-keto-3-deoxyoctonate and Heptose at the Inner Core by Periodate Oxidation. Analytical Biochemistry **267:**161-168.

103. **Liu Y-H, Offler CE, Ruan Y-L.** 2014. A simple, rapid, and reliable protocol to localize hydrogen peroxide in large plant organs by DAB-mediated tissue printing. Frontiers in Plant Science **5**.

104. **Bunderson M, Brooks DM, Walker DL, Rosenfeld ME, Coffin JD, Beall HD.** 2004. Arsenic exposure exacerbates atherosclerotic plaque formation and increases nitrotyrosine and leukotriene biosynthesis. Toxicology and Applied Pharmacology **201:**32-39.

105. **Hill BL, Purcell AH.** 1995. Acquisition and retention of *Xylella fastidiosa* by an efficient vector, *Graphocephala atropunctata*. Phytopathology **85:**209-212.

106. **Love MI, Huber W, Anders S.** 2014. Moderated estimation of fold change and dispersion for RNA-seq data with DESeq2. Genome Biol. **15:**550.

107. **Grimplet J, Cramer GR, Dickerson JA, Mathiason K, Van Hemert J, Fennell AY.** 2009. VitisNet:" Omics" integration through grapevine molecular networks. PloS One **4:**e8365.

108. **Licausi F, Ohme‐Takagi M, Perata P.** 2013. APETALA2/Ethylene Responsive Factor (AP2/ERF) transcription factors: mediators of stress responses and developmental programs. New Phytologist **199:**639-649.

109. **Chen A, Dubcovsky J.** 2012. Wheat TILLING mutants show that the vernalization gene VRN1 down-regulates the flowering repressor VRN2 in leaves but is not essential for flowering. PLoS Genetics **8**(12):e1003134.

CHAPTER III: Disruption in the biosynthesis of L-rhamnose precursors modifies cell surface polysaccharide production and virulence for the bacterial phytopathogen *Xylella fastidiosa*

ABSTRACT

L-rhamnose is a naturally occurring deoxy sugar commonly found in bacterial polysaccharides, which are essential virulence factors for many bacterial pathogens. The role of L-rhamnose production in the bacterial plant pathogen *Xylella fastidiosa* was investigated by knocking out the dTDP-L-rhamnose biosynthetic operon, *rmlB$_1$ACD*. The mutation affected the production and assembly of the major cell surface polysaccharides, lipopolysaccharide (LPS) and exopolysaccharide (EPS). Specifically, LPS O antigen assembly was altered, and the *ΔrmlB$_1$ACD* mutant produced less EPS compared with wild type. Furthermore, the *ΔrmlB$_1$ACD* mutant strain was affected in critical biofilm-associated behaviors, such as attachment to host surfaces. Biologically, the mutant strain was significantly impaired in plant host colonization, including systemic movement, and these plants exhibited fewer Pierce's disease symptoms. Taken together, these results establish diverse roles for L-rhamnose biosynthesis in *X. fastidiosa* biology and host-pathogen interactions.

INTRODUCTION

Xylella fastidiosa is a destructive xylem-limited bacterial plant pathogen that is obligately transmitted by xylem-feeding sharpshooters (1). It is the causal agent of several economically important diseases on agricultural and ornamental crops, notably Pierce's disease of grapevine. *X. fastidiosa* colonizes the vector foregut by attaching to and

forming robust biofilms within the insect mouthparts. Cells are subsequently inoculated into plant xylem vessels during insect feeding on xylem sap (2). *X. fastidiosa* attaches to vessel walls and develops into biofilms that colonize the xylem tissue network, leading to the occlusion of water flow throughout the plant. This is followed by water stress symptoms, such as severe leaf scorching, and ultimately plant death (3). In the case of Pierce's disease of grapevine, additional symptoms include irregular periderm development, premature leaf abscission, and raisining of grape clusters (1). In both the insect and plant host environments, biofilm formation is important for the dissemination of inoculum and progression of infection. *X. fastidiosa* cell surface components, such as the proteinaceous adhesins HxfA and HxfB and types I and IV pili, were demonstrated to contribute to various stages of biofilm formation and host colonization (4-8), but more recently, cell surface polysaccharides have been implicated in this biological process (9-11).

We demonstrated previously that the lipopolysaccharide (LPS) O antigen of *X. fastidiosa* is composed primarily of L-rhamnose. L-rhamnose is a common component of bacterial cell surface polysaccharides and glycoproteins, and it is ubiquitous in both Gram-negative and Gram-positive bacteria. Many notable mammalian and plant bacterial pathogens, e.g. *Salmonella enterica* and *Xanthomonas campestris*, possess L-rhamnose-containing polysaccharides (12, 13). In addition to pathogenic microbes, rhamnose-rich polysaccharides are also found in plant growth-promoting rhizobacteria (e.g. *Rhizobium* spp. and *Azospirillum* spp.) where they contribute to establishing an effective plant-microbe association (14, 15). Loss of the rhamnose-rich O antigen significantly altered *X.*

fastidiosa adhesion dynamics within plant and insect hosts, consequently affecting biofilm formation and virulence (9, 10). Furthermore, this mutation also compromised cell membrane integrity, increasing sensitivity of the cells to oxidative stress. Thus, the focus of our study was to elucidate the specific contributions of L-rhamnose monosaccharide precursors in *X. fastidiosa* pathology.

Genes involved in the biosynthesis of dTDP-L-rhamnose (the activated monosaccharide form of L-rhamnose) have been identified in several bacteria. However, the gene order varies from species to species, and in some cases, the genes are not always located together (12). Using comparative genomics, we have identified four *X. fastidiosa* genes that encode proteins which putatively catalyze the synthesis of dTDP-rhamnose from glucose-1-phosphate (map order): $rmlB_1$ (XP0208), *rmlA* (XP0209), *rmlC* (XP0210), and *rmlD* (XP0211) (13, 16). These genes are located together in an operon. We also identified an additional, unlinked copy of *rmlB*, designated $rmlB_2$ (XP1617). The first enzyme of the pathway, RmlA (glucose-1-phosphate thymidylyltransferase), converts glucose-1-phosphate to dTDP-glucose; RmlB (dTDP-D-glucose-4,6-dehydratase) catalyzes the dehydration of dTDP-d-glucose to form dTDP-4-keto 6-deoxy-D-glucose; RmlC (dTDP-6-deoxy-D-xylo-4-hexulose 3,5-epimerase) catalyzes a double epimerisation reaction at positions C3 and C5; and RmlD (dTDP-6-deoxy-L-lyxo-4-hexulose reductase) reduces the C4 keto function to generate the final product, dTDP-L-Rhamnose (12, 13).

Mutations in the *rml* locus in *Xanthomonas campestris* pv. campestris (*Xcc*), a close relative of *X. fastidiosa*, affected O antigen biosynthesis and caused a reduction in

EPS production (13). EPS, which is a major component of the extracellular matrix surrounding mature biofilms (17), was also shown to be essential for *X. fastidiosa* transmission and virulence *in planta*. Mutants disrupted in EPS biosynthesis were severely affected in biofilm formation, resulting in avirulence in grapevines and reduced transmission rates by blue-green sharpshooters (*Graphocephala atropunctata*) (11). Similar defects in the production of surface polysaccharides, and consequently reductions in bacterial virulence, were also seen in *rml* mutants in the enteric pathogens *Escherichia coli* and *Salmonella enterica*. Additionally, loss of rhamnose production in rhizobial symbionts inhibited establishment and nodule formation *in planta*, suggesting that the production and utilization of rhamnose monosaccharides is highly conserved across diverse microbial lifestyles (14, 18, 19). In this study, we demonstrate that the production of dTDP-L-rhamnose precursors in *X. fastidiosa* contributes to the production and assembly of the prominent bacterial surface polysaccharides, LPS and EPS. Furthermore, we show that these alterations in LPS and EPS affect biofilm-associated behaviors and increase sensitivity of the cells to exogenous stress, which consequently impacts the ability of *X. fastidiosa* to successfully colonize and cause Pierce's disease in a susceptible grapevine host.

RESULTS

Genetic organization of dTDP-L-rhamnose biosynthetic genes in *Xylella fastidiosa* and a close relative, *Xanthomonas campestris* pv campestris. The *X. fastidiosa* *rmlB$_1$ACD* gene cluster is orthologous to L-rhamnose biosynthetic genes in *X. campestris* pv campestris (73% identity). In addition to putative functions in LPS biosynthesis, the genomic context of the *rmlB$_1$ACD* operon implies possible coordination of LPS/EPS biosynthesis via regulation of the *rmlB$_1$ACD* operon. Two xanthan biosynthesis genes, *xanA* and *xanB*, are located immediately downstream (85% identity) (Fig. 3.1) but do not appear to be part of the *rmlB$_1$ACD* operon. *xanA* and *xanB* genes are implicated in fastidian gum production in a different strain of *X. fastidiosa* causing Citrus Variegated Chlorosis (20).

Deletion of the *rmlB$_1$ACD* operon affects the production and assembly of cell surface polysaccharides. To determine whether *rmlB$_1$ACD* contributes to the assembly of LPS, deoxycholate polyacrylamide gel electrophoresis (DOC-PAGE) analysis was performed with purified LPS from wild type, *ΔrmlB$_1$ACD*, and *rml/rml+ X. fastidiosa* cells. The wild type LPS profile exhibited a diffuse, high molecular weight O antigen (Fig. 3.2A, arrow) which is consistent with what has been demonstrated previously (9). No diffuse O antigen was observed in *ΔrmlB$_1$ACD* mutant LPS, similar to the *wzy* mutant described in Chapter II. Restoration of O antigen occurred in the *rml/rml+* complemented strain (Fig. 3.2A). These results suggest that *rmlB$_1$ACD* contributes to the incorporation of rhamnose into the high molecular weight O antigen, and lack of L-rhamnose production disrupts

Figure 3.1. Genetic organization of the *Xylella fastidiosa* dTDP-L-rhamnose biosynthetic operon

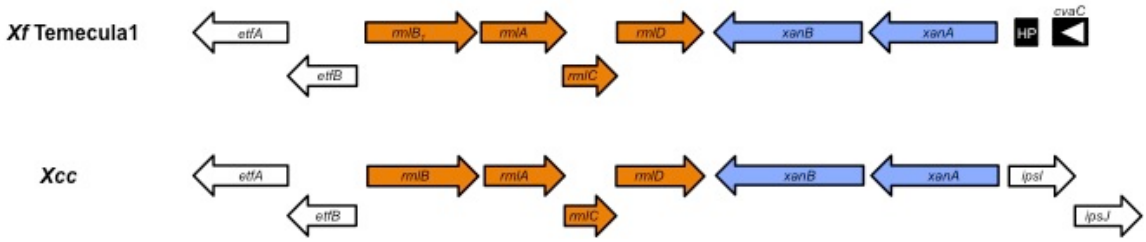

Genetic organization of the *rml* operon of *X. fastidiosa* (*Xf*) Temecula1 isolate (causing Pierce's disease of grapevine) and *Xanthomonas campestris* pv. campestris (*Xcc*), a close relative. The *rml* locus is composed of four open reading frames (ORFs) designated *rmlB*$_1$, *rmlA, rmlC,* and *rmlD* (map order). These genes are contiguous, transcribed in the same direction, and arranged in the same manner as those in *Xcc*. Comparisons of the deduced amino acid sequences of *Xf* RmlB$_1$, RmlA, RmlC and RmlD with those of *Xcc* revealed strong amino acid sequence identity (73%). Furthermore, similarity of the downstream xanthan biosynthesis enzymes (XanA, XanB*;* 85% amino acid sequence identity) suggests a putative role for these enzymes in EPS production in the Temecula1 isolate.

this process. Because similar sugar precursors are utilized in the synthesis of both LPS and EPS, mutations in one biosynthetic pathway can often have pleiotropic affects, thus altering the production of multiple polysaccharides. The *ΔrmlB$_1$ACD* mutant produced less EPS compared with wild type, when grown on EPS-inducing media, suggesting that the production of rhamnose precursors may also play a role in *X. fastidiosa* EPS biosynthesis (Fig. 3.2B). However, we did not observe differences in EPS production when cells were grown on standard PD3 medium, which was used for all of the remaining assays.

Rhamnose biosynthesis contributes to cell attachment and formation of a mature biofilm. To quantify the contribution of L-rhamnose production in cell attachment and cell-cell aggregation (two critical steps in biofilm formation), we evaluated the ability of wild type and *ΔrmlB$_1$ACD X. fastidiosa* cells to attach to a solid surface and to each other. The *ΔrmlB$_1$ACD* mutant showed a significant increase in attachment to glass tubes compared with the wild type strain ($P < 0.05$) (Fig. 3.3A). Taken together, these results suggest that changes in cell surface properties have consequently affected the adhesive properties of the cell. Cell-cell aggregation was also significantly reduced in *Δ rmlB$_1$ACD* cells, compared with the wild type parent ($P < 0.0001$) (Fig. 3.3B). Because surface attachment and cell-cell aggregation are the first steps in biofilm formation, we qualitatively analyzed biofilm formation in liquid cultures of wild type and *Δ rmlB$_1$ACD X. fastidiosa* strains, where biofilm is visualized as a ring of cells at the air-liquid

Figure 3.2. LPS and EPS profiles of *Xylella fastidiosa* strains

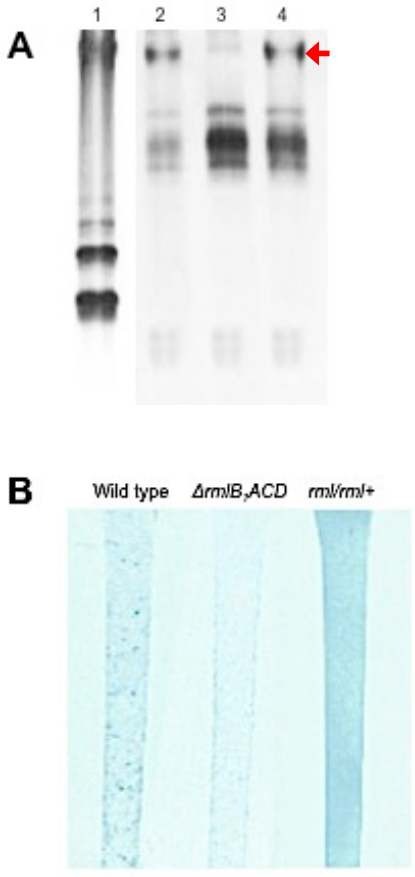

(**A**) Purified LPS analyzed on an 18% deoxycholate–polyacrylamide electrophoretic gel demonstrated that O antigen production is affected in the *ΔrmlB$_1$ACD* mutant strain. Lane 1 = *Escherichia coli* 055:B5 standard; 2 = Wild type *X. fastidiosa*; 3 = *ΔrmlB$_1$ACD*; 4 = *rml/rml+*. Arrow indicates the production of O antigen seen in wild type and *rml/rml+* LPS. (**B**) Alcian Blue 8GX staining of cell lawns printed onto nitrocellulose membrane. Qualitative analysis demonstrated that *ΔrmlB$_1$ACD* mutant cells were impaired in EPS production, compared with wild type and the *rml/rml+* complemented strain.

interface. Following 7 days of incubation in PD3 liquid medium, both strains were capable of attaching to the glass surface and initiating biofilm formation. However, the wild type biofilm was visually thicker than the *ΔrmlB$_1$ACD* mutant biofilm (Fig. 3.3C).

Depletion of rhamnose biosynthesis affects cell tolerance to oxidative stress. Bacterial cell surface polysaccharides serve as important barriers to antimicrobial compounds and host-derived toxins. Utilizing a disk diffusion assay, we evaluated the contribution of rhamnose to the protection against exogenous oxidative stress. The *ΔrmlB$_1$ACD* mutant was significantly more sensitive to H_2O_2 compared with the wild type and complemented strains, indicating that disruption in the biosynthesis of rhamnose affects the integrity of the outer membrane ($P < 0.01$) (Fig. 3.4A,B).

Loss of rhamnose biosynthesis affects virulence and plant host colonization. Grapevines inoculated with *ΔrmlB$_1$ACD* mutant cells showed significantly fewer PD symptoms over the course of the study, compared with wild type and *rml/rml+* complemented strains (Fig. 3.5A). Grapevines inoculated with wild type and *rml/rml+* strains began eliciting noticeable leaf scorch symptoms beginning around 5 weeks post-inoculation. However, grapevines inoculated with *ΔrmlB$_1$ACD* mutant cells did not exhibit significant leaf scorch symptoms until around 9 weeks post-inoculation, and overall, these vines exhibited significantly less disease severity than wild type and *rml/rml+ X. fastidiosa* strains ($P < 0.05$) (Fig. 3.5B). By 18 weeks post-inoculation, over

Figure 3.3. Contribution of rhamnose to biofilm formation

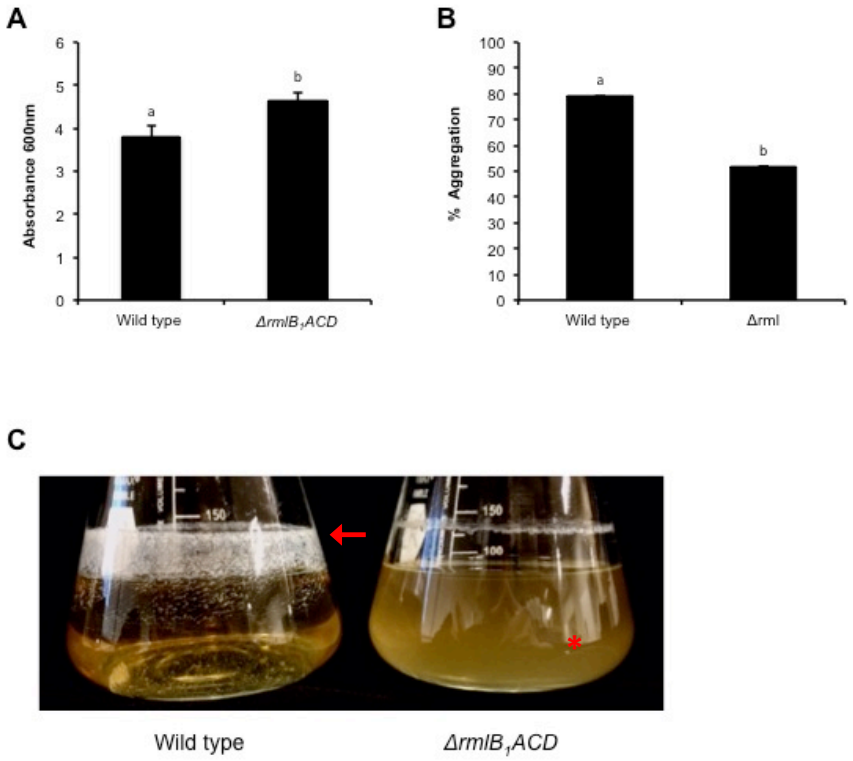

The *ΔrmlB$_1$ACD* mutant attached significantly more to a glass surface than wild type *X. fastidiosa* cells **(A).** Data are means of three independent assays with 9 total replicates. Bars with different letters are significantly different ($P < 0.05$). The *ΔrmlB$_1$ACD* mutant was significantly reduced in cell-cell aggregation **(B)** and biofilm formation **(C)**. Biofilm formation was visualized at the air-liquid interface. Biofilms of wild type *X. fastidiosa* cells were consistently thicker than *ΔrmlB$_1$ACD* mutant cells (arrow). The reduction in cell-cell aggregation could also be seen as turbidity in the liquid culture (*). Data are means of three independent assays with 9 total replicates. Bars with different letters are significantly different ($P < 0.0001$).

Figure 3.4. The production of rhamnose protects *Xylella fastidiosa* against oxidative stress

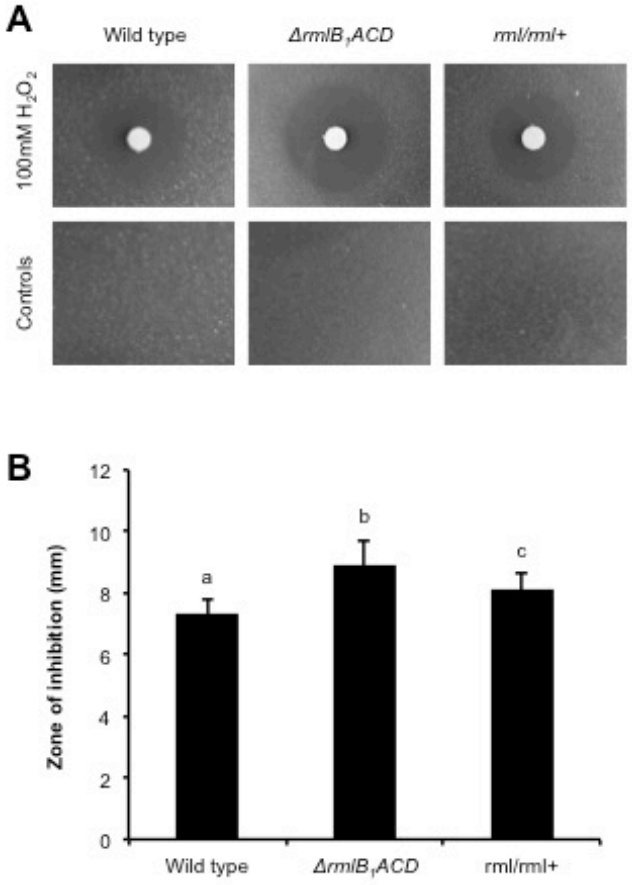

A disk inhibition assay was performed using 100 mM hydrogen peroxide **(A,B)**. The *ΔrmlB1ACD* mutant was significantly less tolerant, qualitatively and quantitatively, to oxidative stress than the wild type and *rml/rml+* complemented strains. Data are means of three independent assays with 9 total replicates. Bars with different letters are significantly different ($P < 0.01$).

half of the leaves on wild type and *rml/rml+* complemented strains exhibited scorching (rating a 3.5 and 3, respectively). In contrast, only one or two leaves on *ΔrmlB$_1$ACD* plants exhibited marginal necrosis (rating of 1.7) (Fig. 3.5C). To quantify the contribution of rhamnose to host colonization, we performed bacterial isolations at 5 weeks post-inoculation from local petioles (point of inoculation, POI) and again at 12 weeks post inoculation from local and systemic petioles (25 cm above the POI). At 5 weeks post-inoculation, the average number of *ΔrmlB$_1$ACD* mutant cells recovered from petioles was significantly less than wild type and *rml/rml+* average populations ($P < 0.05$) (Table 3.1). At 12 weeks post-inoculation, the average number of *ΔrmlB$_1$ACD* mutant cells recovered from local petioles was significantly less than wild type plants (data not shown). In systemic petioles, the average number of *ΔrmlB$_1$ACD* mutant cells recovered from petioles remained significantly less than wild type and *rml/rml+* plants ($P < 0.05$) (Table 3.1). Furthermore, we recovered wild type *X. fastidiosa* from 95% of vines inoculated with that strain, in contrast with only 19% recovery of the mutant strain from *ΔrmlB$_1$ACD*-inoculated vines.

Tylose development in *ΔrmlB$_1$ACD*-inoculated vines is attenuated. Vascular occlusions are commonly produced by plants in response to infection by vascular pathogens. Tyloses are outgrowths of the xylem parenchyma cell into the vessel lumen and are abundant in PD-susceptible grapevines (21). We examined tylose formation at 18 weeks post-inoculation in vines inoculated with wild type, *ΔrmlB$_1$ACD* or *rml/rml+ X. fastidiosa* cells or 1X PBS control. We observed pronounced differences in the

Figure 3.5. The production of L-rhamnose contributes to host colonization and virulence in a susceptible grapevine variety

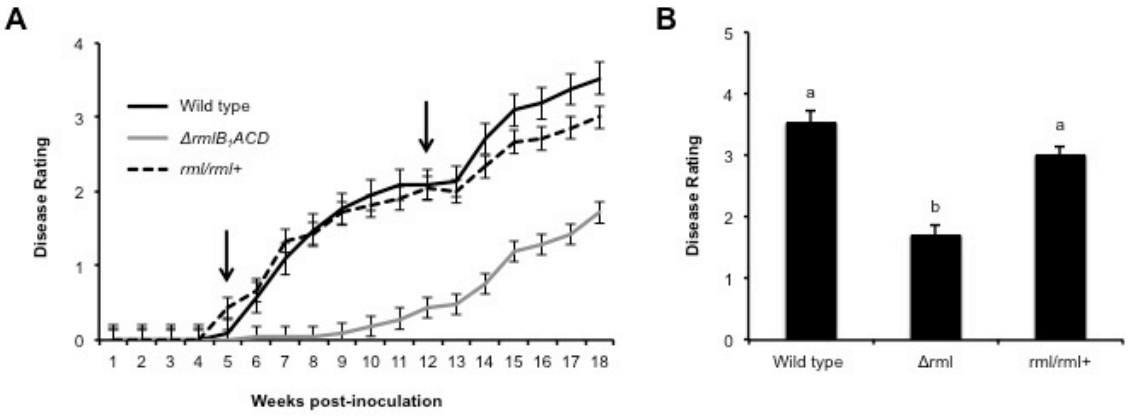

(A) PD symptom progression over the course of the assay. Arrows indicate sampling time points for bacterial isolations. **(B)** Average disease rating at 18 weeks post-inoculation. The *ΔrmlB1ACD* mutant-inoculated plants exhibited a significantly lower degree of PD symptoms overall, compared with wild type and *rml/rml*+-inoculated plants. Data are means of three independent assays with 21 total replications. Bars with different letters are statistically different ($P < 0.05$).

Table 3.1. ***Xylella fastidiosa*** **populations in Chardonnay leaf petioles**

Distance[a]	Weeks[b]	Wild type (CFU)	*ΔrmlB,ACD* (CFU)	*rml/rml+* (CFU)
POI	5	9.11E+08 A[*]	1.51E+07 B	2.25E+09 A
25 cm	12	4.23E+07 A	2.00E+05 B	2.79E+07 A

[a] Point of inoculation (POI) or distance above POI in centimeters
[b] Time post-inoculation
[*] Values with different letters are statistically different ($P < 0.05$).

Figure 3.6. *ΔrmlB$_1$ACD*-inoculated vines contain fewer tyloses

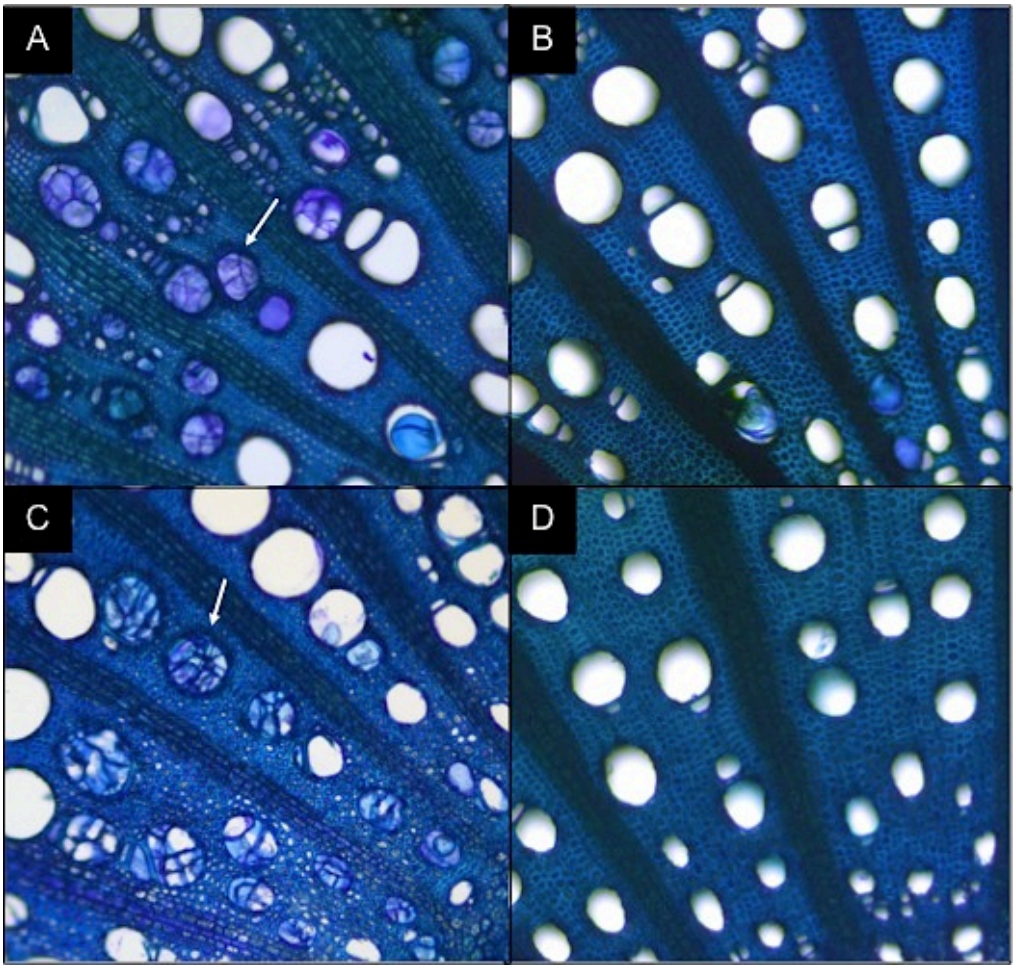

Micrographs display tylose production in cross sections of grapevine xylem (brightfield Toluidine Blue O). Images represent grapevines at 18 weeks post-inoculation treated with wild type **(A)**, *ΔrmlB$_1$ACD* **(B)**, or *rml/rml+ X. fastidiosa* cells **(C)** or 1X PBS buffer **(D)**. Arrows point to xylem vessels completely occluded with multiple tyloses seen in wild type and *rml/rml+*-inoculated vines. Tyloses were largely absent in the xylem vessels of *ΔrmlB$_1$ACD* mutant-inoculated vines. No tyloses were present in the stems of 1X PBS-inoculated vines.

abundance of tyloses in response to wild type vs *ΔrmlB$_1$ACD* mutant-inoculated plants. In wild type-inoculated vines, tyloses were present in nearly all xylem vessels (Fig. 3.6A), and vessels were often completely occluded with multiple tyloses. In contrast, *ΔrmlB$_1$ACD* mutant-inoculated vines contained very few tyloses (Fig. 3.6B). In the case where a tylose was present, it was often one large tylose that only partially occluded the vessel. *Rml/rml+* vines complemented the level of tylose production seen in wild type-inoculated vines (Fig. 3.6C), and all 1X PBS control vines were free of occlusions (Fig. 3.6D).

DISCUSSION

Polysaccharides are important components of the bacterial cell surface that greatly contribute to cell survival and interactions with potential hosts. In both pathogenic and symbiotic plant-bacteria interactions, the biosynthesis of monosaccharide precursors, particularly rhamnose, plays an important role in the production of the polysaccharides LPS and EPS, which contribute to successful host associations. Thus far, there is little evidence implicating these rhamnose precursors in *X. fastidiosa* biology and host-pathogen interactions. L-rhamnose is synthesized as an activated nucleotide sugar (e.g. dTDP-L-rhamnose) by the enzymes RmlA, RmlB, RmlC, and RmlD. Sequence analysis of the *X. fastidiosa* genome identified four ORFs, which showed high homology to the rhamnose biosynthetic operon (*rmlB$_1$ACD*) in *Xcc*, a close relative. To assess the role of L-rhamnose biosynthesis in LPS and EPS production and assembly in *X. fastidiosa,* an *ΔrmlB$_1$ACD* mutant strain was constructed in the Temecula1, Pierce's disease isolate.

LPS serves as an important barrier to toxic compounds and for maintaining cell function and integrity (22). To determine whether L-rhamnose precursors contributed to LPS biosynthesis, DOC PAGE analysis of purified LPS was performed. Wild type *X. fastidiosa* produced a diffuse O antigen-containing LPS (9), but no O antigen-containing LPS was observed in *ΔrmlB$_1$ACD* mutant cells. This mirrors the phenotype of the *wzy* mutant in Chapter II. This implicates the *rml* operon in the incorporation of rhamnose monomers into the O antigen. Therefore, we propose that the *rml* operon should be included in LPS biosynthesis gene clusters, specifically genes involved in production and assembly of O antigen, for future studies. In many bacterial pathogens, the same sugar precursors are utilized in the synthesis of both LPS and EPS. Consequently, mutations in LPS biosynthetic genes typically affect EPS production as well (23, 24). *X. fastidiosa* is predicted to produce an EPS that is similar to xanthan gum. This is supported by the fact that *X. fastidiosa* has an operon with high homology to the *Xcc gum* operon (25), which encodes the enzymes involved in the biosynthesis of xanthan gum (11, 30). Based on genomic analysis, rhamnose is not predicted to be a constituent of *X. fastidiosa* EPS. Yet, the *ΔrmlB$_1$ACD* mutant produced smaller amounts of EPS than wild type cells, when grown on EPS-inducing media, indicating that disruption of the *rml* operon also affects the biosynthesis of this polysaccharide. EPS also contributes to the ability of *X. fastidiosa* to colonize and cause disease in grapevine (11), but for all other experiments in this study, *X. fastidiosa* strains were grown on standard PD3 medium, which does not induce EPS production. Furthermore, cells were subjected to rinses and OD adjustments in

buffer prior to inoculation. Thus, we do not attribute the observed phenotypic differences to defects in EPS production.

LPS and EPS play important roles in the construction of bacterial biofilms, where they contribute to initial cell attachment and biofilm maturation, respectively (26). Mature biofilm formation on a glass surface by the *ΔrmlB$_1$ACD* mutant strain was severely impaired, compared with wild type cells. We attribute this to significant alterations in cell attachment and cell-cell aggregation. The *ΔrmlB$_1$ACD* mutant cells exhibited enhanced attachment to a glass surface, which is similar to the phenotype of the *X. fastidiosa wzy* mutant and is consistent with reports in other bacteria containing O antigen mutations (9, 27, 28). The hyperattachment phenotype exhibited by the *ΔrmlB$_1$ACD* mutant, combined with reduced cell-cell aggregation and EPS production, likely locks these cells in the initial attachment stages of biofilm formation and hinders the subsequent steps of microcolony formation and construction of a 3-dimensional biofilm. Although biofilm formation contributes to the occlusion of xylem vessels, the development of disease also depends on the ability of *X. fastidiosa* to spread systemically from the point of infection (3). Grapevines inoculated with the *ΔrmlB$_1$ACD* mutant contained significantly fewer populations in systemic tissue, and Pierce's disease symptoms were significantly reduced in these plants, compared with wild type and *rml/rml+*-inoculated vines. We speculate that the hyperattachment phenotype likely hinders *ΔrmlB$_1$ACD* cells from moving effectively through the xylem network.

Cell surface polysaccharides serve important protective functions for bacterial cells (29-31), such as increasing tolerance to antimicrobial compounds, desiccation, and

host defense responses. We demonstrate that the production of rhamnose-rich polysaccharides protects the cells against oxidative stress, which is likely encountered by *X. fastidiosa* as it colonizes the plant. This may partially explain why *ΔrmlB$_1$ACD* mutant cells were impaired in host colonization, as these cells were significantly more sensitive to hydrogen peroxide treatment. Both LPS and EPS have been implicated specifically in the protection against hydrogen peroxide (9, 32-36), which is a type of toxic reactive oxygen species produced during the oxidative burst, a hallmark of plant basal defense responses. We have evidence demonstrating that the rhamnose-rich O antigen serves to shield wild type *X. fastidiosa* cells from recognition by the grapevine immune system, allowing them to evade early recognition by the grapevine host (Chapter II). A similar scenario occurs in *Salmonella enterica* subsp. *enterica* sv. (*S.*) Typhimurium where the O antigen aids in evasion of the murine immune system (37). We speculate that O antigen alterations in *ΔrmlB$_1$ACD* mutant cells hastens detection by the grapevine immune system, resulting in the swift deployment of defense responses that effectively reduce bacterial populations *in planta*. The reduction in tyloses seen in these vines corroborates this hypothesis. Plants produce tyloses in an effort to block systemic movement of vascular pathogens, and it has been established that PD-infected vines produce an abundance of tyloses. Specifically, tyloses can occur in over 60% of the vessels in a transverse section of vascular tissue (21). Since the *ΔrmlB$_1$ACD* mutant is impaired in virulence and host colonization, it is likely that the plant does not deem it necessary to allocate resources towards building these structural barriers.

In this study, we demonstrate the importance of L-rhamnose production in the biosynthesis of *X. fastidiosa* cell surface polysaccharides that are critical to virulence in the grapevine host. Future studies investigating the functional characterization and regulation of the *rml* operon would greatly contribute to our understanding of polysaccharide biosynthesis and assembly in this bacterial pathogen. Strains of *X. fastidiosa* exhibit incredible host specificity, but presently, the determinants of this specificity are unknown. Previous reports comparing the genomes of two *Xanthomonas* spp. with differing host specificities implicated *rml*-linked O antigen biosynthesis in pathogen host-range selection (38). We demonstrated in Chapter II that the rhamnose-rich O antigen is critical for the *X. fastidiosa*-grapevine interaction. However, there has been little focus on O antigen structural and functional characterization in other prominent *X. fastidiosa* strains, which exhibit strict host specificity. Comparison of the *rml* operons in these other prominent strains is warranted, as specific O antigen composition and structure may play crucial roles in the creation of successful *X. fastidiosa*-host adaptations.

MATERIALS AND METHODS

Bacterial strains, plasmids, and primers. All bacterial strains, plasmids, and primers used in this study are listed in Table 3.2.

Media and growth of bacterial strains. *X. fastidiosa* strains were grown at 28°C in PD3 liquid and solid medium. *E. coli* strains were grown at 37°C in liquid and solid Luria-Bertani medium. When appropriate, kanamycin and chloramphenicol were added at 5μg/mL for *X. fastidiosa* strains. For selection of *E. coli* transformants, spectinomycin and kanamycin were added at 100 and 30μg/mL, respectively.

DNA Manipulations. Genomic DNA was extracted using the Qiagen DNeasy Blood and Tissue Kit (Qiagen, Valencia, CA, U.S.A.). Plasmid DNA was extracted using the Zyppy^{tm} plasmid miniprep kit (Zymo Research Corporation, Irvine, CA, U.S.A.). DNA fragments were amplified using Takara Ex-Taq DNA polymerase (Takara Bio USA, Madison, WI, U.S.A.). Synthetic oligonucleotide primers were ordered from Integrated DNA Technologies (Coralville, IN, U.S.A.). Restriction enzymes were purchased from New England Biolabs (Ipswich, MA, U.S.A.).

Table 3.2. Bacterial strains and plasmids used in this study

Strain or plasmid	Relevant characteristics	Reference, source
Plasmids		
pCR8/GW/TOPO	Gateway TA cloning vector, Sp^r	Invitrogen
TOPO XL	TA cloning vector, Km^r, Zeo^r	Invitrogen
pAX1Cm	pAX1 with cat and multiple cloning site, Cm^r	Matsumoto et al. 2009
pJR8	pCR8/GW/TOPO with 5.48kb *rmlB$_1$ACD* operon (including flanking regions), Sp^r	This study
pJR15	pJR8 digested with restriction enzymes BsiWi and BspEI, with Tn-5 EZ Tn5 <kan-2> marker, creating Δ,*rmlB$_1$ACD*, Km^r, Sp^r	This study
pJR12	TOPO XL with wild type *rmlB$_1$ACD* operon, including native promoter, Km^r, Zeo^r	This study
pJR13	pAX1Cm with wild type *rmlB$_1$ACD* operon, including native promoter, Cm^r	This study
Xylella fastidiosa		
Temecula1	subsp. *fastidiosa*, wild type isolated from grape	Guilhabert et al. 2001
Temecula *ΔrmlB$_1$ACD* (JR16)	Km^r, knockout in *rmlB$_1$ACD* operon	This study
Temecula *rmlB$_1$ACD/ rmlB$_1$ACD*+(JR17)	Km^r, Cm^r, knockout in *rmlB$_1$ACD* complemented by chromosomal integration of wild type *rmlB$_1$ACD* operon, including native promoter, between PD0702/PD0703 (NS1)	This study
Escherichia coli		
Top 10	F– *endA1 recA1 galE15 galK16 nupG rpsL* Δ*lacX74* Φ*80lacZ*Δ*M15 araD139* Δ(*araleu*)7697 *mcrA* Δ(*mrr-hsdRMS-mcrBC*)	Invitrogen

[a]Sp^r, Km^r, Amp^r, Zeo^r and Cm^r indicate resistance to Spectinomycin, Kanamycin, Ampicillin, Zeocin, and Chloramphenicol, respectively. NS1 represents a neutral site located between the two pseudogenes PD0702 and PD0703 in the *X. fastidiosa* Temecula1 genome.

Mutagenesis and Complementation. The primer pair Rml_LF for 5'-ACCATCCAAGTGTTCGGCGATGATA-3' and Rml_RF rev 5'-GTTCCTATTCCGCGCCTCACGCTAC-3' was used to amplify a 5.48 kb genomic DNA fragment containing the *rmlB1ACD* operon and its flanking regions, which was cloned into pCR8/GW/TOPO (Life Technologies, Grand Island, NY, U.S.A.) to create pJR8. This resulting plasmid was digested with BspEI and BsiWi (New England Biolabs, Ipswich, MA, U.S.A.), removing most of the ORF of *rmlB$_1$ACD.* The Ez-Tn5 <kan-2> transposon was introduced using the Ez-Tn5 *in vitro* transposome kit (Epicentre Technologies, Madison, WI, U.S.A.). All transformants were screened for appropriate antibiotic resistance and a plasmid with the <kan-2> cassette inserted into *ΔrmlB$_1$ACD* was confirmed by polymerase chain reaction (PCR) amplification and sequence analysis to create pJR15. To create the *ΔrmlB$_1$ACD* mutant, 200 ng of pJR15 DNA was electroporated into electrocompetent *X. fastidiosa* Temecula1 cells, as previously described (39). Transformants were plated onto PD3 solid media supplemented with kanamycin at 5 μg/mL. Genomic DNA was extracted from putative mutants and confirmation of recombination was performed by amplification of the regions to the left and right flank of the disrupted *rml* operon using primers Rml_del F 5′-TTAACGCGACCTCTTGACGATCTCG -3′ and Rml_del R 5′-GATGGAGAATGGGATTGGCAACGTG-3′, followed by sequence analysis.

For the construction of the *rmlB$_1$ACD/rmlB$_1$ACD*+ complemented strain (denoted as *rml/rml*+), a 3.73kb genomic DNA fragment containing the wild type *rmlB$_1$ACD* operon and its upstream regulatory region was PCR amplified and cloned into TOPO XL

(Life Technologies, Grand Island, NY, U.S.A.) to create pJR12. The cloned DNA fragment was digested with restriction enzymes XhoI and SpeI and ligated into the XbaI site of the chromosomal complementation plasmid pAX1Cm (Matsumoto et al. 2009) to create pJR13. Confirmation of sequence fidelity of the cloned region was performed via sequencing. Following transformation into *ΔrmlB$_1$ACD* mutant electrocompetent cells, homologous recombination was confirmed by amplification of the flanking regions of the cloning site: PW-For 5′-AGAAGAGCGCGAGATT GAGTTGGA-3′ and PW-Rev 5′-AAACAGGCTTCACATGG CTCAACG-3′.

LPS extraction and analysis. LPS extractions were performed based on the method of Marolda et al. (40), with some modification. Briefly, *X. fastidiosa* cells were grown on solid PD3 medium for 7 days at 28°C. Following incubation, cells were harvested with 1X PBS buffer and spun down to form dense pellets. Cell pellets were stored at -80°C until LPS extractions. Prior to LPS extractions, cell pellets were washed 2x with 1X PBS buffer and suspended in 300 μL Solution A (0.05M Na_2HPO_4 x $7H_2O$, 0.005M EDTA; pH 7) + 40 μL Proteinase K (Qiagen #19131). Suspensions were incubated overnight at room temperature. LPS was extracted from cell pellets using a hot phenol/water method, and resulting LPS was further purified using dialysis (MWCO 1 kD). Following purification, LPS was quantified using the Purpald Assay (41). LPS profiles were analyzed using an 18% deoxycholate–polyacrylamide electrophoretic gel (DOC PAGE) (42), and visualized with the Bio-Rad Silver Stain kit (Bio-Rad, Hercules, CA).

EPS production. To visualize EPS production, Wild type, *ΔrmlB$_1$ACD,* or *rml/rml+ X. fastidiosa* cells were blotted onto dry nitrocellulose membrane, according to the methods of Killiny and Almeida (43). Briefly, *X. fastidiosa* strains were grown on solid PD3 at 28°C for 7 days. Following incubation, cells were harvested and adjusted to an OD_{600} of 0.25, and then 20 µL aliquots were striped onto XFM with 0.01% pectin. Plates were incubated for an additional 7 days at 28°C. Small strips of NCM membrane (0.45 µm; Bio-Rad, Hercules, CA) were overlaid onto the cell stripe and blotted for 1 h. The lifted prints were stained for 15 min with 1% Alcian blue 8GX in 3% acetic acid and then rinsed once in 3% acetic acid for 15 min.

Cell attachment and aggregation assays. *X. fastidiosa* strains were tested for their ability to attach to a glass surface according to a previously published protocol (44). Briefly, wild type or *ΔrmlB$_1$ACD X. fastidiosa* strains were grown on solid PD3 media (with or without antibiotics) at 28°C for 7 days. Following incubation, cells were harvested in liquid PD3 medium and adjusted to an OD_{600} of 0.25 ($1x10^8$ CFU/mL). Subsequently, 500 µL of each cell suspension was added to 5 mL of liquid PD3 medium in a 13 x 100 mm glass test tube and incubated at 28°C for 7 days at 100 rpm. Following incubation, 500 µL of filtered, 1% crystal violet stain was added to the liquid medium and allowed to incubate for 20 min. The medium was discarded, and the tube was rinsed three times with deionized water. The stained, attached cells were dissolved in 2 mL of 95% ethanol, and absorbance of the eluent was measured at 600 nm. A pairwise analysis of variance (ANOVA) was used to determine significance among the treatments. Prior to

the test, data were checked for normality and homogeneity of variance and met these criteria. Post hoc comparisons amongst the treatments used Tukey's honestly significant difference (HSD) test at $P = 0.05$.

Using established protocols (5, 45), we quantified the ability of cells to aggregate to one another. Briefly, *X. fastidiosa* strains were grown and prepared in glass tubes as described above. Tubes were incubated at 28°C, without agitation, for 10 days. Following incubation, the cells were gently dispersed and any formed aggregates were allowed to settle for 20 min. The turbidity of the upper culture medium, consisting primarily of planktonic cells, was measured at 540 nm. This measurement was termed "OD of the upper culture" (ODUC). The upper culture medium was returned to the original tube, thoroughly homogenized by vortexing, and 1 mL was measured at 540 nm. This measurement was termed "OD of the total culture" (ODTC). The percentage of aggregated cells was calculated according to the methods of Burdman et al (45). A student's t-test ($P = 0.01$) was used to determine significance among the treatments. Prior to the test, data were checked for normality and homogeneity of variance and met these criteria.

Biofilm formation. Wild type or *ΔrmlB$_1$ACD X. fastidiosa* strains were grown on solid PD3 media (with or without antibiotics) at 28°C for 7 days. Following incubation, cells were harvested in liquid PD3 medium and adjusted to an OD_{600} of 0.25 ($1x10^8$ CFU/mL). Subsequently, cell suspensions were added to 100 mL of liquid PD3 medium in glass

flasks and incubated at 28°C for 7 days at 180 rpm. Biofilm was visualized at the air-liquid interface.

Disk inhibition assay. *X. fastidiosa* strains were tested for their sensitivity to oxidative stress (via exogenously applied H_2O_2). Briefly, wild type, *ΔrmlB$_1$ACD*, or *rml/rml+ X. fastidiosa* strains were grown on solid PD3 medium (with or without antibiotics) at 28°C for 7 days. Following incubation, small agar squares containing colonies were excised from the plates and added to individual Falcon tubes containing 30 mL of liquid PD3. The liquid cultures were incubated at 28°C and 150 rpm for 4 days. Following incubation, cell suspensions were adjusted to an OD_{600} of 0.1 and diluted 1:10 in 3 mL of PD3 containing 0.8% agar. The suspension was gently vortexed and immediately overlaid onto solid PD3 medium. Following incubation at 28°C for two days, a Whatman paper disk saturated with 10 μL of 100 mM H_2O_2 was placed in the center of the plate. After 7 days of incubation at 28°C, the zone of inhibition was measured. Data was analyzed using the Kruskal-Wallis test for nonparametric one-way ANOVA. Prior to the test, data were checked for normality and homogeneity of variance and did not meet these criteria. Post hoc comparisons amongst the treatments used Mann-Whitney U tests at $P = 0.01$.

Pathogenicity assays. *Vitis vinifera* 'Chardonnay' vines were needle-inoculated (46) with wild type, *ΔrmlB$_1$ACD*, or *rml/rml+ X. fastidiosa* cells or a 1X PBS buffer control. Cells of *X. fastidiosa* strains were harvested from plates of PD3 media in 1X PBS buffer,

and suspensions were adjusted to an OD_{600} of 0.25 ($1x10^8$ CFU/mL). Each vine was inoculated twice (with a 20 μL drop) on the main stem. Three independent trials of 7 plants were used. Upon the appearance of PD symptoms, vines were rated weekly on an established PD rating scale of 0 to 5, with 0 representing a healthy plant and 5 representing a dead plant. Scores of 1-4 represent an increase in the severity of PD-related leaf scorching and vine decline (5).

We quantified wild type, *ΔrmlB$_1$ACD*, or *rml/rml+ X. fastidiosa* populations per gram of tissue by isolating cells from the point of inoculation and from systemic tissue (25 cm above the point of inoculation). Isolations were performed twice: at 5 and 12 weeks post-inoculation. Petioles were surface sterilized and ground in 2 mL of sterile 1X PBS. The resulting macerate was diluted and plated onto solid PD3 medium according to standard methods. Total CFU/g tissue was determined, and data was analyzed using the Kruskal-Wallis test for nonparametric one-way ANOVA. Prior to the test, data were checked for normality and homogeneity of variance and did not meet these criteria. Post hoc comparisons amongst the treatments used Mann-Whitney U tests at $P = 0.05$.

Tylose formation. Stem sections of *Vitis vinifera* 'Chardonnay' vines were harvested at 18 weeks post-inoculation with wild type, *ΔrmlB$_1$ACD*, *rml/rml+*or 1X PBS negative control. Tissue was fixed in 80% ethanol prior to histological examination. Freehand sections were made of approximately 100 μm, stained with Toluidine Blue O (0.05%), and observed using a brightfield microscope (DM4000, Leica Microsystems CMS GmbH, Wetzlar, Germany).

LITERATURE CITED

1. **Janse JD, Obradovic A.** 2010. *Xylella fastidiosa*: its biology, diagnosis, control and risks. Journal of Plant Pathology **92:**S1. 35-S31. 48.

2. **Alhaddad H, Coudron TA, Backus EA, Schreiber F.** 2011. Comparative behavioral and protein study of salivary secretions in *Homalodisca spp.* sharpshooters (Hemiptera: Cicadellidae: Cicadellinae). Annals of the Entomological Society of America **104:**543-552.

3. **Chatterjee S, Almeida RPP, Lindow S.** 2008. Living in two Worlds: The Plant and Insect Lifestyles of *Xylella fastidiosa*. Annual Review of Phytopathology **46:**243-271.

4. **Feil H, Feil WS, Lindow SE.** 2007. Contribution of Fimbrial and Afimbrial Adhesins of *Xylella fastidiosa* to Attachment to Surfaces and Virulence to Grape. Phytopathology **97:**318-324.

5. **Guilhabert MR, Kirkpatrick BC.** 2005. Identification of *Xylella fastidiosa* antivirulence genes: hemagglutinin adhesins contribute to *X. fastidiosa* biofilm maturation and colonization and attenuate virulence. Molecular Plant-Microbe Interactions **18:**856-868.

6. **Voegel TM, Warren JG, Matsumoto A, Igo MM, Kirkpatrick BC.** 2010. Localization and characterization of *Xylella fastidiosa* haemagglutinin adhesins. Microbiology **156:**2172-2179.

7. **Killiny N, Almeida RPP.** 2009. *Xylella fastidiosa* Afimbrial Adhesins Mediate Cell Transmission to Plants by Leafhopper Vectors. Applied and Environmental Microbiology **75:**521-528.

8. **Li Y, Hao G, Galvani CD, Meng Y, Fuente LDL, Hoch HC, Burr TJ.** 2007. Type I and type IV pili of *Xylella fastidiosa* affect twitching motility, biofilm formation and cell–cell aggregation. Microbiology **153:**719-726.

9. **Clifford JC, Rapicavoli JN, Roper MC.** 2013. A Rhamnose-Rich O-Antigen Mediates Adhesion, Virulence, and Host Colonization for the Xylem-Limited Phytopathogen *Xylella fastidiosa*. Molecular Plant-Microbe Interactions **26:**676-685.

10. **Rapicavoli JN, Kinsinger N, Perring TM, Backus EA, Shugart HJ, Walker S, Roper MC.** 2015. O Antigen Modulates Insect Vector Acquisition of the Bacterial Plant Pathogen *Xylella fastidiosa*. Applied and Environmental Microbiology **81:**8145-8154.

11. **Killiny N, Martinez RH, Dumenyo CK, Cooksey DA, Almeida RPP.** 2013. The Exopolysaccharide of *Xylella fastidiosa* Is Essential for Biofilm Formation, Plant Virulence, and Vector Transmission. Molecular Plant-Microbe Interactions **26:**1044-1053.

12. **Giraud M-F, Naismith JH.** 2000. The rhamnose pathway. Current Opinion in Structural Biology **10:**687-696.

13. **Köplin R, Wang G, Hötte B, Priefer UB, Pühler A.** 1993. A 3.9-kb DNA region of *Xanthomonas campestris* pv. campestris that is necessary for lipopolysaccharide production encodes a set of enzymes involved in the synthesis of dTDP-rhamnose. Journal of Bacteriology **175:**7786-7792.

14. **Marie C, Deakin WJ, Ojanen-Reuhs T, Diallo E, Reuhs B, Broughton WJ, Perret X.** 2004. TtsI, a key regulator of Rhizobium species NGR234 is required for type III-dependent protein secretion and synthesis of rhamnose-rich polysaccharides. Molecular Plant-Microbe Interactions **17:**958-966.

15. **Jofré E, Lagares A, Mori G.** 2004. Disruption of dTDP-rhamnose biosynthesis modifies lipopolysaccharide core, exopolysaccharide production, and root colonization in *Azospirillum brasilense*. FEMS Microbiology Letters **231:**267-275.

16. **Jiang XM, Neal B, Santiago F, Lee SJ, Romana LK, Reeves PR.** 1991. Structure and sequence of the rfb (O antigen) gene cluster of *Salmonella* serovar typhimurium (strain LT2). Molecular Microbiology **5:**695-713.

17. **Flemming H-C, Wingender J.** 2010. The biofilm matrix. Nature Reviews Microbiology **8:**623-633.

18. **Marolda CL, Valvano MA.** 1995. Genetic analysis of the dTDP-rhamnose biosynthesis region of the *Escherichia coli* VW187 (O7: K1) rfb gene cluster: identification of functional homologs of rfbB and rfbA in the rff cluster and correct location of the rffE gene. Journal of bacteriology **177:**5539-5546.

19. **Gao M, D'Haeze W, De Rycke R, Wolucka B, Holsters M.** 2001. Knockout of an azorhizobial dTDP-L-rhamnose synthase affects lipopolysaccharide and extracellular polysaccharide production and disables symbiosis with *Sesbania rostrata*. Molecular Plant-Microbe Interactions **14:**857-866.

20. **da Silva FR, Vettore AL, Kemper EL, Leite A, Arruda P.** 2001. Fastidian gum: the *Xylella fastidiosa* exopolysaccharide possibly involved in bacterial pathogenicity. FEMS Microbiology Letters **203:**165-171.

21. **Sun Q, Sun Y, Walker MA, Labavitch JM.** 2013. Vascular occlusions in grapevines with Pierce's disease make disease symptom development worse. Plant Physiology **161:**1529-1541.

22. **Valvano MA, Messner P, Kosma P.** 2002. Novel pathways for biosynthesis of nucleotide-activated glycero-manno-heptose precursors of bacterial glycoproteins and cell surface polysaccharides. Microbiology **148:**1979-1989.

23. **Köplin R, Arnold W, Hötte B, Simon R, Wang G, Pühler A.** 1992. Genetics of xanthan production in *Xanthomonas campestris*: the xanA and xanB genes are involved in UDP-glucose and GDP-mannose biosynthesis. Journal of Bacteriology **174:**191-199.

24. **Rocchetta HL, Pacan JC, Lam JS.** 1998. Synthesis of the A-band polysaccharide sugar D-rhamnose requires Rmd and WbpW: identification of multiple AlgA homologues, WbpW and ORF488, in *Pseudomonas aeruginosa*. Molecular Microbiology **29:**1419-1434.

25. **Simpson AJG, Reinach FC, Arruda P, Abreu FA, Acencio M, Alvarenga R, Alves LMC, Araya JE, Baia GS, Baptista CS, Barros MH, Bonaccorsi ED, Bordin S, Bove JM, Briones MRS, Bueno MRP, Camargo AA, Camargo LEA, Carraro DM, Carrer H, Colauto NB, Colombo C, Costa FF, Costa MCR, Costa-Neto CM, Coutinho LL, Cristofani M, Dias-Neto E, Docena C, El-Dorry H, Facincani AP, Ferreira AJS, Ferreira VCA, Ferro JA, Fraga JS, Franca SC, Franco MC, Frohme M, Furlan LR, Garnier M, Goldman GH, Goldman MHS, Gomes SL, Gruber A, Ho PL, Hoheisel JD, Junqueira ML, Kemper EL, Kitajima JP, Krieger JE, et al.** 2000. The genome sequence of the plant pathogen *Xylella fastidiosa*. Nature **406:**151-157.

26. **Donlan RM.** 2002. Biofilms: microbial life on surfaces. Emerging Infectious Diseases **8:**881-890.

27. **Petrocelli S, Tondo ML, Daurelio LD, Orellano EG.** 2012. Modifications of *Xanthomonas axonopodis* pv. citri lipopolysaccharide affect the basal response and the virulence process during citrus canker. PloS One **7:**e40051.

28. **Abarca-Grau AM, Burbank LP, De Paz HD, Crespo-Rivas JC, Marco-Noales E, López MM, Vinardell JM, Von Bodman SB, Penyalver R.** 2012. Role for Rhizobium rhizogenes K84 cell envelope polysaccharides in surface interactions. Applied and Environmental Microbiology **78:**1644-1651.

29. **Raetz CRH, Whitfield C.** 2002. Lipopolysaccharide endotoxins. Annual Review of Biochemistry **71:**635.

30. **Roper MC, Greve LC, Labavitch JM, Kirkpatrick BC.** 2007. Detection and Visualization of an Exopolysaccharide Produced by *Xylella fastidiosa* In Vitro and In Planta. Applied and Environmental Microbiology **73:**7252-7258.

31. **Kotra LP, Golemi D, Amro NA, Liu G-Y, Mobashery S.** 1999. Dynamics of the Lipopolysaccharide Assembly on the Surface of *Escherichia coli*. Journal of the American Chemical Society **121:**8707-8711.

32. **Lehman AP, Long SR.** 2013. Exopolysaccharides from *Sinorhizobium meliloti* can protect against H2O2-dependent damage. Journal of Bacteriology **195:**5362-5369.

33. **Davies BW, Walker GC.** 2007. Identification of novel *Sinorhizobium meliloti* mutants compromised for oxidative stress protection and symbiosis. Journal of Bacteriology **189:**2110-2113.

34. **Fones H, Preston GM.** 2012. Reactive oxygen and oxidative stress tolerance in plant pathogenic *Pseudomonas*. FEMS Microbiology Letters **327:**1-8.

35. **Kiraly Z, El‐Zahaby H, Klement Z.** 1997. Role of extracellular polysaccharide (EPS) slime of plant pathogenic bacteria in protecting cells to reactive oxygen species. Journal of Phytopathology **145:**59-68.

36. **Berry MC, McGhee GC, Zhao Y, Sundin GW.** 2009. Effect of a waaL mutation on lipopolysaccharide composition, oxidative stress survival, and virulence in *Erwinia amylovora*. FEMS Microbiology Letters **291:**80-87.

37. **Duerr CU, Zenk SF, Chassin C, Pott J, Gütle D, Hensel M, Hornef MW.** 2009. O-antigen delays lipopolysaccharide recognition and impairs antibacterial host defense in murine intestinal epithelial cells. PLoS Pathogens **5:**e1000567.

38. **da Silva AR, Ferro JA, Reinach F, Farah C, Furlan L, Quaggio R, Monteiro-Vitorello C, Van Sluys M, Almeida Na, Alves L.** 2002. Comparison of the genomes of two *Xanthomonas* pathogens with differing host specificities. Nature **417:**459-463.

39. **Guilhabert MR, Hoffman LM, Mills DA, Kirkpatrick BC.** 2001. Transposon Mutagenesis of *Xylella fastidiosa* by Electroporation of Tn5 Synaptic Complexes. Molecular Plant-Microbe Interactions **14:**701-706.

40. **Marolda CL, Lahiry P, Vinés E, Salidías S, Valvano MA.** 2006. Micromethods for the characterization of lipid A-core and O-antigen lipopolysaccharide. *In* Brockhausen I (ed), Methods in Molecular Biology, vol 347. Humana Press, Inc., Totowa, NJ.

41. **Lee C-H, Tsai C-M.** 1999. Quantification of Bacterial Lipopolysaccharides by the Purpald Assay: Measuring Formaldehyde Generated from 2-keto-3-deoxyoctonate and Heptose at the Inner Core by Periodate Oxidation. Analytical Biochemistry **267:**161-168.

42. **Krauss JH, Weckesser J, Mayer H.** 1988. Electrophoretic analysis of lipopolysaccharides of purple nonsulfur bacteria. International Journal of Systematic and Evolutionary Microbiology **38:**157-163.

43. **Chatterjee S, Killiny N, Almeida RP, Lindow SE.** 2010. Role of cyclic di-GMP in *Xylella fastidiosa* biofilm formation, plant virulence, and insect transmission. Molecular Plant-Microbe Interactions **23:**1356-1363.

44. **Espinosa-Urgel M, Salido A, Ramos J-L.** 2000. Genetic analysis of functions involved in adhesion of *Pseudomonas putida* to seeds. Journal of Bacteriology **182:**2363-2369.

45. **Burdman S, Jurkevitch E, Soria‐Díaz ME, Serrano AMG, Okon Y.** 2000. Extracellular polysaccharide composition of *Azospirillum brasilense* and its relation with cell aggregation. FEMS Microbiology Letters **189:**259-264.

46. **Hill BL, Purcell AH.** 1995. Acquisition and retention of *Xylella fastidiosa* by an efficient vector, *Graphocephala atropunctata*. Phytopathology **85:**209-212.